

Monitoring Phenology of Boreal Trees Using Remote Sensing

by

Kyle Springer

A thesis submitted in partial fulfillment of the requirements for the degree of

Master of Science

in

Plant Biology

Department of Biological Sciences  
University of Alberta

© Kyle Springer, 2018

## **Abstract**

Terrestrial vegetation contributes strongly to dynamic biosphere-atmosphere exchanges of mass and energy, through activities such as photosynthesis, that help shape the Earth's climate. The boreal forest is located in high latitudes and subject to large seasonal temperature fluctuations and a changing climate. Understanding the response of the boreal forest to seasonal and climate changes requires a means of effectively monitoring vegetation phenology at large spatial and temporal scales. Optical remote sensing can be applied at such scales, providing a powerful means of observing how ecosystems respond to changing environmental conditions. However, continued work that integrates both optical remote sensing and plant physiology at multiple scales is necessary to correctly apply and interpret large scale remote sampling of vegetation. Key questions regarding the application of optical remote sensing across ecosystems remain unanswered: 1) which remote sensing metrics are most effective at monitoring phenology of different functional types? and 2) how do these remote sensing metrics relate to actual changes in plant physiology when sampling different vegetation?

To address these questions, experimental forest stands for several boreal tree species, both evergreen and deciduous were established in pots in Edmonton, Alberta, Canada, allowing for continuous monitoring across seasons using a variety of metrics to track phenology of representative boreal vegetation at multiple scales. This involved the use of different optical indices: the normalized difference vegetation index (NDVI), the photochemical reflectance index (PRI), the chlorophyll/carotenoid index (CCI), and steady-state chlorophyll fluorescence ( $F_s$ ), as an analogue of solar-induced fluorescence (SIF). These optical metrics were then compared to actual rates of photosynthesis to determine their efficacy in tracking seasonal changes in photosynthetic activity, or photosynthetic phenology. Results indicated that NDVI and PRI

exhibited a complementary ability to monitor photosynthetic phenology of both evergreen and deciduous functional types. NDVI effectively tracked photosynthetic phenology of deciduous species, but less so for evergreens, while PRI closely paralleled photosynthetic phenology of evergreens, but less so for deciduous species. CCI showed strong parallels with photosynthetic activity in both evergreen and deciduous species, with  $F_S$  showing a similar ability. These results indicated subtle differences in seasonal patterns of optical metrics and photosynthetic activity across and within functional types. Overall, these results revealed the efficacy of different remote sensing metrics at tracking photosynthetic phenology of different boreal tree species. This project provides an important foundation for the assessment of plant physiology by means of optical remote sensing, expanding the value of large-scale ecosystem monitoring.

## Preface

This thesis is an original work by Kyle R. Springer. This study was supported by iCORE/AITF (G224150012 & 200700172), NSERC (RGPIN-2015-05129), CFI (26793), and NASA ABoVE (NNX15AT78A) grants to John A. Gamon. The data chapter of this thesis was co-authored, with research, analysis and writing led by Kyle R. Springer. Co-authors were involved in development of the project and the experiment design, data collection, data analysis, and providing editorial comments.

A version of Chapter 2 has been published as: Kyle R. Springer, Ran Wang, and John A. Gamon. 2017. "Parallel Seasonal Patterns of Photosynthesis, Fluorescence, and Reflectance Indices in Boreal Trees". *Remote Sensing*. 8: 691. K.R.S. was the primary author. K.R.S. and J.A.G. conceived and designed the experiments; K.R.S. and R.W. performed the experiments; K.R.S. and R.W. analyzed the data; and K.R.S. wrote the manuscript draft, with J.A.G. and R.W. providing revisions.

## Acknowledgements

Looking back at where I was 5 years ago, an uncertain third year undergraduate, it seems like the most improbable of outcomes that I have would end up cultivating the passion for plants that I now have. Even a few years ago, I could hardly even see myself going to graduate school. Yet here I am, at the end of my time working towards my MSc and becoming a card-carrying botanist.

I would first like to thank my supervisor, Dr. John Gamon, as I most certainly would not be where I am today without his influence. It was Dr. Gamon who first introduced me to this unique way of looking at plants. Since then, Dr. Gamon has helped cultivate my skills for scientific research and writing, providing extensive and constructive feedback on how my work can always be better, even after seven rounds of revisions. Pushing me to always do better will be something that I will appreciate, wherever the future takes me.

I would also like to thank my committee members Dr. Janice Cooke and Dr. David Hik, for their comments, suggestions and general feedback on my work over the past few years. I have had the pleasure of working with Dr. Cooke for several years now and fully appreciate the botanical knowledge and skills that I have developed in my experiences with her, realizing how far I have come since first learning about plant physiology, which now seems like a lifetime ago. From Dr. Hik, I have seen the balanced demeanor that is essential to deal with the ups and downs of scientific research, and now know how imperative it is to take a step back and set practical goals so as not to be overwhelmed by unrealistic expectations.

I have also had the pleasure of working with the current and past member of our lab, Ran Wang, Olga Kovalchuk, and Scott Williamson, over the past few years. In particular, I would like to thank Ran Wang for all his assistance during my time as a graduate student, not only for his aid with my research but for helping me adjust to the life of a grad student, or lack thereof in some cases. Thanks are also extended to Steven Williams, whose experience and knowledge was invaluable for the proper care of my plants.

Finally, I would like to thank my family and friends that supported me while I pursued my passion for working with plants, which at times may have seemed like an obsession. This undertaking could not have been completed without the support from every one of you. Thank you all.

# Table of Contents

Abstract .....	ii
Preface .....	iv
Acknowledgements.....	v
Table of Contents.....	vi
List of Tables .....	viii
List of Figures.....	ix
List of Abbreviations .....	xi
Chapter 1: Introduction.....	1
1.1 The Current State of the Boreal Forest.....	1
1.2 Plant Processes in Response to Environmental Changes.....	4
1.3 Utilizing Remote Sensing.....	7
1.4 Linking Remote Sensing and Plant Physiology .....	9
1.5 The Complementary Nature of Optical Indices .....	10
1.6 Research Objectives .....	12
1.7 References .....	15
Chapter 2: Parallel Seasonal Patterns of Photosynthesis, Fluorescence, and Reflectance Indices in Boreal Trees.....	24
2.1 Introduction .....	24
2.2 Materials and Methods .....	29
2.2.1 Plant Culture .....	29
2.2.2 Data Collection .....	31
2.2.3 Environmental Conditions .....	31
2.2.4 Canopy Reflectance and Optical Indices .....	31
2.2.5 Gas Exchange.....	32
2.2.6 Chlorophyll Fluorescence .....	33
2.2.7 Data Analysis .....	33
2.3 Results .....	34
2.3.1 Seasonal Environmental Conditions.....	34
2.3.2 Seasonal Patterns of Photosynthesis and Remote Sensing Metrics .....	35
2.3.3 Comparison of optical metrics to photosynthesis .....	41
2.4 Discussion .....	48

2.4.1 Seasonal Patterns and Variation.....	48
2.4.2 Complementarity Hypothesis.....	51
2.4.3 Differences Between Species Within Functional Types.....	52
2.4.4 Other Causes of Variation in Stand-Level Sampling.....	53
2.5 Conclusions .....	54
2.6 References .....	57
Chapter 3: Discussion and Conclusions .....	63
3.1 Summary and Contributions.....	63
3.2 Limitations and Future Work .....	65
3.2.1 Expanding Upon Small-Scale Studies .....	65
3.2.2 Upscaling with New Technologies .....	66
3.3 Conclusions .....	67
3.4 References .....	68
Bibliography .....	70
Appendix .....	80

## List of Tables

<b>Table 2.1:</b>	Calculated t-statistics and <i>p</i> -values (asterisks) from paired t-test comparing average summer and winter values of different measurements by type and by species. For evergreen and deciduous types (a), average summer and winter values for each species were used for comparison. For evergreen (b) and deciduous (c) species, summer and winter averages were derived from plant or plot region measurements for each period. Bonferroni corrections were not applied for analyses. Winter was defined as November to March; Summer was defined as Mid-May to Mid-August. See supplemental Figure S3, S4 and Table S2 for additional information on comparisons. *, <i>p</i> < 0.05; **, <i>p</i> < 0.01; ***, <i>p</i> < 0.001; ****, <i>p</i> < 0.0001.....	40
<b>Table 2.2:</b>	Coefficient of determination ( $R^2$ ) and <i>p</i> -values (asterisks) for regressions between canopy-level optical indices (normalized difference vegetation index (NDVI), photochemical reflectance index (PRI), chlorophyll/carotenoid index (CCI), and steady-state fluorescence ( $F_s$ )) and photosynthetic rate for evergreen (a) and deciduous (b) species. Data points from the spring transition in 2016 for <i>P. glauca</i> and <i>P. mariana</i> were excluded from analyses. The sample size for $F_s$ was smaller than for reflectance indices, and is indicated in parentheses. *, <i>p</i> < 0.05; **, <i>p</i> < 0.01; ***, <i>p</i> < 0.001; ****, <i>p</i> < 0.0001. ....	41
<b>Table 2.3:</b>	<i>p</i> -values for comparison of regression slopes (interaction) between evergreen and deciduous species grouped by type for optical measurements and photosynthetic rate (a), and between optical indices and $F_s$ (b).....	43
<b>Table 2.4:</b>	<i>p</i> -values from ANCOVA analysis comparing regression slopes (interaction) of optical measurements NDVI (a), PRI (b), CCI (c), and $F_s$ (d), plotted against photosynthetic rate between each study species. *, <i>p</i> < 0.05; **, <i>p</i> < 0.01; ***, <i>p</i> < 0.001; ****, <i>p</i> < 0.0001.....	44
<b>Table 2.5:</b>	Coefficient of determination ( $R^2$ ) and <i>p</i> -values (asterisks) for regressions between canopy-level optical indices NDVI, PRI, CCI and $F_s$ for evergreen (a) and deciduous (b) species. Data points from the spring transition in 2016 for <i>P. glauca</i> and <i>P. mariana</i> were excluded from analyses. *, <i>p</i> < 0.05; **, <i>p</i> < 0.01; ***, <i>p</i> < 0.001; ****, <i>p</i> < 0.0001.....	45
<b>Table 2.6:</b>	<i>p</i> -values from ANCOVA analysis comparing regression slopes of optical indices NDVI (a), PRI (b), and CCI (c), plotted against $F_s$ between each study species. * <i>p</i> < 0.05; ** <i>p</i> < 0.01; *** <i>p</i> < 0.001; **** <i>p</i> < 0.0001.....	47



## List of Figures

- Figure 1.1:** Mean annual surface air temperature anomaly in 2016 compared to the period of 1965-2015. The inset shows the temperature anomaly averaged by latitude for the same comparison. Results are based on the National Aeronautics and Space Administration Goddard Institute for Space Sciences (NASA GISS) temperature analysis [8,9]. ..... 2
- Figure 1.2:** Hypothesized relationships between NDVI (a and b), PRI (c and d) and CCI (e and f) and productivity for annual or deciduous (left) or evergreen (right) vegetation. The hypothetical relationships between CCI and productivity are indicated in red to illustrate the current hypothesis of this thesis. More positive values indicate greater photosynthetic carbon uptake, given as Net Ecosystem Exchange (NEE) or Gross Ecosystem Exchange (GEE). Modified from Gamon 2015 [61]. ..... 11
- Figure 1.3:** Synthetic plots of boreal tree species established on the rooftop of the Biological Sciences Building. Species sampled include trembling aspen (*Populus tremuloides*) and balsam poplar (*Populus balsamifera*) as broad-leaf species, and tamarack (*Larix laricina*), a deciduous conifer, and three evergreen species: black spruce (*Picea mariana*), white spruce (*Picea glauca*), and jack pine (*Pinus banksiana*). Image date: September 28, 2017. .... 13
- Figure 2.1:** Representation of the light-use efficiency (LUE) model in black, stating that gross primary productivity (GPP) is a function of absorbed photosynthetically active radiation (APAR:  $f_{PAR} \times PAR$ ) and efficiency ( $\epsilon$ ). Red text shows optical measurements useful for model parameterization and validation, including solar-induced fluorescence (SIF), the chlorophyll/carotenoid index (CCI), the normalized difference vegetation index (NDVI), and the photochemical reflectance index (PRI) (modified from Gamon 2015) [31]. ..... 28
- Figure 2.2:** Depiction of experimental set-up on the rooftop of the Biological Sciences Building at the University of Alberta, illustrating the monocultural plots established on the rooftop (a), the arrangement of plants, approximate regions within each plot sampled for canopy reflectance (red), and plants sampled for gas exchange (blue) and fluorescence (blue and green) in each plot (b), representative entire canopies during the growing season (June 2016), winter (December 2016), and following snowfall in the winter (January 2017) of evergreen (c) and deciduous (d) species, and representative mature, sun-lit branchlets from evergreen plants (e) and leaves from deciduous plants (f) near the tops of trees that were used for measuring gas exchange and leaf area (branchlets and leaves indicated in red). For gas exchange sampling, plants on the northern edge of the plot were sampled to avoid interference with measurements of canopy optical signals. For canopy reflectance, the same regions of the plot were sampled throughout the study. For leaf-level measurements (gas exchange and fluorescence), the same plants were used throughout the study; for evergreens, the same branchlets were used for gas exchange and leaf area measurements. .... 30
- Figure 2.3:** Seasonal dynamics of photosynthetic photon flux density (PPFD;  $\mu\text{mol photons m}^{-2} \text{s}^{-1}$ ) and temperature ( $^{\circ}\text{C}$ ) from December 2015 to January 2016. PPFD is expressed

as a midday average, taken as the period between 13:00 and 14:00 (UTC-06), and temperature is expressed as daily (24-hour) averages. Long-term normal (1981-2010) daily average temperature by month is also shown. Error bars denote  $\pm$ SD of the mean. Between 20 November and 20 January, the sun did not clear buildings to the south due to low solar elevation, causing anomalously low PPFD values during this period... 35

**Figure 2.4:** Annual patterns of midday average temperature (grey line), optical indices and photosynthetic metrics for evergreen and deciduous species. Evergreen species (a-e) included *P. mariana* (black), *P. banksiana* (red), and *P. glauca* (blue). Deciduous species (f-j) included *L. laricina* (black), *P. tremuloides* (red), and *P. balsamifera* (blue). Optical indices (b-d, g-i) were calculated from reflectance measurements at the canopy-level. Fluorescence ( $F_s$ ) was measured at the leaf-level. Data points shown were obtained near solar noon from December 2015 to January 2017. Open points (a) denote sampling periods during the spring transition, where new branches were sampled for *P. mariana* and *P. glauca* during gas exchange measurements. The winter period is indicated by the grey regions (November-March). Annotations on figures indicate the effects of snow (S), repotting (R), and new-leaf expansion (E). For deciduous trees, data were restricted to periods with fully formed leaves during the growing season. Error bars denote  $\pm$ SE of the mean..... 38

**Figure 2.5:** Relationships between photosynthetic rate ( $\mu\text{mol CO}_2 \text{ m}^{-2} \text{ s}^{-1}$ ) and the NDVI, PRI, CCI, or  $F_s$  for evergreen (a-d) and deciduous (e-h) species. Data points were obtained near solar noon from January 2016 to December 2016. Error bars denote  $\pm$ SE of the mean. Open points (a-d) denote dates when new branches were sampled for *P. mariana* and *P. glauca*; these points were excluded from analyses. The  $R^2$  and significance of each relationship are indicated in Table 2.2. .... 42

**Figure 2.6:** Relationships between  $F_s$  and canopy-level optical indices NDVI, PRI, and CCI for evergreen (a-c) and deciduous (d-f) species. Data points were obtained near solar noon from January 2016 to December 2016. Error bars denote  $\pm$ SE of the mean. The  $R^2$  and significance of each relationship are indicated in Table 2.4..... 46

## List of Abbreviations

NPP	Net Primary Productivity
GPP	Gross Primary Productivity
NEE	Net Ecosystem Exchange
GEE	Gross Ecosystem Exchange
PAR	Photosynthetically Active Radiation
PPFD	Photosynthetic Photon Flux Density
LUE	Light Use Efficiency
APAR	Absorbed Photosynthetically Active Radiation
$f_{PAR}$	Fraction of Absorbed Photosynthetically Active Radiation
$F_S$	Steady-State Chlorophyll Fluorescence
SIF	Solar-Induced Fluorescence
NDVI	Normalized Difference Vegetation Index
PRI	Photochemical Reflectance Index
CCI	Chlorophyll/Carotenoid Index
NPQ	Non-Photochemical Quenching
MODIS	Moderate Resolution Imaging Spectroradiometer
FLEX	FLuorescence EXplorer

# Chapter 1: Introduction

## 1.1 The Current State of the Boreal Forest.

Terrestrial vegetation represents one of the most important components of the biosphere. Globally, the net uptake of carbon by forest ecosystems has been estimated to be as high as 2.4 Pg of Carbon per year [1]. With approximately 4 billion hectares of the Earth's land surface covered by forests [2], forest ecosystems account for approximately 45% of stored biospheric carbon (in plants and soil) and around 50% of all net primary production in terrestrial environments [3]. The circumpolar boreal forest alone covers 1132 million hectares, accounting for approximately one quarter of the total forested area on the planet [1]. The vast boreal region is a substantial global carbon store [4] containing nearly a quarter of the global carbon sinks in forested regions [1]. The boreal region, however, is particularly vulnerable to changes in climate, and is experiencing more rapid change than many other terrestrial ecosystems.

Located at higher latitudes than other forests, the boreal forest is subject to strong seasonal temperature variability and is exhibiting greater temperature changes in response to increasing atmospheric greenhouse gas concentrations in comparison to most other terrestrial ecosystems. This greater susceptibility of higher latitudes to increasing temperatures is a feature of the global climate system known as Arctic amplification [5]. Arctic amplification is the combined product of a suite of processes that act independently or together on different spatial and temporal scales; dynamic interactions between the atmosphere, hydrosphere, cryosphere, and biosphere all contribute to the amplified warming in higher latitudes. Some models suggest that the warming experienced in arctic regions (60°N–90°N) is nearly twice that of global mean warming [6]. When comparing temperature anomaly observed in 2016 to the past 50 years on average, the changes in temperature in higher latitudes is most pronounced (Fig. 1.1).

Changes in climatic conditions are currently having substantial impacts on the ecology and physiology of the boreal region. In climatic zones outside the tropics, plants are exposed to seasons that are either favorable or limiting to photosynthetic activity and growth. In northern latitudes like the boreal region, temperature and photoperiod are the main factors that define the growing season, the favorable growing period of high productivity for plants.

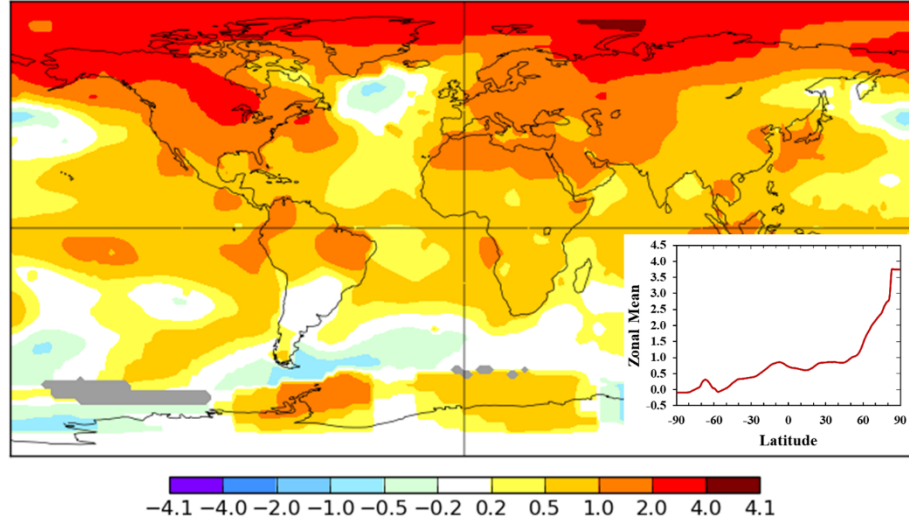


**Figure 1.1:** Mean annual surface air temperature anomaly in 2016 compared to the period of 1965-2015. The inset shows the temperature anomaly averaged by latitude for the same comparison. Results are based on the National Aeronautics and Space Administration Goddard Institute for Space Sciences (NASA GISS) temperature analysis [8,9].

Plant productivity is fundamentally linked to photosynthesis, the biochemical processes for light harvesting and carbon fixation. Photosynthetic capacity, the maximum rate of photosynthesis or carbon assimilation [9], is regulated by the relatively short-term dynamics of the electron transport capacity ( $J_{\max}$ ) and carboxylation capacity ( $V_{\text{cmax}}$ ) of plants [10], both of which have a high sensitivity to temperature changes [11]. As discussed below, photosynthetic dynamics are also tied to seasonal changes in pigment activity and pool sizes, and leaf display. Photosynthesis is expressed on an “instantaneous” basis, typically described as micromoles of carbon assimilated per square meter per second, but productivity is often expressed as carbon accumulation in biomass over days to years. At ecosystem scales, accumulation of carbon is formally described by Gross Primary Productivity (GPP) and Net Primary Productivity (NPP) which are often integrated over a year; GPP is the equivalent to  $\text{CO}_2$  assimilation or photosynthetic rate but is expressed over a longer time period, while NPP accounts for the combined effects of plant photosynthesis and respiration over time [12,13]. While changing climate has no effect on photoperiod, changes in temperature can alter the timing of vernal and autumnal transitions, altering the growing season length and directly impacting vegetation phenology and productivity [14].

Warmer temperatures are likely to cause an earlier spring onset and a delayed fall senescence [14–16], but photoperiod control on phenology for many boreal species may limit the fall extension of the growing season [16]. With changing climate, the onset of leaf emergence and leaf senescence has already advanced and delayed, respectively, in the last several decades [17]. With a longer growing season, forests may yield a greater carbon uptake and productivity as a result of a longer period with green foliage and an extended period of favorable conditions [14]. However, forest growth and productivity in response to climate change may depend on more than the timing of warming and growing season length [18] and may actually be restricted in a warming world.

With boreal forest function and health, including photosynthesis and respiration, being closely linked to temperature and precipitation patterns [19], altered growing season temperature and moisture availability with changing climate will lead to further effects on plant productivity [20]. While boreal species can show positive photosynthetic and growth responses to warming [18], they can also show reduced responses when warming is accompanied by drought. The recent ‘browning’ of boreal regions and the recession of vegetation appears to be a product of drought stress during the growing season, as warmer temperatures and lower moisture availability reduce plant growth and productivity [20–22]. Warmer temperatures also influence the frequency and severity of disturbances such as fires or insect infestations, which directly impact vegetation succession and productivity [23,24].

Shifts in vegetation are already noticeable due to changing climate. The boreal region is a mosaic of different forest types that, due to the harsh conditions, are composed of relatively few tree species [25]. Forest stands are comprised of a mix of conifers, including spruce (*Picea* spp.), pine (*Pinus* spp.), fir (*Abies* spp.) and hemlock (*Tsuga* spp.), larch (*Larix* spp.), and broadleaf deciduous tree species, including poplar (*Populus* spp.), birch (*Betula* spp.), willow (*Salix* spp.), and alder (*Alnus* spp.); The physiology, ecology, and adaptations of these trees have been well studied [26–29], and two primary functional types, evergreen and deciduous, often have contrasting responses to environmental change [18]. The boreal forest itself may see a shift in vegetation composition toward more deciduous trees with a loss of evergreens [19], as warming has been shown to result in greater growth and productivity in deciduous vegetation [18,30] while evergreens may have a lesser growth response to warming [18]. However, the drier conditions that are likely to accompany warming in the boreal region [20] may favor the thicker, less productive evergreen

leaves capable of tolerating drier, more stressful conditions [31]. Trees may also expand into the tundra ecoregion, which is already experiencing northward vegetation encroachment that has contributed to the apparent greening of coastal tundra [21,32], while receding towards the south with a loss of trees near prairie regions [33].

These shifts in vegetation will also change the land surface albedo [19], and alter rates of gas exchange (e.g. evapotranspiration) that will further impact the radiative balance [34]. The combined effects of changing temperatures, atmospheric carbon dioxide (CO<sub>2</sub>) levels, and moisture availability that are associated with climate change will have direct impacts on plant processes [35], causing further feedbacks on the atmosphere and climate [19]. For these reasons, developing improved remote sensing methods to assess actual photosynthesis and productivity of boreal regions has become a high priority for current missions, like NASA's ABoVE project, aimed at monitoring and understanding changing arctic and boreal environments [36].

## **1.2 Plant Processes in Response to Environmental Changes.**

Evergreen-coniferous and deciduous-broadleaf tree species have contrasting phenological strategies [30]. During the growing season, broad-leaf deciduous species have high rates of photosynthesis attributed to the morphology and nutrient content of their foliage [31,37]. High surface area to mass ratio of relatively thin leaves allows for maximized light absorption, reduced internal competition for carbon dioxide, and high stomatal conductance which, when coupled with high nitrogen content, results in a high photosynthetic capacity and high productivity under favorable conditions [31,38,39]. Evergreen species, like conifers, with thicker, less productive leaves, do not have the high peak-season photosynthetic capacity of broad-leaf deciduous species [31,37]. However, the retention of foliage year-round allows for a potentially longer growing season, with leaves able to photosynthesize earlier in the spring and later in the fall when conditions are favorable to evergreens but not to deciduous species [39,40].

Variation in photosynthetic activity across seasons results from exposure of plants to an extended period of cold temperatures and reduced photoperiod, which leads to photosynthetic down-regulation during the transition to winter [41–45]. For plants, the preparations for unfavorable growing conditions begin near the middle of the growing season, with the end of active growth and the formation of buds to protect meristematic tissues [14]. These meristematic changes, along with cellular-level biochemical changes, lead to bud dormancy, the cessation of active growth in

meristematic regions that does not resume under favorable conditions [46], a process shared by both evergreen and deciduous species. Bud dormancy, reduced metabolic activity and nutrient cycling, suppression of growth, leaf senescence, enhanced cold and frost stance, and other cellular and cytoplasmic changes, are characteristic process of plants reaching winter dormancy [46,47]. In this work, the use of the term dormancy, or dormant period/phase, will refer to this suite of processes that are associated with the period of rest for plants. Different functional types, however, have varying strategies for establishing dormancy and dealing with extreme winter conditions.

Evergreen and deciduous vegetation possess contrasting foliar mechanisms for cycling between active and dormant phases. Deciduous species have obvious foliar changes that occur during transition periods that signal the shifts between active growth and downregulation, and photosynthetic activity in deciduous species is closely linked to the seasonal pattern of leaf emergence and senescence [48]. At the end of the growing season, the transition to the dormant phase is clearly marked by the changing of leaf coloring caused by the degradation of chlorophyll in leaves [49] during leaf senescence in the fall. The decline in chlorophyll content, along with other biochemical changes, during senescence results in a decrease in photosynthetic activity [50], which can occur rapidly prior to leaf fall [51]. The spring activation period leading into the growing season is clearly marked by the leaf emergence and the ‘greening’ of canopies, which leads to a rapid increase in photosynthetic activity [51].

However, observing seasonal transitions in physiological activity is more difficult in evergreen conifers. Retaining their leaves year-round, evergreen species exhibit subtle changes in foliage during seasonal transitions that efficiently up- and down-regulate their photosynthetic activity with changing conditions [52]. In order to maintain their leaves in extreme winter conditions, needles undergo a cold-hardening process prior to the overwinter period as signaled by declining temperatures and a shorter photoperiod [42]. The cold-hardening process involves the adjustment of leaf pigment pools that dissipate excess light energy following photosynthetic down-regulation. These changes primarily involve increases in carotenoid pigments associated with photoprotection [50,51], and the reorganization and reduction of chlorophyll pigments [41] to reduce excess energy absorbance and avoid winter damage. Specifically, the reduction of chlorophyll pigments combined with increased photoprotective pigments like lutein and  $\beta$ -carotene and the retention of xanthophyll cycle pigments result in a sustained down regulation of photosystem II (PSII) activity



to prevent photodynamic damage to plant tissues when low air temperatures inhibit photosynthesis [55]. These pigment shifts along with other cellular changes associated with cold-hardening lead to a depression of photosynthetic rates in evergreen foliage during winter months [47]. These adjustments in photoprotective pigmentation and the near complete suppression of photosynthesis during the winter are subsequently reversed during the spring transition, resulting in a rapid recovery of photosynthetic capacity when plants detect above freezing temperatures [41].

In addition to seasonal processes that respond to environmental cues, plants also possess a number of mechanisms to regulate photosynthetic processes that operate within seasons to respond to changing environmental conditions on shorter timescales. When light is absorbed by photosynthetic pigments in leaves, it is either used for photochemistry, or dissipated as heat or fluorescence, to prevent photodamage [56]. Under favorable conditions, or in low light environments, light absorbed by chlorophyll is efficiently used to drive photosynthesis [57]. When light levels become saturating, or plants are under stress, plants possess mechanisms for dissipating excess light energy as heat, referred to as non-photochemical quenching (NPQ) [53,56]. One such method of dissipating excess energy is through the xanthophyll cycle, the de-epoxidation of zeaxanthin from violaxanthin through an intermediary, antheraxanthin [53]. This process is readily reversed (epoxidation) under low light conditions to maintain balance between photoprotection and photochemistry in variable light.

Another primary pathway for excess energy to be dissipated is through chlorophyll fluorescence, the re-emission of excess light [57]. The amount of energy dissipated through fluorescence is dependent on the amount of absorbed photosynthetically active radiation (APAR) assimilated by the plants and how much energy is dissipated through NPQ [56]. Though it occurs rapidly, the total amount of energy dissipated through fluorescence is small, as it represents the remainder of light energy that was not used for photochemistry or dissipated as heat; accordingly, the light emitted through chlorophyll fluorescence occurs at a lower energy level, hence at a longer wavelength, than what was incident [57]. The extent of light dissipation through fluorescence in different seasons is yet unclear, but some studies have shown strong seasonal variability [58].

Together, these processes allow plants to regulate their photosynthetic activity in response to environmental cues on different temporal scales. The time scales for these responses are variable, ranging from fractions of a second to weeks or months. Dissipation of excess light energy through

chlorophyll fluorescence occurs rapidly in response to changing light conditions, photosynthetic rates and NPQ, eventually reaching a steady state within minutes [59]. The dissipation of excess energy as heat through the xanthophyll cycle takes place over a slightly longer period, acting on timescales of minutes to hours, as pigments adjust to changing conditions [60]. On the other hand, changes in foliage or canopy structure related leaf development or senescence [14] and pigment pool size changes related to winter cold hardening [41–45] occur on much longer time scales. Though occurring on very different time scales, these physiological changes relating to energy regulation, as well as changes in photosynthetic activity, can be detected using different remote sensing techniques [61].

### **1.3 Utilizing Remote Sensing**

Remote sensing provides a means of monitoring plant physiological processes at multiple spatial and temporal scales. While conventional, large-scale remote sensing techniques such as satellite (MODIS) and flux tower measurements can be used to quantify broad vegetative patterns (i.e. phenology, GPP) [62], these methods are often unable to resolve finer scale temporal and spatial details that reflect underlying ecosystem physiological mechanisms that drive broad scale patterns [61]. Using optical remote sensing at proximal distances (from the ground or low-flying platforms), it is possible to observe and measure changing compositional properties of plants and forests that drive the physiological processes influencing plant productivity [63,64]. When properly implemented, optical sampling conducted at proximal scales are often comparable with other remote sensing measurements at large spatial and temporal scales [61], providing ground validation of these large-scale metrics and the potential to extrapolate (up-scale) broad, ecosystem-level, patterns and properties from mechanistic processes.

Many vegetation indices derived from optical sampling can be useful in estimating different parameters, both physiological and structural, that impact phenology and productivity [65]. The normalized difference vegetation index (NDVI) has long been used to track changing vegetation “greenness” [66] by quantifying the amount of photosynthetic green plant tissues [67]. Using reflectance in the red and near-infrared wavelengths, NDVI provides an estimate of fraction of photosynthetically active radiation ( $f_{PAR}$ ) that is absorbed by green vegetation [62] (Eq. 1). Vegetation ‘greenness’ has often been employed as a surrogate for photosynthetic activity, particularly at coarse spatial scales, and has been shown to track long-term changes in growing-

season length and productivity in high latitudes [68]. NDVI tracks seasonal phenology of green biomass and leaf display, from budburst to senescence, in annual and deciduous species [69]. Though NDVI is useful in detecting changes in and canopy “greenness” and light absorption over time, as represented by leaf area index and  $f_{PAR}$  [62,69], it is unable to fully resolve changes to physiological processes that control photosynthetic activity [70]. This is particularly a problem when observing evergreen species, as they have much more subtle physiological changes, particularly during transition periods, and exhibit little change in greenness across seasons [71].

$$NDVI = \frac{\rho_{NIR} - \rho_{red}}{\rho_{NIR} + \rho_{red}} \quad (1)$$

Relative to NDVI, the photochemical reflectance index (PRI) is capable of detecting more subtle change in foliage relating to the regulation of photosynthetic activity [72]. This index evaluates reflectance in the 531 nm waveband as compared to 570 nm as a reference waveband [73] (Eq. 2) to detect pigmentation responses to environmental cues, particularly in evergreen species; these responses are easily missed when using NDVI [43]. Over shorter, diurnal time-scales, PRI responses are driven by changes in the xanthophyll cycle, a facultative response, while responses over seasonal timescales reflect changes in pigment pool size (carotenoid/chlorophyll ratios), a constitutive response [43,74]. Proper interpretation of PRI responses is dependent on sampling method and scale, and a number of studies have calculated PRI with slight differences from the original equation [70,75,76].

$$PRI = \frac{\rho_{531nm} - \rho_{570nm}}{\rho_{531nm} + \rho_{570nm}} \quad (2)$$

More recently, the chlorophyll/carotenoid index (CCI) has been proposed as an alternative indicator of photosynthetic activity, particularly in evergreens [45]. CCI was originally derived from NASA’s satellite-based MODIS sensor using bands 1 (645 nm, a terrestrial band) and 11 (531 nm, an ocean band) (Eq. 3). Like the PRI, CCI is sensitive to changes in pigment pool sizes and can accurately track seasonally changing chlorophyll/carotenoid levels at both the leaf and stand level, as changes in pigment pool sizes have a broader spectral response, compared to the changes to the xanthophyll cycle, which affects a narrow waveband [45]. However, unlike PRI, CCI has the potential to be applied over much larger spatial and temporal scales, as it can be derived from reprocessed MODIS satellite data (MODIS Collection 6) in a dataset that now spans

almost two decades. The potential of CCI as an indicator of seasonal photosynthetic activity was originally outlined for evergreen species; similar studies on its application to deciduous species have not yet been reported [45].

$$CCI = \frac{\rho_{B11} - \rho_{B1}}{\rho_{B11} + \rho_{B1}} \quad (3)$$

Chlorophyll fluorescence can also provide information regarding photosynthetic performance, as it indicates the amount of absorbed light energy used for photochemistry or dissipated as heat [77]. As outlined in a recent review [56], changes in fluorescence can reflect changing photosynthetic activity as the fluorescence signal is influenced by a number of internal and external factors, such as leaf chlorophyll content, chloroplast movements, leaf orientation and structure, and solar illumination. Traditionally, chlorophyll fluorescence has been measured at leaf-level using the pulse-amplitude modulation (PAM) technique, which delivers a saturating pulse of light [56]. While this limits the application of PAM to proximal measurements, with the advent of high-spectral resolution spectrometers capable of resolving narrow absorption bands in the solar spectrum (Fraunhofer lines), fluorescence can now be passively measured remotely detected as a small signal present in the “gaps” of the solar spectrum [78]. The resulting measurement has been termed solar-induced fluorescence (SIF), and has been shown to be closely linked to gross primary productivity (GPP) when aggregated over large spatial and temporal scales [58,79,80]. However, due to the coarse spatial and temporal scales of many satellite-based measurements, satellite SIF measurements are unable to resolve underlying mechanisms driving seasonal dynamics of GPP. Proximal and airborne fluorescence studies are needed to better understand the mechanisms driving the SIF signal.

#### **1.4 Linking Remote Sensing and Plant Physiology**

A common approach for applying optical remote sensing to estimate plant productivity and photosynthetic activity at stand to global scales employs the light-use efficiency (LUE) model. This model represents plant productivity, often in different forms, as a function of solar radiation absorbed by plants and the conversion efficiency of absorbed light [81]. The model expresses plant productivity (GPP) as a function of the amount of absorbed photosynthetically active radiation (APAR) and the efficiency ( $\epsilon$ ) of plants in converting absorbed light into fixed carbon [62,82] (Eq. 4). The  $\epsilon$  term of the model represents the photosynthetic light-use efficiency of vegetation (i.e.

physiological control of photosynthesis) which is also impacted by abiotic conditions such as temperature and humidity [83]. The APAR term of the model can be broken down further and defined as the product of incoming photosynthetically active radiation (PAR), or photosynthetic photon flux density (PPFD), and the fraction of that photosynthetically active radiation ( $f_{PAR}$ ) that is absorbed by photosynthetic plant structures to drive photosynthesis through photochemistry [61] (Eq. 5).

$$GPP = APAR \times \varepsilon \quad (4)$$

$$APAR = f_{PAR} \times PAR \quad (5)$$

The application of remote sensing with respect to this model derives from the ability of different remotely measured optical indices to provide means of estimating different terms of the LUE model. Together, NDVI and PRI provide complementary information in the LUE model by providing a means of estimating the two main terms in the LUE model [61]. NDVI is sensitive to canopy ‘greenness’ and can be used to estimate the fraction of light absorbed by photosynthetic structures ( $f_{PAR}$ ) [81]. PRI is sensitive to processes relating to the thermal dissipation of light energy and can be used to estimate photosynthetic efficiency ( $\varepsilon$ ) [84]. Being a relatively new optical index, the specific role of CCI in the LUE model, and its responsiveness to evergreen and deciduous species, is still unclear. CCI has been shown to be sensitive to changes in pigmentation associated with photoprotection and thermal dissipation of light energy [45], indicating it may be representative of the efficiency ( $\varepsilon$ ) term of the model, similar to PRI. However, it may be more similar to SIF, which is sensitive to both the absorbed radiation and efficiency terms of the model, and potentially a more direct indicator of plant productivity (GPP) [45,61].

### 1.5 The Complementary Nature of Optical Indices

Recent reviews [61,85] have proposed that across ecosystems different functional types (optical types) have varying relationships to NDVI, PRI and GPP that are driven by contrasting structural, physiological, and environmental controls on plant productivity and optical properties. This proposed relationship has led to the development of the “complementarity hypothesis”, which outlines how the variation in optical signals across functional types may provide complementary information about photosynthetic phenology [61]. Accordingly, hypothetical relationships between individual optical indices and productivity have been proposed (Fig. 1.2).

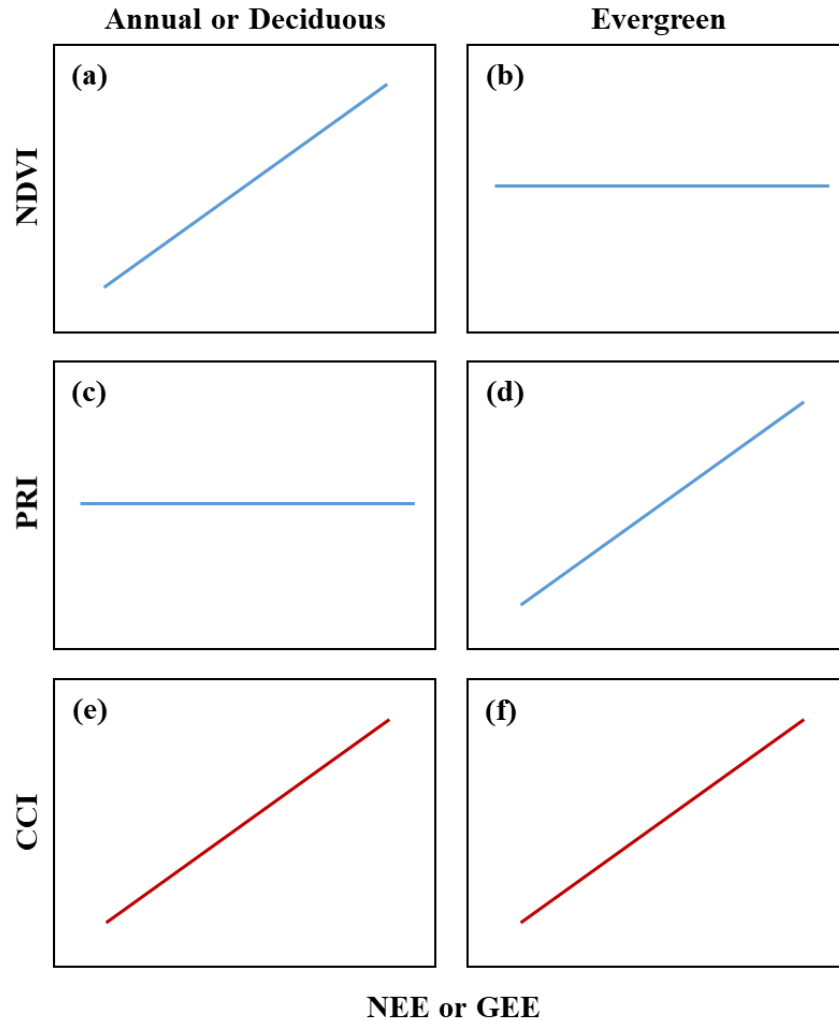


**Figure 1.2:** Hypothesized relationships between NDVI (a and b), PRI (c and d) and CCI (e and f) and productivity for annual or deciduous (left) or evergreen (right) vegetation. The hypothetical relationships between CCI and productivity are indicated in red to illustrate the current hypothesis of this thesis. More positive values indicate greater photosynthetic carbon uptake, given as Net Ecosystem Exchange (NEE) or Gross Ecosystem Exchange (GEE). Modified from Gamon 2015 [61].

In the case of deciduous vegetation, where photosynthesis is strongly driven by canopy structural changes relating to green leaf area and therefore green  $f_{PAR}$ , photosynthetic phenology and GPP should be highly detectable using NDVI (Fig. 1.2a). In evergreen vegetation, NDVI should not relate well to productivity, as there is little structural variation in evergreen vegetation over seasons (Fig. 1.2b). PRI should relate poorly to productivity in deciduous species (Fig. 1.2c) that have less

variation in efficiency ( $\epsilon$ ) than evergreens. On the other hand, PRI would strongly relate to productivity in evergreens (Fig. 1.2d), as changes in efficiency driven by seasonal changes in pigment pool size are readily detected by PRI [43,44,70].

Being recently defined, CCI had not been included in the original complementarity hypothesis. While it has been shown to be similar to PRI in relationship to identifying seasonal photosynthetic activity in evergreens [45], the broader spectral response of CCI may allow for detection of structural changes related to APAR in deciduous species. This would indicate that CCI may be a direct indicator of seasonal dynamics of GPP in both deciduous and evergreen vegetation (Fig. 1.2e,f). This would be similar to SIF, which may also be directly relatable to productivity in both functional types on seasonal time scales, as is also sensitive to both absorbed radiation (APAR), affected by canopy structure, and changes in photosynthetic efficiency [56]. This leads to the hypothesized positive CCI response to NEE for annuals, deciduous, and evergreen vegetation, as illustrated in Figure 1.2.

The boreal forest provides a unique opportunity to test the complementarity hypothesis as it is home to a varying mix of both evergreen and deciduous tree species having strong seasonal changes in photosynthetic activity. Based on the current understanding of the behaviour of optical indices in sampling different vegetation, relationships between some indices and productivity are relatively well known, while others require further testing.

## **1.6 Research Objectives**

Given the expectation for the boreal forest to undergo substantial change as our climate continues to shift [19], accurate methods of assessing changes in phenology of boreal trees over large spatial and temporal scales are necessary to fully understand how the boreal region will respond to changes in environmental conditions. The main purpose of this research is to explore the relationship between optical remote sensing and the phenology of boreal trees, and to evaluate the hypothetical relationships between different optical indices and seasonal changes in plant productivity as outlined in the complementarity hypothesis. Developing a stronger understanding of which optical parameters are most effective at tracking seasonal changes in photosynthetic activity, or photosynthetic phenology, in multiple functional and species types at large scales requires studies that provide a more mechanistic understanding of how these remote sensing metrics relate to plant physiology at smaller scales.

This project took place on the rooftop of the Biological Sciences Building at the University of Alberta, Canada (53.528861, -113.525972), where a total of six boreal tree species, three evergreens and three deciduous, were exposed to a seasonally changing boreal climate. This small-scale study provided the necessary setting to link remotely detected optical indices with actual plant photosynthetic activity and canopy phenology. The establishment of rooftop tree plots (Figure 1.3) allowed for remote and proximal physiological measurements to be performed concurrently and at relatively high temporal resolutions across seasons.



**Figure 1.3:** Synthetic plots of boreal tree species established on the rooftop of the Biological Sciences Building. Species sampled include trembling aspen (*Populus tremuloides* Michx.) and balsam poplar (*Populus balsamifera* L.) as broad-leaf species, and tamarack (*Larix laricina* (Du Roi) K. Koch), a deciduous conifer, and three evergreen species: black spruce (*Picea mariana* (Mill.) Britton, Sterns & Poggenb.), white spruce (*Picea glauca* (Moench) Voss), and jack pine (*Pinus banksiana* Lamb.). Image date: September 28, 2017.

The following data chapter examines the ability of remotely sensed optical indices to observe seasonal changes in photosynthetic activity, or photosynthetic phenology, of six boreal tree species. The remote sensing metrics included: the normalized difference vegetation index (NDVI), the photochemical reflectance index (PRI), the chlorophyll/carotenoid index (CCI). At the leaf scale, steady-state chlorophyll fluorescence ( $F_s$ ) was used to provide a measure of solar-induced fluorescence (SIF). Understanding the phenology of these metrics at proximal scales, using a plot-



level setting to represent an entire forest stand is a foundation for the proper interpretation and application of remote measurements of entire ecosystems through large-scale airborne or satellite platforms. The seasonal responses of these metrics were then compared to the seasonal changes in photosynthetic activity to directly test the expanded relationships put forth by the complementarity hypothesis. Specifically, the hypothesis predicted that NDVI and PRI would relate well to photosynthetic activity for deciduous and evergreen vegetation, respectively. Novel aspects of the study explored CCI and fluorescence as potential indicators of photosynthetic activity for evergreen and deciduous species. The following chapter demonstrates that optical indices and fluorescence can be effective indicators of photosynthetic phenology, illustrating that some indices showing parallel seasonal patterns to photosynthesis and to other remote sensing metrics, but with noticeable differences between metrics when sampling across species and functional types. This study provides crucial information about the link between different optical measurements and plant physiology that will inform future efforts to monitor the health and functioning of entire ecosystems as the biosphere responds to changing climatic conditions.

## 1.7 References

1. Pan, Y.; Birdsey, R. A.; Fang, J.; Houghton, R.; Kauppi, P. E.; Kurz, W. A.; Phillips, O. L.; Shvidenko, A.; Lewis, S. L.; Canadell, J. G. A Large and Persistent Carbon Sink in the World's Forests. *Science* 2011, 333, 988–993.
2. Dixon, R. K.; Browne, S.; Houghton, R. A.; Solomon, A. M.; Trexler, M. C.; Wosniewski, J. Carbon pools and flux of global forest ecosystems. *Science* 1994, 263, 185–190.
3. Sabine, C. L.; Heimann, M.; Artaxo, P.; Bakker, D. C. E.; Chen, C.-T. A.; Field, C. B.; Gruber, N.; Le Quéré, C.; Prinn, R. G.; Richey, J. E. Current status and past trends of the global carbon cycle. In *The Global Carbon Cycle: Integrating Humans, Climate, and the Natural World*; 2004; Vol. 62, pp. 17–44.
4. Goodale, C. L.; Apps, M. J.; Birdsey, R. A.; Field, C. B.; Heath, L. S.; Houghton, R. A.; Jenkins, J. C.; Kohlmaier, G. H.; Kurz, W.; Liu, S.; Nabuurs, G.; Nilsson, S.; Shvidenko, A. Z. Forest carbon sinks in the Northern Hemisphere. *Ecol. Appl.* 2002, 12, 891–899.
5. Serreze, M. C.; Barry, R. G. Processes and impacts of Arctic amplification: A research synthesis. *Glob. Planet. Change* 2011, 77, 85–96.
6. Winton, M. Amplified Arctic climate change: What does surface albedo feedback have to do with it? *Geophys. Res. Lett.* 2006, 33, 1–4.
7. GISTEMP Team GISS Surface Temperature Analysis (GISTEMP) <https://data.giss.nasa.gov/gistemp/> (accessed Sep 21, 2017).
8. Hansen, J.; Ruedy, R.; Sato, M.; Lo, K. Global surface temperature change. *Rev. Geophys.* 2010, 48, RG4004.
9. Bhatia, S.; Sharma, K. *Microenvironmentation in Micropropagation*; Elsevier Inc., 2015.
10. Walker, A. P.; Beckerman, A. P.; Gu, L.; Kattge, J.; Cernusak, L. A.; Domingues, T. F.; Scales, J. C.; Wohlfahrt, G.; Wullschleger, S. D.; Woodward, F. I. The relationship of leaf photosynthetic traits - V<sub>c</sub>max and J<sub>max</sub> - to leaf nitrogen, leaf phosphorus, and specific leaf area: A meta-analysis and modeling study. *Ecol. Evol.* 2014, 4, 3218–3235.

11. Kattge, J.; Knorr, W. Temperature acclimation in a biochemical model of photosynthesis: A reanalysis of data from 36 species. *Plant, Cell Environ.* 2007, 30, 1176–1190.
12. Lloyd, J. The CO<sub>2</sub> dependence of photosynthesis, plant growth responses to elevated CO<sub>2</sub> concentrations and their interaction with soil nutrient status, II. Temperate and boreal forest productivity and the combined effects of increasing CO<sub>2</sub> concentrations and increased nitrogen deposition at a global scale. *Funct. Ecol.* 1999, 13, 439–459.
13. Olson, J. S. Productivity of Forest Ecosystems. In *Productivity of World Ecosystems*; National Academy of Sciences: Washington, DC, 1975; pp. 33–43.
14. Estiarte, M.; Peñuelas, J. Alteration of the phenology of leaf senescence and fall in winter deciduous species by climate change: Effects on nutrient proficiency. *Glob. Chang. Biol.* 2015, 21, 1005–1017.
15. Hanes, J. M.; Richardson, A. D.; Klosterman, S. Mesic Temperate Deciduous Forest Phenology. In *Phenology: An Integrative Environmental Science*; Schwartz, M. D., Ed.; Springer, Dordrecht, 2013; pp. 211–224.
16. Richardson, A. D.; Keenan, T. F.; Migliavacca, M.; Ryu, Y.; Sonnentag, O.; Toomey, M. Climate change, phenology, and phenological control of vegetation feedbacks to the climate system. *Agric. For. Meteorol.* 2013, 169, 156–173.
17. Gordo, O.; Sanz, J. J. Long-term temporal changes of plant phenology in the Western Mediterranean. *Glob. Chang. Biol.* 2009, 15, 1930–1948.
18. Way, D. A.; Oren, R. Differential responses to changes in growth temperature between trees from different functional groups and biomes: a review and synthesis of data. *Tree Physiol.* 2010, 669–688.
19. Bonan, G. B. Forests and climate change: forcings, feedbacks, and the climate benefits of forests. *Science* 2008, 320, 1444–1449.
20. Bunn, A. G.; Goetz, S. J.; Kimball, J. S.; Zhang, K. Northern high-latitude ecosystems respond to climate change. *Eos, Trans. Am. Geophys. Union* 2007, 88, 333–335.

21. Goetz, S. J.; Bunn, A. G.; Fiske, G. J.; Houghton, R. A. Satellite-observed photosynthetic trends across boreal North America associated with climate and fire disturbance. *Proc. Natl. Acad. Sci. U. S. A.* 2005, 102, 13521–5.
22. de Jong, R.; Verbesselt, J.; Schaepman, M. E.; de Bruin, S. Trend changes in global greening and browning: Contribution of short-term trends to longer-term change. *Glob. Chang. Biol.* 2012, 18, 642–655.
23. Seidl, R.; Thom, D.; Kautz, M.; Martin-Benito, D.; Peltoniemi, M.; Vacchiano, G.; Wild, J.; Ascoli, D.; Petr, M.; Honkaniemi, J.; Lexer, M. J.; Trotsiuk, V.; Mairota, P.; Svoboda, M.; Fabrika, M.; Nagel, T. A.; Reyer, C. P. O. Forest disturbances under climate change. *Nat. Clim. Chang.* 2017, 7, 395–402.
24. Gustafson, E. J.; Shvidenko, A. Z.; Sturtevant, B. R.; Scheller, R. M. Predicting global change effects on forest biomass and composition in south-central Siberia. *Ecol. Appl.* 2010, 20, 700–715.
25. Black, T. A.; Gaumont-Guay, D.; Jassa, R. S.; D'Amico, B.; Jarvis, P. G.; Gower, S. T.; Kelliher, F. M.; Dunn, A. L.; Wofsy, S. C. Measurement of CO<sub>2</sub> exchange between boreal forest and the atmosphere. In *The Carbon Balance of Forest Biomes*; Griffith, H.; Jarvis, P., Eds.; Taylor & Francis Group: New York, NY, 2005; Vol. 57, pp. 151–186.
26. Tjoelker, M. G.; Oleksyn, J.; Reich, P. B. Seedlings of five boreal tree species differ in acclimation of photosynthesis to elevated CO<sub>2</sub> and temperature. *Tree Physiol.* 1998, 18, 715–726.
27. Soolanayakanahally, R. Y.; Guy, R. D.; Silim, S. N.; Drewes, E. C.; Schroeder, W. R. Enhanced assimilation rate and water use efficiency with latitude through increased photosynthetic capacity and internal conductance in balsam poplar (*Populus balsamifera* L.). *Plant, Cell Environ.* 2009, 32, 1821–1832.
28. Burns, R. M.; Honkala, B. H. *Silvics of North America: 1. Conifers*. Agricultural Handbook 654; 654th ed.; U.S. Department of Agriculture, Forest Service: Washington, DC, 1990.
29. Burns, R. M.; Honkala, B. H. *Silvics of North America: 2. Hardwoods*. Agriculture Handbook 654; U.S. Department of Agriculture, Forest Service: Washington, DC, 1990.

30. Barr, A.; Black, T. A.; McCaughey, H. Climatic and Phenological Controls of the Carbon and Energy Balances of Three Contrasting Boreal Forest Ecosystems in Western Canada. In *Phenology of Ecosystem Processes*; Noormets, A., Ed.; Springer: New York, NY, 2009; pp. 3–34.
31. Givnish, T. J. Adaptive significance of evergreen vs. deciduous leaves: Solving the triple paradox. *Silva Fenn.* 2002, 36, 703–743.
32. Bhatt, U. S.; Walker, D. A.; Reynolds, M. K.; Comiso, J. C.; Epstein, H. E.; Jia, G.; Gens, R.; Pinzon, J. E.; Tucker, C. J.; Tweedie, C. E.; Webber, P. J. Circumpolar Arctic tundra vegetation change is linked to sea ice decline. *Earth Interact.* 2010, 14.
33. Fischlin, A.; Midgley, G. F.; Price, J. T.; Leemans, R.; Gopal, B.; Turley, C.; Rounsevell, M. D. A.; Dube, O. P.; Tarazona, J.; Velichko, A. A. *Ecosystems, their properties, goods and services*; 2007; Vol. 48.
34. Swann, A. L.; Fung, I. Y.; Levis, S.; Bonan, G. B.; Doney, S. C. Changes in Arctic vegetation amplify high-latitude warming through the greenhouse effect. *Proc. Natl. Acad. Sci.* 2010, 107, 1295–1300.
35. MacDonald, G. M. Global warming and the Arctic: a new world beyond the reach of the Grinnellian niche? *J. Exp. Biol.* 2010, 213, 855–861.
36. NASA-ABOVE A Notional Airborne Science Research Strategy for NASA's Arctic Boreal Vulnerability Experiment (ABOVE); 2016.
37. Reich, P. B.; Ellsworth, D. S.; Walters, M. B. Leaf structure (specific leaf area) modulates photosynthesis – nitrogen relations: evidence from within and across species and functional groups. *Funct. Ecol.* 1998, 12, 948–958.
38. Van Ommen Kloeke, A. E. E.; Douma, J. C.; Ordoñez, J. C.; Reich, P. B.; Van Bodegom, P. M. Global quantification of contrasting leaf life span strategies for deciduous and evergreen species in response to environmental conditions. *Glob. Ecol. Biogeogr.* 2012, 21, 224–235.
39. Sánchez-Azofeifa, G. A.; Castro, K.; Wright, S. J.; Gamon, J.; Kalacska, M.; Rivard, B.; Schnitzer, S. A.; Feng, J. L. Differences in leaf traits, leaf internal structure, and spectral reflectance between two communities of lianas and trees: Implications for remote sensing in tropical environments. *Remote Sens. Environ.* 2009, 113, 2076–2088.

40. Gower, S. T.; Richards, J. H. Larches: Deciduous Conifers in an Evergreen World carbon gain similar to evergreens. *Bioscience* 1990, 40, 818–826.
41. Ottander, C.; Campbell, D.; Öquist, G. Seasonal changes in photosystem II organisation and pigment composition in *Pinus sylvestris*. *Planta* 1995, 197, 176–183.
42. Öquist, G.; Huner, N. P. A. Photosynthesis of Overwintering Plants. *Annu. Rev. Plant Biol.* 2003, 54, 329–355.
43. Wong, C. Y. S.; Gamon, J. A. Three causes of variation in the photochemical reflectance index (PRI) in evergreen conifers. *New Phytol.* 2015, 206, 187–195.
44. Wong, C. Y. S.; Gamon, J. A. The photochemical reflectance index provides an optical indicator of spring photosynthetic activation in evergreen conifers. *New Phytol.* 2015, 206, 196–208.
45. Gamon, J. A.; Huemmrich, K. F.; Wong, C. Y. S.; Ensminger, I.; Garrity, S.; Hollinger, D. Y.; Noormets, A.; Peñuelas, J. A remotely sensed pigment index reveals photosynthetic phenology in evergreen conifers. *Proc. Natl. Acad. Sci. U. S. A.* 2016, 113, 13087–13092.
46. Rohde, A.; Bhalerao, R. P. Plant dormancy in the perennial context. *Trends Plant Sci.* 2007, 12, 217–223.
47. Havranek, W. M.; Tranquillini, W. Physiological Processes during Winter Dormancy and Their Ecological Significance. In *Ecophysiology of Coniferous Forests*; ACADEMIC PRESS, INC., 1995; pp. 95–124.
48. D’Odorico, P.; Gonsamo, A.; Gough, C. M.; Bohrer, G.; Morison, J.; Wilkinson, M.; Hanson, P. J.; Gianelle, D.; Fuentes, J. D.; Buchmann, N. The match and mismatch between photosynthesis and land surface phenology of deciduous forests. *Agric. For. Meteorol.* 2015, 214–215, 25–38.
49. Hörtensteiner, S. Chlorophyll Degradation During Senescence. *Annu. Rev. Plant Biol.* 2006, 57, 55–77.
50. Thakur, N.; Sharma, V.; Kishore, K. Leaf senescence: an overview. *Indian J. Plant Physiol.* 2016, 21, 225–238.

51. Wilson, K. B.; Baldocchi, D. D.; Hanson, P. J. Leaf age affects the seasonal pattern of photosynthetic capacity and net ecosystem exchange of carbon in a deciduous forest. *Plant, Cell Environ.* 2001, 24, 571–583.
52. Ensminger, I.; Sveshnikov, D.; Campbell, D. A.; Funk, C.; Jansson, S.; Lloyd, J.; Shibistova, O.; Öquist, G. Intermittent low temperatures constrain spring recovery of photosynthesis in boreal Scots pine forests. *Glob. Chang. Biol.* 2004, 10, 995–1008.
53. Demmig-Adams, B.; Adams, W. W. The role of xanthophyll cycle carotenoids in the protection of photosynthesis. *Trends Plant Sci.* 1996, 1, 21–26.
54. Adams, W. W.; Demmig-Adams, B.; Rosenstiel, T. N.; Brightwell, A. K.; Ebbert, V. Photosynthesis and Photoprotection in Overwintering Plants. *Plant Biol.* 2002, 4, 545–557.
55. Adams, W. W.; Demmig-Adams, B. Carotenoid composition and down-regulation of photosystem II in three conifer species during the winter. *Physiol. Plant.* 1994, 92, 451–458.
56. Porcar-Castell, A.; Tyystjärvi, E.; Atherton, J.; Van Der Tol, C.; Flexas, J.; Pfündel, E. E.; Moreno, J.; Frankenberg, C.; Berry, J. A. Linking chlorophyll a fluorescence to photosynthesis for remote sensing applications: Mechanisms and challenges. *J. Exp. Bot.* 2014, 65, 4065–4095.
57. Maxwell, K.; Johnson, G. N. Chlorophyll fluorescence - a practical guide. *J. Exp. Bot.* 2000, 51, 659–668.
58. Joiner, J.; Yoshida, Y.; Vasilkov, A. P.; Schaefer, K.; Jung, M.; Guanter, L.; Zhang, Y.; Garrity, S.; Middleton, E. M.; Huemmrich, K. F.; Gu, L.; Belelli Marchesini, L. The seasonal cycle of satellite chlorophyll fluorescence observations and its relationship to vegetation phenology and ecosystem atmosphere carbon exchange. *Remote Sens. Environ.* 2014, 152, 375–391.
59. Jones, H. G. *Plants and Microclimate: A Quantitative Approach to Environmental Plant Physiology*; 3rd ed.; Cambridge University Press: Cambridge, United Kingdom, 2014.
60. Demmig, B.; Winter, K.; Krüger, A.; Czygan, F. C. Photoinhibition and zeaxanthin formation in intact leaves: a possible role of the xanthophyll cycle in the dissipation of excess light energy. *Plant Physiol.* 1987, 84, 218–224.

61. Gamon, J. A. Reviews and Syntheses: Optical sampling of the flux tower footprint. *Biogeosciences* 2015, 12, 4509–4523.
62. Running, S. W.; Nemani, R. R.; Heinsch, F. A.; Zhao, M.; Reeves, M.; Hashimoto, H. A Continuous Satellite-Derived Measure of Global Terrestrial Primary Production. *Bioscience* 2004, 54, 547.
63. Balzarolo, M.; Vescovo, L.; Hammerle, A.; Gianelle, D.; Papale, D.; Tomelleri, E.; Wohlfahrt, G. On the relationship between ecosystem-scale hyperspectral reflectance and CO<sub>2</sub> exchange in European mountain grasslands. *Biogeosciences* 2015, 12, 3089–3108.
64. Gamon, J. A.; Cheng, Y.; Claudio, H.; MacKinney, L.; Sims, D. A. A mobile tram system for systematic sampling of ecosystem optical properties. *Remote Sens. Environ.* 2006, 103, 246–254.
65. Balzarolo, M.; Vicca, S.; Nguy-Robertson, A. L.; Bonal, D.; Elbers, J. A.; Fu, Y. H.; Grünwald, T.; Horemans, J. A.; Papale, D.; Peñuelas, J.; Suyker, A.; Veroustraete, F. Matching the phenology of Net Ecosystem Exchange and vegetation indices estimated with MODIS and FLUXNET in-situ observations. *Remote Sens. Environ.* 2016, 174, 290–300.
66. Tucker, C. J.; Townshend, J. R. G.; Goff, T. E. African land-cover classification using satellite data. *Science* 1985, 227, 369–75.
67. Sims, D. A.; Luo, H.; Hastings, S.; Oechel, W. C.; Rahman, A. F.; Gamon, J. A. Parallel adjustments in vegetation greenness and ecosystem CO<sub>2</sub> exchange in response to drought in a Southern California chaparral ecosystem. *Remote Sens. Environ.* 2006, 103, 289–303.
68. Park, T.; Ganguly, S.; Tømmervik, H.; Euskirchen, E. S.; Høgda, K.; Karlsen, S. R.; Brovkin, V.; Nemani, R. R.; Myneni, R. B. Changes in growing season duration and productivity of northern vegetation inferred from long-term remote sensing data. *Environ. Res. Lett.* 2016, 11, 84001.
69. Gamon, J. A.; Field, C. B.; Goulden, M. L.; Griffin, K. L.; Hartley, A. E.; Joel, G.; Peñuelas, J.; Valentini, R. Relationships Between NDVI, Canopy Structure, and Photosynthesis in Three Californian Vegetation Types. *Ecol. Appl.* 1995, 5, 28–41.
70. Gamon, J. A.; Kovalchuck, O.; Wong, C. Y. S.; Harris, A.; Garrity, S. R. Monitoring seasonal and diurnal changes in photosynthetic pigments with automated PRI and NDVI sensors. *Biogeosciences* 2015, 12, 4149–4159.



71. Jönsson, A. M.; Eklundh, L.; Hellström, M.; Barring, L.; Jönsson, P. Annual changes in MODIS vegetation indices of Swedish coniferous forests in relation to snow dynamics and tree phenology. *Remote Sens. Environ.* 2010, 114, 2719–2730.
72. Gamon, J. A.; Peñuelas, J.; Field, C. B. A Narrow-Waveband Spectral Index That Tracks Diurnal Changes in Photosynthetic Efficiency. *Remote Sens. Environ.* 1992, 44, 35–44.
73. Gamon, J. A.; Serrano, L.; Surfus, J. S. The photochemical reflectance index: an optical indicator of photosynthetic radiation use efficiency across species, functional types, and nutrient levels. *Oecologia* 1997, 112, 492–501.
74. Gamon, J. A.; Berry, J. A. Facultative and constitutive pigment effects on the Photochemical Reflectance Index (PRI) in sun and shade conifer needles. *Isr. J. Plant Sci.* 2012, 60, 85–95.
75. Garbulsky, M. F.; Peñuelas, J.; Ogaya, R.; Filella, I. Leaf and stand-level carbon uptake of a Mediterranean forest estimated using the satellite-derived reflectance indices EVI and PRI. *Int. J. Remote Sens.* 2013, 34, 1282–1296.
76. Goerner, A.; Reichstein, M.; Rambal, S. Tracking seasonal drought effects on ecosystem light use efficiency with satellite-based PRI in a Mediterranean forest. *Remote Sens. Environ.* 2009, 113, 1101–1111.
77. Baker, N. R.; Rosenqvist, E. Applications of chlorophyll fluorescence can improve crop production strategies: An examination of future possibilities. *J. Exp. Bot.* 2004, 55, 1607–1621.
78. Meroni, M.; Rossini, M.; Guanter, L.; Alonso, L.; Rascher, U.; Colombo, R.; Moreno, J. Remote sensing of solar-induced chlorophyll fluorescence: Review of methods and applications. *Remote Sens. Environ.* 2009, 113, 2037–2051.
79. Frankenberg, C.; Fisher, J. B.; Worden, J.; Badgley, G.; Saatchi, S. S.; Lee, J. E.; Toon, G. C.; Butz, A.; Jung, M.; Kuze, A.; Yokota, T. New global observations of the terrestrial carbon cycle from GOSAT: Patterns of plant fluorescence with gross primary productivity. *Geophys. Res. Lett.* 2011, 38, 1–6.
80. Walther, S.; Voigt, M.; Thum, T.; Gonsamo, A.; Zhang, Y.; Köhler, P.; Jung, M.; Varlagin, A.; Guanter, L. Satellite chlorophyll fluorescence measurements reveal large-scale decoupling of

photosynthesis and greenness dynamics in boreal evergreen forests. *Glob. Chang. Biol.* 2016, 22, 2979–2996.

81. Monteith, J. L. Climate and the efficiency of crop production in Britain. *Phil. Trans. R. Soc. Lond. B* 1977, 281, 277–294.

82. Gamon, J. A.; Qiu, H.-L. Ecological applications of remote sensing at multiple scales. In *Handbook of Functional Plant Ecology*; Pugnaire, F. I.; Valladares, F., Eds.; Marcel Dekker, Inc.: New York, USA, 1999; pp. 805–846.

83. Heinsch, F. A.; Zhao, M.; Running, S. W.; Kimball, J. S.; Nemani, R. R.; Davis, K. J.; Bolstad, P. V.; Cook, B. D.; Desai, A. R.; Ricciuto, D. M.; Law, B. E.; Oechel, W. C.; Kwon, H.; Luo, H.; Wofsy, S. C.; Dunn, A. L.; Munger, J. W.; Baldocchi, D. D.; Xu, L.; Hollinger, D. Y.; Richardson, A. D.; Stoy, P. C.; Siqueira, M. B. S.; Monson, R. K.; Burns, S. P.; Flanagan, L. B. Evaluation of remote sensing based terrestrial productivity from MODIS using regional tower eddy flux network observations. *IEEE Trans. Geosci. Remote Sens.* 2006, 44, 1908–1923.

84. Gamon, J. A.; Field, C. B.; Fredeen, A. L.; Thayer, S. Assessing photosynthetic downregulation in sunflower stands with an optically-based model. *Photosynth. Res.* 2001, 67, 113–25.

85. Garbulsky, M. F.; Peñuelas, J.; Gamon, J.; Inoue, Y.; Filella, I. The photochemical reflectance index (PRI) and the remote sensing of leaf, canopy and ecosystem radiation use efficiencies. A review and meta-analysis. *Remote Sens. Environ.* 2011, 115, 281–297.

## **Chapter 2: Parallel Seasonal Patterns of Photosynthesis, Fluorescence, and Reflectance Indices in Boreal Trees**

### **Abstract**

Tree species in the boreal forest cycle between periods of active growth and dormancy and alter their photosynthetic processes in response to changing environmental conditions. For deciduous species, these changes are readily visible, while evergreen species have subtler foliar changes during seasonal transitions. In this study, we used remotely sensed optical indices to observe seasonal changes in photosynthetic activity, or photosynthetic phenology, of six boreal tree species. We evaluated the normalized difference vegetation index (NDVI), the photochemical reflectance index (PRI), the chlorophyll/carotenoid index (CCI), and steady-state chlorophyll fluorescence ( $F_s$ ) as a measure of solar-induced fluorescence (SIF), and compared these optical metrics to gas exchange to determine their efficacy in detecting seasonal changes in plant photosynthetic activity. The NDVI and PRI exhibited complementary responses. The NDVI paralleled photosynthetic phenology in deciduous species, but less so evergreens. The PRI closely paralleled photosynthetic activity in evergreens, but less so in deciduous species. The CCI and  $F_s$  tracked photosynthetic phenology in both deciduous and evergreen species. The seasonal patterns of optical metrics and photosynthetic activity revealed subtle differences across and within functional types. With the CCI and fluorescence becoming available from satellite sensors, they offer new opportunities for assessing photosynthetic phenology, particularly for evergreen species, which have been difficult to assess with previous methods.

### **2.1 Introduction**

Forests cover approximately 4 billion hectares of the earth's land surface [1]; the circumpolar boreal forest accounts for approximately one-quarter (1132 million hectares) of that total [2]. The boreal region, known to be a substantial store of carbon [3], is experiencing a significant change in climate. The combined effects of increasing atmospheric carbon dioxide ( $CO_2$ ) levels and increasing temperatures associated with climate change will impact a number of plant processes [4], and these effects are amplified at higher latitudes. These changes in climate are expected to impact growing-season length, and directly influence phenology by altering the timing of seasonal transitions that are defined by changing temperatures and photoperiod [5].

In boreal forests, tree species cycle between periods of active growth and dormancy in response to a changing temperature and day-length [5]. Different boreal species utilize contrasting mechanisms to deal with extreme seasonal variation. For deciduous species, the onset of dormancy is easily observed by changing of leaf coloring and leaf senescence, while spring activation is marked by budburst and greening of canopies. Evergreens, however, have subtler changes in foliage during seasonal transitions. To maintain their leaves going into dormancy and to avoid winter damage, needles undergo a cold-hardening [6], which involves the adjustment of leaf pigments pools, primarily carotenoids and chlorophylls, in order to protect the photosynthetic systems and dissipate excess light energy during dormancy. These adjustments are then reversed leading into the growing season [7].

In addition to these seasonal changes, plants regulate photosynthetic processes in response to changing environmental conditions on shorter timescales. Under favorable conditions, light absorbed by chlorophyll is used to drive photosynthesis through photochemistry [8]. Under stress, plants have several mechanisms to dissipate excess light energy in the form of heat, known as non-photochemical quenching (NPQ) [9]. One method of dissipation is through the xanthophyll cycle, the interconversion of three carotenoid pigments to distribute absorbed light energy between productive photochemistry and non-destructive energy dissipation [9]. Plants also dissipate excess energy by emitting a small fraction of absorbed light through emission as chlorophyll fluorescence at longer wavelengths than those which were absorbed [8]. Fluorescence is driven by the amount of absorbed photosynthetically active radiation (APAR), but is also modified by NPQ [10].

Chlorophyll fluorescence acts rapidly, dissipating energy within nanoseconds in response to changing light, and adjusting to steady-state levels over minutes [11], whereas the xanthophyll cycle acts on timescales from minutes to hours [12]. Pigment pool sizes and foliage structure adjust on longer timescales, from hours to seasons [13–15]. Together, these mechanisms of energy regulation provide several possible ways of assessing changing photosynthetic activity through optical remote sensing.

The normalized difference vegetation index (NDVI) is often used to track changing vegetation “greenness” as a surrogate for photosynthetic activity, and has been shown to track long-term changes in growing-season length and productivity in high latitudes [16]. In deciduous vegetation, the NDVI tracks seasonal phenology of green biomass, from budburst to senescence [17]. The

NDVI utilizes reflectance in red and near-infrared wavelengths to estimate the fraction of photosynthetically active radiation ( $f_{PAR}$ ) that is absorbed by green plant material [18]. Though the NDVI can detect structural changes, such as the leaf area index and  $f_{PAR}$  [17,18], it misses less visible changes in physiological processes controlling photosynthetic activity, particularly in evergreen species [15,19] that see little change in greenness from spring budburst through the growing season and into winter dormancy [20].

The photochemical reflectance index (PRI), on the other hand, detects subtle changes in regulatory processes related to photosynthetic activity [21]. The PRI can detect pigment responses to environmental cues, primarily in evergreen species, that the NDVI can miss [13]. Over diurnal time-scales, PRI responses are driven by changes in the xanthophyll cycle, a facultative response, while responses over seasonal timescales reflect changes in pigment pool size (carotenoid/chlorophyll ratios), a constitutive response [22]. This index evaluates reflectance in the 531 nm waveband in comparison to 570 nm as a reference waveband [23]. A variety of other wavebands have been used to calculate the PRI. Some sensors provide the PRI using the 532 nm instead of the 531 nm waveband; this formulation is functionally similar to the PRI calculated using the original 531 nm waveband, and detects both facultative and constitutive responses depending upon the sampling period [19]. On the other hand, a number of studies report other PRI formulas using different reference wavebands (e.g., Moderate Resolution Imaging Spectroradiometer PRI: MODIS PRI) [24,25], which primarily detect pigment pool size variation when applied over seasonal timescales or across canopies [19]. Thus, the proper interpretation of the PRI can depend upon the formula and sampling scale used.

The chlorophyll/carotenoid index (CCI) provides another indicator of photosynthetic activity, particularly in evergreens. Like the PRI, this index is sensitive to changes in pigment pools at both stand- and leaf-levels, and can accurately track seasonally changing chlorophyll/carotenoid levels indicating an important role of carotenoid pigments in winter downregulation [15]. The CCI can be derived from NASA's satellite-based MODIS sensor using bands 1 (645 nm, a terrestrial band) and 11 (531 nm, an ocean band), allowing for evaluation of terrestrial vegetation across large spatial scales. Unlike the xanthophyll cycle, which affects a narrow waveband, pigment pool size changes detectable with the CCI have a broad spectral response [15]. While the CCI has been

shown to be a potent index capable of quantifying of seasonal photosynthetic activity at leaf- and canopy-scales for evergreens [15], similar studies on deciduous species have not yet been reported.

Chlorophyll fluorescence can also provide information on photosynthetic performance [26], and can reflect changing photosynthetic activity driven by both internal and external factors. Chlorophyll fluorescence has often been measured using the pulse-amplitude modulation (PAM) technique, which is restricted to the leaf-level due to the requirement of a saturating pulse [10]. With high resolution spectrometers that can resolve atmospheric absorption bands (Fraunhofer lines), fluorescence can now be passively detected from a distance as a small signal present in the “gaps” of the solar spectrum [27]. This solar-induced fluorescence (SIF) is closely linked to gross primary productivity (GPP) [28–30], however, the coarse spatial and temporal scales of many satellite-based SIF measurements cannot resolve detailed seasonal dynamics or explain underlying mechanisms driving changes in GPP. At leaf-scales, the PAM method can measure steady-state chlorophyll fluorescence ( $F_s$ ) without delivering a saturating pulse of light, which is an analogous measurement to SIF measured at large scales, as both can be measured under ambient light, allowing for more mechanistic studies of individual leaves and canopies.

Together, the NDVI and PRI can provide complementary information in estimating the two main terms in the light-use efficiency (LUE) model [31] (Fig. 2.1). This model expresses GPP as a function of APAR, and the efficiency ( $\epsilon$ ) of converting absorbed radiation into fixed carbon [18,32]. APAR is the product of photosynthetically active radiation (PAR) or photosynthetic photon flux density (PPFD) and the fraction of PAR that is absorbed for photosynthesis ( $f_{PAR}$ ). The NDVI can be used to estimate light absorption as  $f_{PAR}$  [32], whereas the PRI can be used to estimate efficiency ( $\epsilon$ ) [33]. The precise role of the CCI in the LUE model is still unclear, although it is similar to the PRI in that it is sensitive to changing pigment pool size [15]. Like SIF, the CCI may be sensitive to both APAR and efficiency ( $\epsilon$ ), and is therefore a direct indicator of GPP [15,31].

Recent reviews [31,34] have proposed that different vegetation, or optical types, have contrasting structural and physiological controls influencing productivity and optical signatures, which leads to varying relationships between GPP and optical indices such as the NDVI and PRI across ecosystems; we describe this as the “complementarity hypothesis”. Accordingly, photosynthetic phenology of deciduous vegetation should relate to  $f_{PAR}$ , and be strongly detectable by the NDVI, whereas the NDVI of evergreens, with little temporal variation in  $f_{PAR}$ , should relate poorly to

primary productivity. Conversely, deciduous vegetation should have little seasonal variation in  $\epsilon$  detectable by the PRI, whereas changes in  $\epsilon$  in evergreens should be largely driven by changing pigment pool sizes [13,14,19], leading to strong relationships between the PRI and primary productivity. As a newly defined index, the CCI has not previously been considered in the complementarity hypothesis [15]. We predict that, on seasonal timescales, the CCI will be similar to SIF, sensitive to both canopy structure influencing absorbed radiation (APAR) and photosynthetic downregulation [10]. Both metrics should be indicators of GPP in both deciduous and evergreen vegetation (Fig. 2.1).

$$\begin{array}{ccc}
 \text{SIF, CCI?} & \text{NDVI} & \text{PRI} \\
 \swarrow & \downarrow & \swarrow \\
 \mathbf{GPP = (f_{PAR} \times PAR) \times \epsilon}
 \end{array}$$

**Figure 2.1:** Representation of the light-use efficiency (LUE) model in black, stating that gross primary productivity (GPP) is a function of absorbed photosynthetically active radiation (APAR:  $f_{PAR} \times PAR$ ) and efficiency ( $\epsilon$ ). Red text shows optical measurements useful for model parameterization and validation, including solar-induced fluorescence (SIF), the chlorophyll/carotenoid index (CCI), the normalized difference vegetation index (NDVI), and the photochemical reflectance index (PRI) (modified from Gamon 2015) [31].

Further understanding of the mechanisms underlying reflectance indices and fluorescence in different functional types and natural environments is essential to the proposed FLuorescence EXplorer (FLEX) mission, which will enable both reflectance indices and SIF to assess photosynthetic phenology from satellites [35]. This mission will provide insight into ecosystem phenology and productivity beyond that of satellite missions providing reflectance (MODIS) or SIF (e.g. Orbiting Carbon Observatory-2: OCO-2) by allowing concurrent measurements of reflectance indices and SIF at finer scales. In support of this mission, ground-based studies are needed to clarify the utility of both reflectance indices and fluorescence as indicators of photosynthesis for different functional types.

The goals of this study were to evaluate the efficacy of reflectance indices (NDVI, PRI, and CCI) and fluorescence ( $F_s$ ) in tracking photosynthetic phenology, by comparing the responses of these metrics in boreal trees that undergo large seasonal swings in photosynthetic activity. This study also evaluated the complementarity hypothesis by considering the efficacy of these metrics in

estimating photosynthetic activity in evergreen and deciduous species. This study demonstrates that reflectance indices and fluorescence can be used to as indicators of photosynthetic phenology, showing seasonal patterns that parallel photosynthetic activity, but with noticeable differences across and within different functional types.

## **2.2 Materials and Methods**

Six different tree species were grown on the south-facing rooftop of the Biological Sciences Building at the University of Alberta, Canada (53.528861, -113.525972). Adjacent to the southern edge of the boreal forest, the study location was exposed to seasonal weather conditions similar to the boreal region. The trees used for this study included three winter deciduous species—trembling aspen (*Populus tremuloides*) and balsam poplar (*Populus balsamifera*), two broad-leaf species, and tamarack (*Larix laricina*), a deciduous conifer—and three evergreen species: black spruce (*Picea mariana*) white spruce (*Picea glauca*), and jack pine (*Pinus banksiana*) (Fig. 2.2). In the spring of 2015, trees were planted in deep pots and arranged in monocultural plots. Due to limitations of space and time, this study had an unreplicated design at the species level.

### **2.2.1 Plant Culture**

Trees were supplied by Tree Time Services Inc. (Edmonton, AB, CAN) and were initially grown from seed sourced from Alberta-based suppliers at Tree Times' nursery located in Smoky Lake, AB. The trees were potted in 2.83 L pots (TP414, Stuewe & Sons, Tangent, OR, USA) in the spring of 2015. One-year-old seedlings of each species, except white spruce seedlings, which were 2 years old, were planted in a mixture of 3:1 potting soil (Sunshine Mix 4, Sun Gro Horticulture, Agawam, MA, USA) and topsoil. The mix was supplemented with a slow-release fertilizer (Nutricote 14-14-14, Sun Gro Horticulture, Agawam, MA, USA), at ca. 150 grams per 60 liters of soil. To help the trees overwinter in the first year, plants were placed in 1.2 m × 1.2 m plywood frames. The trees were repotted into 6.23 L pots (TP616, Stuewe & Sons, Tangent, OR, USA) in April 2016, to allow for adequate moisture and nutrient availability, avoid potential root restriction, and provide greater spacing of the plants. To provide insulation during the winter and better emulate non-container conditions, the tree-pots were surrounded by small pots of peat. During the 2015 growing season, the trees were watered daily and fertilized periodically with a 400 ppm mixture of 20-20-20 fertilizer. In June 2016, the plants were fertilized with a 200 ppm mixture of 20-20-20 fertilizer to provide additional nutrients for the growing season.



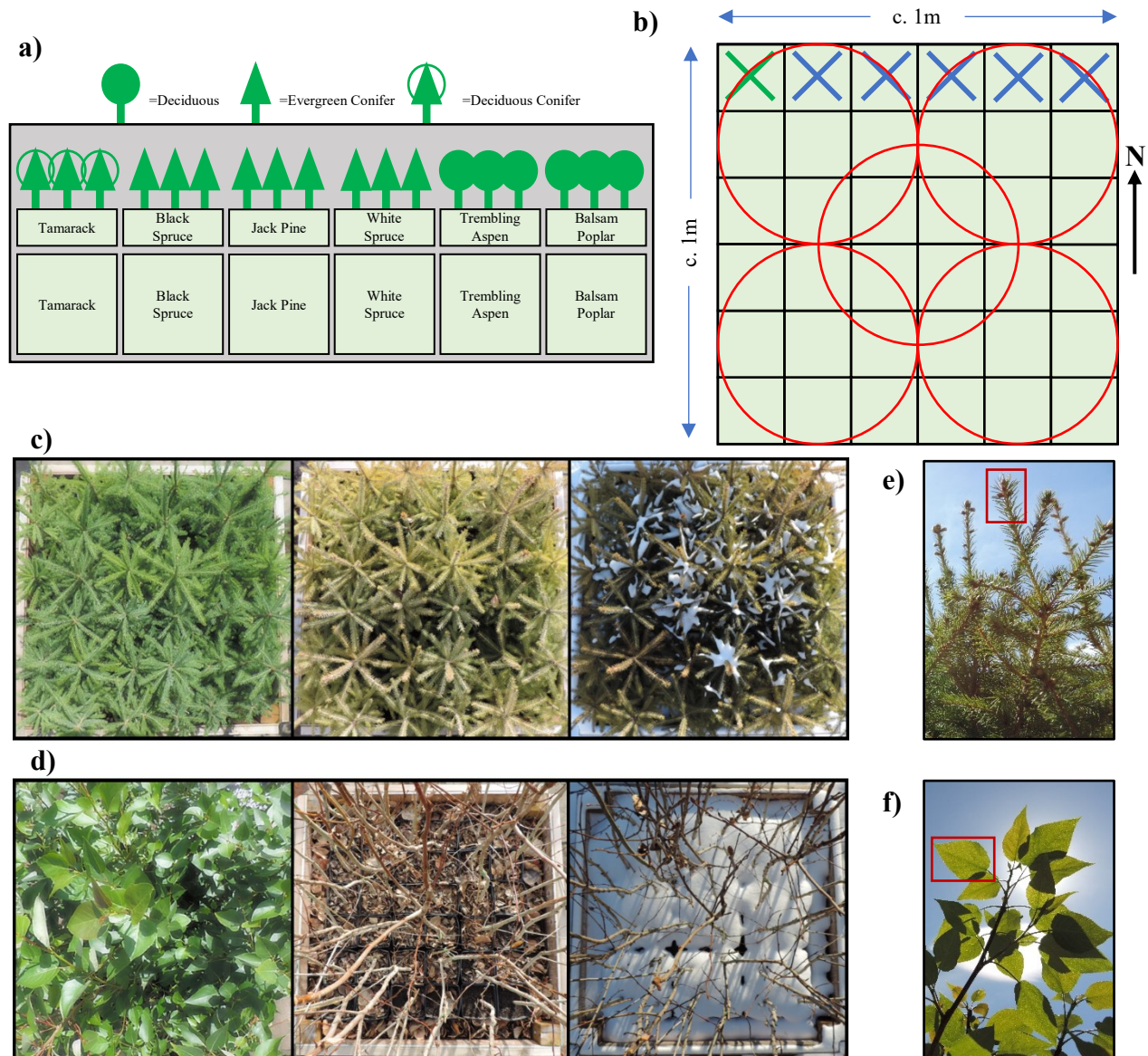


**Figure 2.2:** Depiction of experimental set-up on the rooftop of the Biological Sciences Building at the University of Alberta, illustrating the monocultural plots established on the rooftop (a), the arrangement of plants, approximate regions within each plot sampled for canopy reflectance (red), and plants sampled for gas exchange (blue) and fluorescence (blue and green) in each plot (b), representative entire canopies during the growing season (June 2016), winter (December 2016), and following snowfall in the winter (January 2017) of evergreen (c) and deciduous (d) species, and representative mature, sun-lit branchlets from evergreen plants (e) and leaves from deciduous plants (f) near the tops of trees that were used for measuring gas exchange and leaf area (branchlets and leaves indicated in red). For gas exchange sampling, plants on the northern edge of the plot were sampled to avoid interference with measurements of canopy optical signals. For canopy reflectance, the same regions of the plot were sampled throughout the study. For leaf-level measurements (gas exchange and fluorescence), the same plants were used throughout the study; for evergreens, the same branchlets were used for gas exchange and leaf area measurements.

### **2.2.2 Data Collection**

Data were collected from December 2015 to January 2017, covering a full yearly growth cycle. For each species, one monocultural plot composed of 36 plants (ca. 1 m x 1 m) was established for sampling (Fig. 2.2b). Photosynthetic rate, canopy reflectance, and steady-state fluorescence measurements were taken approximately every 2 weeks (weather permitting) between 12:30 and 14:30 UTC-06 (within ~1 h of solar noon); to ensure maximal sunlight and reduce potential cloud-cover impacts, data were collected on mostly sunny days. When all data could not be collected on a single day, due to the small window for sampling around solar noon, sampling occurred on sequential days under near-identical conditions. See supplemental Table S1 for a summary of measurements performed.

### **2.2.3 Environmental Conditions**

An automated weather station provided air temperature (S-THB-M002, Onset, Bourne, MA, USA) and PPFD (S-LIA-M003, Onset, Bourne, MA, USA) data, collected every minute on a data logger (U30-NRC, Onset, Bourne, MA, USA). Temperature and PPFD were aggregated into 15 min averages. PPFD was expressed as midday averages (13:00–14:00; UTC–06) and temperature was expressed as daily averages. Daily average temperature expressed as 30-year climate normals (1981–2010) by month were obtained from the Edmonton City Centre A Climate Normals Station (Climate ID 301228) [36].

### **2.2.4 Canopy Reflectance and Optical Indices**

Canopy-level reflectance measurements were collected using a dual-detector field spectrometer (UniSpec-DC; PP Systems, Amesbury, MA, USA) equipped with two fibre-optics. A downward-looking fibre (UNI684; PP Systems), fitted with a field-of-view restrictor (UNI688; PP Systems) to limit the field of view to ca. 15°, measured target reflectance, while an upward-facing fibre (UNI686; PP Systems), attached to a cosine receptor (UNI435; PP Systems), detected incoming irradiance. Five measurements were taken at different locations above each monoculture and mixed plot (center, NW, NE, SW, and SE) approximately 1 m above the top of the canopy (Fig. 2.2b). These replicate measurements were performed to account for spatial heterogeneity in the canopy.

Canopy reflectance was calculated by referencing the downward-looking target radiance ( $R_t$ ) spectrum to the upward-looking irradiance ( $I_t$ ) spectrum. This ratio was corrected to reflectance

( $\rho_\lambda$ ), by means of a cross-calibration procedure using  $I_\lambda$  and  $R_\lambda$  measurements ( $R_{panel_\lambda}$ ) from a standard reference panel (Spectralon, LabSphere, North Sutton, NH, USA) under the same conditions, immediately prior to and following sampling (Eq. 1) [37].

$$\rho_\lambda = \frac{R_{target_\lambda}}{I_\lambda} \times \frac{I_\lambda}{R_{panel_\lambda}} \quad (1)$$

Optical indices were then calculated using the canopy reflectance ( $\rho_\lambda$ ) from each measurement. Index values were calculated utilizing 630 and 800 nm for the NDVI (Eq. 2), 532 and 570 nm for the PRI (Eq. 3), and 532 and 630 nm for the CCI (Eq. 4). The CCI was originally calculated using reflectance in MODIS bands 1 (650 nm, a terrestrial band) and 11 (530 nm, an ocean band) [15]. For this experiment, the CCI was calculated using reflectance in the 532 and 630 nm wavebands (Eq. 4).

$$NDVI = \frac{\rho_{800nm} - \rho_{630nm}}{\rho_{800nm} + \rho_{630nm}} \quad (2)$$

$$PRI = \frac{\rho_{532nm} - \rho_{570nm}}{\rho_{532nm} + \rho_{570nm}} \quad (3)$$

$$CCI = \frac{\rho_{532nm} - \rho_{630nm}}{\rho_{532nm} + \rho_{630nm}} \quad (4)$$

Each optical index was averaged for all five canopy reflectance measurements, creating a single average canopy value for each sampling data.

### 2.2.5 Gas Exchange

Photosynthetic rate, expressed as net CO<sub>2</sub> assimilation, was measured using a portable gas exchange system (LI-6400; LI-COR, Lincoln, NE, USA). Leaves, or bundles of leaves in the case of conifers, were placed inside a 6 cm<sup>2</sup> leaf gas exchange chamber (6400-02B, LI-COR, Lincoln, NE, USA). The chamber monitored CO<sub>2</sub> assimilation rates under 1500  $\mu\text{mol photons m}^{-2} \text{s}^{-1}$  to determine light-saturated photosynthetic rate ( $\mu\text{mol CO}_2 \text{ m}^{-2} \text{s}^{-1}$ ) [14]; light-saturated photosynthetic rate was confirmed through light-response curves that were performed on each species in July 2016 (supplemental Figure S1). The reference CO<sub>2</sub> was set to 400  $\mu\text{mol mol}^{-1}$  to match atmospheric concentrations. The chamber air flow was set to 400  $\mu\text{mol s}^{-1}$ , with temperature and humidity set to match ambient conditions. Following a 1–3 min acclimation period after the leaf-clip was set on a plant, five consecutive measurements were taken from a single branch or

leaf on each plant from a total of five plants of each species. Technical replicates from individual branches or leaves were sampled to account for temporal variability in photosynthesis when sampling each plant and were averaged to yield a single plant-level measurement. The photosynthetic rate of each species at the plot level was determined by averaging the measurements from all individuals of a given species at a single sampling interval, creating a single average midday photosynthetic rate for each plot and sampling data. Leaf area for broad-leaf species (*P. tremuloides*, *P. balsamifera*) were determined by the 6 cm<sup>2</sup> leaf chamber area; for needle-leaved species, leaf area was determined from the size (length and width measured by a caliper) and number of needles present in the gas chamber during sampling. Non-destructive means of measuring leaf area were necessary as to not alter canopy structure or plant physiology over seasons and to preserve the canopy for optical measurements. For each species, mature leaf tissues were sampled whenever possible; new tissues were sampled for *P. mariana* and *P. glauca* during the spring of 2016 when the elongation of new branches did not allow for sampling of mature sunlit tissues.

### **2.2.6 Chlorophyll Fluorescence**

Chlorophyll fluorescence was measured using a portable fluorometer (Mini-PAM; Walz, Effeltrich, Germany) fitted with a fibre-optic and leaf-clip holder (2030-B; Walz, Effeltrich, Germany). Leaves sampled were kept as close to their original orientation as possible to maintain ambient illumination during sampling; needles were bundled together in a flat plane prior to clamping to maximize the sampling area. The fluorometer recorded  $F_S$  under ambient illumination, without a saturating pulse of light, which was used as an indicator of SIF. Three leaves, or bundles of needles, were measured from six individual plants for each species. The replicates for each plant provided a measure of spatial variability of  $F_S$  within each plant and were averaged to yield a single plant-level measurement.  $F_S$  for each species at the plot level was determined by averaging the measurements from all individuals of a given species for a given sampling interval. Fluorescence was not sampled during winter months (Dec-Jan) when low PPFD values due to low solar elevation and building shade resulted in poor fluorescence signals.

### **2.2.7 Data Analysis**

Data collected for this experiment were compared across a full year to examine the seasonal course of optical indices, fluorescence, and photosynthetic activity through seasonal transitions. Data

were visually inspected through time course plots, to describe the phenology of optical and photosynthetic measurements. Seasonal variation of each variable was analyzed through paired t-tests comparing summer and winter period averages for each measure (from plants or canopy regions) within each plot. Summer was defined from May 15 – August 16: the period during the growing season starting 10 days after obvious active growth, when deciduous vegetation was in full leaf flush, (May 5), and ending 10 days prior to observed cessation of growth and changing foliage color throughout the canopies (August 26). Winter was defined from November 1 – March 1: the period starting 10 days after full leaf senescence for deciduous trees (Oct 22, 2016), and ending 10 days prior to any visible changes to evergreen buds (Mar 11, 2016). Regression analyses were performed to compare annual photosynthetic measurements and optical metrics that were averaged to the plot level at each time point. ANCOVA (general linear model evaluating interaction) was used to test differences between the slopes of relationships tested in regression analyses of the two functional types, aggregating species as either evergreen or deciduous, as well as comparing slopes of individual species. As there was no species-level plot replication available in this within-subjects study design, the analyses of plot differences were interpreted as species differences. Statistical analyses were performed using the standard package of R.

## **2.3 Results**

### ***2.3.1 Seasonal Environmental Conditions***

Daily temperature and midday PPFD showed strong seasonal changes typical of boreal regions (Fig. 2.3). During the spring transition, temperatures ranged from  $\sim 0$  °C in February and March, to  $>20$  °C by April. Midday temperatures typically exceeded 20 °C in summer months, from May to August. It was an unusually warm year (Fig. 2.3), and warm weather ( $>15$  °C) persisted throughout September, with midday temperatures rarely below 0 °C until mid-November. Midday temperatures in winter months were typically around  $-8$  °C, with extreme cold periods having midday temperatures of around  $-20$  °C, primarily in early December. Summer midday PPFD values often exceeded  $1500 \mu\text{mol m}^{-2} \text{s}^{-1}$ , while the spring and fall experienced clear-day PPFD values of around  $1000 \mu\text{mol m}^{-2} \text{s}^{-1}$  prior to, and following, the spring and fall equinoxes, respectively. The study site microclimate was warmer than the long-term average (Fig. 2.3), in part because it was a warm year, but also due to the additional thermal mass of the building.

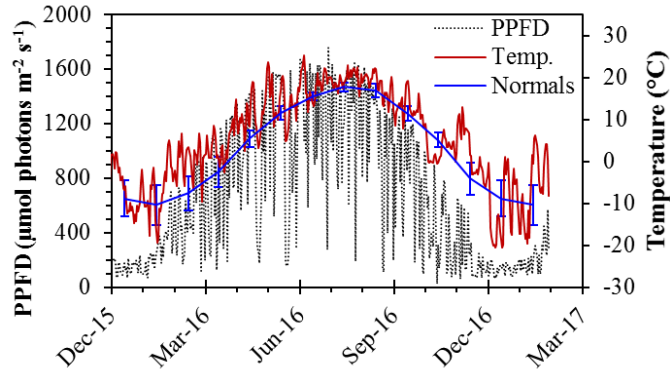


**Figure 2.3:** Seasonal dynamics of photosynthetic photon flux density (PPFD;  $\mu\text{mol photons m}^{-2} \text{s}^{-1}$ ) and temperature ( $^{\circ}\text{C}$ ) from December 2015 to January 2016. PPFD is expressed as a midday average, taken as the period between 13:00 and 14:00 (UTC-06), and temperature is expressed as daily (24-hour) averages. Long-term normal (1981–2010) daily average temperature by month is also shown. Error bars denote  $\pm\text{SD}$  of the mean. Between 20 November and 20 January, the sun did not clear buildings to the south due to low solar elevation, causing anomalously low PPFD values during this period.

### 2.3.2 Seasonal Patterns of Photosynthesis and Remote Sensing Metrics

The seasonal patterns, or phenology, of each measured variable described in the following section are based upon visual inspection of the data. Photosynthetic activity, fluorescence, and reflectance indices often exhibited parallel responses to seasonally changing environmental conditions. However, indices showed subtle differences from each other that indicated variation in their ability to track photosynthetic phenology. Key differences in optical behavior were observed between evergreen and deciduous species, and further interspecific differences were also evident between some species within each functional type.

Photosynthetic rate and most optical metrics followed clear seasonal patterns as temperature for both evergreen (Fig. 2.4a–e) and deciduous (Fig. 2.4f–j) species. Abrupt changes in canopy index values in the winter months for deciduous and evergreen species coincided with the presence of snow on the canopies. Deciduous species showed abrupt changes, over several weeks, in both photosynthesis and optical indices during transitions, while more gradual seasonal transitions, over several months, were observed in evergreen species for both optical metrics and photosynthetic rate. Relationships between each measured variable and temperature are illustrated in supplemental Figure S2. For deciduous species, leaf-level sampling methods were limited to periods when fully formed foliage was present, and canopy-level optical sampling was influenced

by bare soil and remaining stems in the absence of foliage. Small dips in index values in April, during the spring transition, were related to the repotting and increased spacing of trees.

In evergreens, photosynthetic rate responded gradually, over several months (Feb-May), to seasonally changing temperature (Fig. 2.4a). Spring activation began in March, with photosynthetic rates increasing to summer maxima (ca.  $10 \mu\text{mol CO}_2 \text{ m}^{-2} \text{ s}^{-1}$ ) by mid-June. During the spring transition, a large drop in photosynthetic rate was observed for the spruce species (*P. mariana* and *P. glauca*) that coincided with the sampling of newly emerged branches following budburst (also indicated by open symbols; Fig. 2.4a); this drop was not seen in *P. banksiana* as mature needles were sampled through the transition. Following the growing season, photosynthetic rate gradually decreased, reaching near-zero again by November.

Deciduous species displayed rapid changes, over several weeks, in photosynthesis in the spring (April) and fall (Sept-Oct), during early leaf development and senescence, respectively, with winter periods lacking foliage for sampling (Fig. 2.4f). For the broad-leaf deciduous species, the spring transition was very rapid, with sampling periods limited to before budburst and following early leaf expansion. *L. laricina* showed more gradual spring activation than the broad-leaf deciduous species. Maximum photosynthetic rates varied greatly during the growing season for broad-leaf species, but were regularly above  $10 \mu\text{mol CO}_2 \text{ m}^{-2} \text{ s}^{-1}$  until the start of the fall transition, while *L. laricina* had more consistent photosynthetic rates (ca.  $10 \mu\text{mol CO}_2 \text{ m}^{-2} \text{ s}^{-1}$ ) during the growing season. During the fall transition, photosynthetic rates for broad-leaf species decreased more abruptly than for *L. laricina*, with near-zero rates by the end of September and mid-October, respectively.

For evergreens, except for declines during periods of snow, the NDVI was relatively constant through the year (ca. 0.8) increasing slightly with bud burst and decreasing slightly in the fall (Fig. 2.4b). The drop in NDVI in the spring coincided with a brief period of decreased tree density following repotting. For deciduous species, canopy-level NDVI values increased abruptly in spring and decreased abruptly in the fall (Fig. 2.4g); these changes occurred over several weeks in April and Sept-Oct, respectively. Maximum values of the NDVI (ca. 0.85) were seen in the early summer, when trees were flush with foliage. Prior to the rapid spring transition, when trees lacked foliage and mostly bare soil was being sampled, NDVI values were approximately half (ca. 0.4) the summer maximum. Similar values were seen in late-fall following senescence, when canopies

had no green foliage. Snow caused marked declines in the NDVI, and minimum values of the NDVI (ca. 0.1–0.2) occurred in the winter months when snow was present.

Seasonal patterns of the PRI varied for deciduous and evergreens species. For evergreens, seasonal PRI patterns closely followed temperature and increased gradually, over several months (Mar-May), from winter minima (ca.  $-0.2$ : *P. mariana* and *P. glauca*; and ca.  $-0.27$ : *P. banksiana*) to near-growing season maxima (ca.  $-0.03$  and ca.  $-0.06$ , respectively), following the spring transition (Fig. 2.4c). The PRI for *P. banksiana* increased slightly (ca.  $-0.04$ ) towards the end of the summer, during a period when needles were elongating following vertical shoot growth. Through the fall, PRI values decreased gradually, over several months (Sept-Nov), to winter minima (ca.  $-0.2$ : *P. mariana* and *P. glauca*; and ca.  $-0.27$ : *P. banksiana*). Over the winter period, spikes in the PRI corresponded with periods of snow.

PRI values for deciduous species had less overall variation than was seen with evergreens (Fig. 2.4h), but still showed indications of seasonal changes associated with spring leaf development and fall senescence. Prior to the growing season, PRI values were slightly higher for the broad-leaf deciduous species (ca.  $-0.8$ ) compared to *L. laricina* (ca.  $-0.14$ ). Following the spring transition, PRI values increased sharply, over several weeks (April), to maximum growing season values (ca.  $-0.03$ ). The fall senescence period saw a gradual decrease, over several months (Aug-Oct), in the PRI. During leaf senescence, when leaves visibly yellowed, values slightly dropped below those prior to the spring transition (ca.  $-0.16$ ), then increased slightly after leaf-fall.

For evergreens, the CCI showed strong seasonal variation that roughly coincided with changes in temperature (Fig. 2.4d). Winter values of the CCI were lower for *P. banksiana* (ca.  $-0.25$ ) than the spruce species (ca.  $-0.1$ ), and *P. banksiana* trees were visibly stressed during this period, showing a red-yellow needle coloring. During the spring transition, the CCI increased overall several months (Mar-May) for all evergreen species. The maximum CCI occurred in early summer for *P. mariana* and *P. glauca* (ca.  $0.2$ ), which coincided with the later stages of budburst, when new branches were nearly fully elongated and developed. The maximum CCI for *P. banksiana* (ca.  $0.2$ ) was seen later in the summer, during a period when needles were elongating following vertical shoot growth. The CCI gradually decreased through the summer and fall transition for both spruce species. This fall decrease was more abrupt for *P. banksiana* than for *P. mariana* and *P. glauca*. Abrupt increases in the CCI seen in the winter months coincided with periods of snow cover.



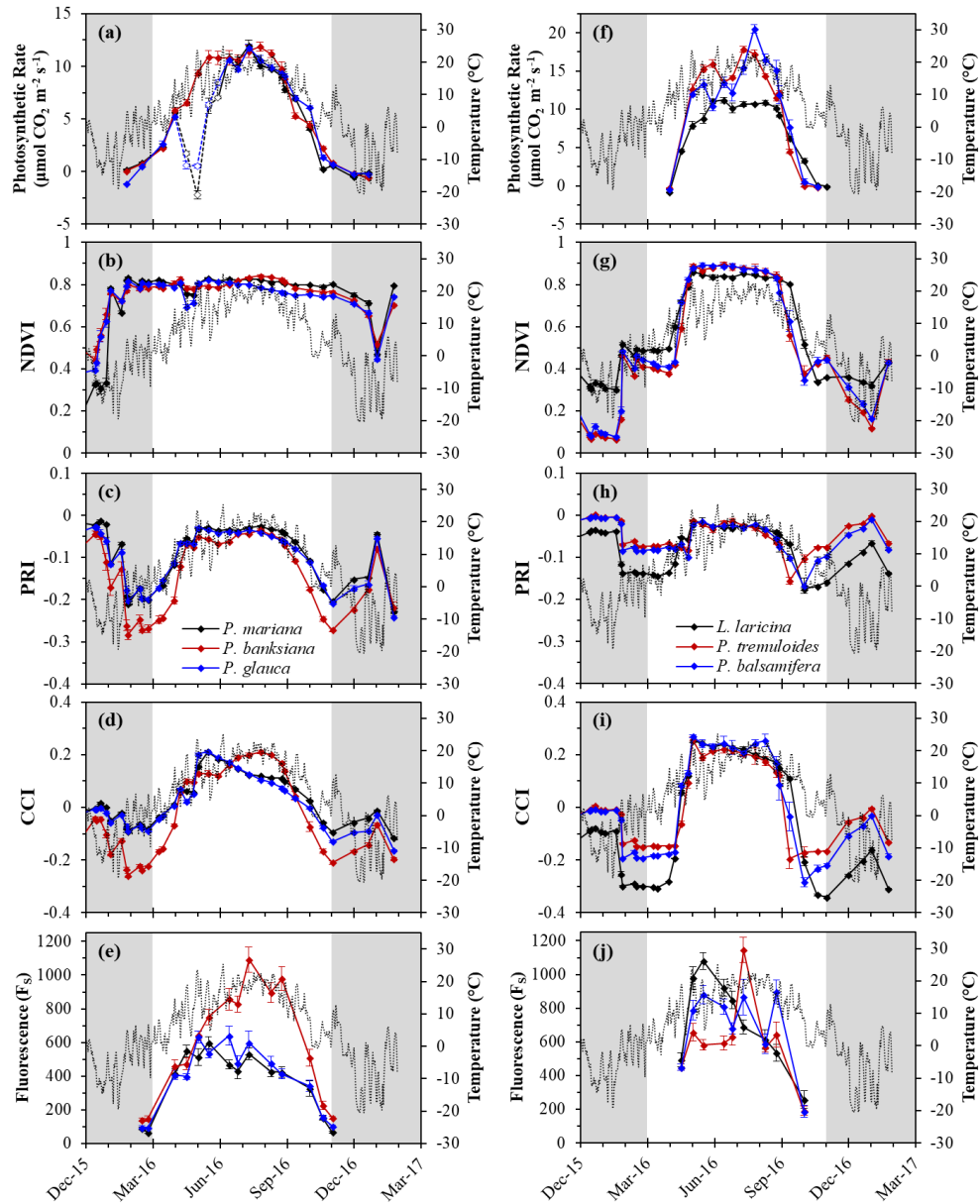


**Figure 2.4:** Annual patterns of midday average temperature (grey line), optical indices and photosynthetic metrics for evergreen and deciduous species. Evergreen species (a–e) included *P. mariana* (black), *P. banksiana* (red), and *P. glauca* (blue). Deciduous species (f–j) included *L. laricina* (black), *P. tremuloides* (red), and *P. balsamifera* (blue). Optical indices (b–d, g–i) were calculated from reflectance measurements at the canopy-level. Fluorescence ( $F_s$ ) was measured at the leaf-level. Data points shown were obtained near solar noon from December 2015 to January 2017. Open points (a) denote sampling periods during the spring transition, where new branches were sampled for *P. mariana* and *P. glauca* during gas exchange measurements. The winter period is indicated by the grey regions (November–March). Annotations on figures indicate the effects of snow (S), repotting (R), and new-leaf expansion (E). For deciduous trees, data were restricted to periods with fully formed leaves during the growing season. Error bars denote  $\pm$ SE of the mean.

For deciduous species, the CCI also showed clear seasonal variation (Fig. 2.4i), with abrupt spring and fall transition periods. Overwinter values of the CCI were high for broad-leaf deciduous species (ca.  $-0.18$ ) compared to *L. laricina* (ca.  $-0.3$ ). The spring transition showed a sharp and rapid increase in the CCI from overwinter values to maximum growing season values (ca.  $0.24$ ) in early summer. This increase began earlier for *L. laricina* than for *P. tremuloides* and *P. balsamifera* due to the earlier budburst for *L. laricina*. CCI values declined slightly during the middle of the growing season, followed by an abrupt decrease during fall senescence. This decrease occurred later for *L. laricina*, coinciding with a later onset of senescence. Increases in the CCI during winter also coincided with the presence of snow.

In evergreens, seasonal patterns in  $F_S$  roughly paralleled temperature changes (Fig. 2.4e).  $F_S$  values increased during the spring transition to maximum values during the growing season, before declining during the fall. Like the CCI, maximum values of  $F_S$  for *P. glauca* and *P. mariana* were observed early in the growing season, corresponding to a period of new branch development following budburst. While *P. banksiana* had a similar spring transition period,  $F_S$  values continued to increase until peaking near the end of the growing season, when new needles expanded following shoot elongation. Following the growing season maximum,  $F_S$  values decreased during the fall transition.

For deciduous species,  $F_S$  roughly paralleled seasonal temperature changes (Fig. 2.4j), but was highly variable during the growing season. Patterns in  $F_S$  appeared different across species during the growing season. However, similar patterns were seen across species immediately following budburst, when  $F_S$  values all increased, and during the fall transition, when  $F_S$  declined during a period of visible chlorophyll loss.  $F_S$  for *L. laricina* was highest following budburst, and gradually decreased through the growing season until the end of senescence; this early season spike occurred when preformed needles were sampled from new buds during the spring transition. For *P. tremuloides*,  $F_S$  was relatively constant during the growing season, apart from a spike in mid-July.  $F_S$  signals for *P. balsamifera* were highly variable throughout the growing season.

To evaluate seasonal variation, statistical comparisons of the average summer and winter values (see supplemental Figure S3) of each measured variable, indicated in Table 2.1, show that photosynthetic rates were significantly different in summer and winter periods for evergreen ( $p < 0.001$ ) and deciduous ( $p < 0.05$ ) species grouped by type, and among individual evergreen and

deciduous species ( $p < 0.001$ ), indicating clear seasonal variability in photosynthesis. For evergreens as a type (Table 2.1a), NDVI was not significantly different in summer and winter periods ( $p > 0.05$ ), but among individual species (Table 2.1b), summer and winter periods had significantly different NDVI values ( $p < 0.01$ ), indicating subtle seasonal variation. Summer and winter NDVI values were significantly different for deciduous species grouped by type (Table 2.1a;  $p < 0.01$ ) and among species (Table 2.1c;  $p < 0.0001$ ), indicating clear seasonal variation. Average summer and winter PRI were significantly different for evergreens grouped by type (Table 2.1a;  $p < 0.01$ ), and for each species (Table 2.1b;  $p < 0.0001$ ), indicating clear seasonal variation in PRI. There was no significant difference between average summer and winter PRI values for the deciduous types (Table 2.1a;  $p > 0.05$ ) but differences were significant for each species (Table 2.1a;  $p < 0.01$ ), indicating subtle seasonal variability in PRI. CCI in summer and winter were significantly different for both evergreen and deciduous types (Table 2.1a;  $p < 0.05$ ), as well as all evergreen ( $p < 0.0001$ ) and deciduous ( $p < 0.01$ ) species (Table 2.1b,c), indicating clear seasonal variability for CCI. Average summer and winter  $F_s$  were significantly different for both evergreen ( $p < 0.05$ ) and deciduous ( $p < 0.001$ ) types (Table 2.1a) as well as all evergreen ( $p < 0.0001$ ) and deciduous ( $p < 0.01$ ) species (Table 2.1b,c), indicating  $F_s$  varied across seasons.

**Table 2.1:** Calculated t-statistics and  $p$ -values (asterisks) from paired t-test comparing average summer and winter values of different measurements by type and by species. For evergreen and deciduous types (a), average summer and winter values for each species were used for comparison. For evergreen (b) and deciduous (c) species, summer and winter averages were derived from plant or plot region measurements for each period. Bonferroni corrections were not applied for analyses. Winter was defined as November to March; Summer was defined as Mid-May to Mid-August. See supplemental Figure S3, S4 and Table S2 for additional information on comparisons. \*,  $p < 0.05$ ; \*\*,  $p < 0.01$ ; \*\*\*,  $p < 0.001$ ; \*\*\*\*,  $p < 0.0001$ .

		Photosynthetic Rate		NDVI		PRI		CCI		$F_s$	
a)	Evergreen spp.	85.762	***	3.373		13.274	**	6.236	*	5.233	*
	Deciduous spp.	9.060	*	21.280	**	3.086		7.779	*	36.420	***
b)	<i>P. mariana</i>	22.239	****	8.012	**	72.815	****	72.022	****	11.995	****
	<i>P. banksiana</i>	15.549	****	8.279	**	30.160	****	86.473	****	21.730	****
	<i>P. glauca</i>	28.247	****	15.679	****	67.416	****	151.682	****	15.595	****
c)	<i>L. laricina</i>	21.667	****	59.100	****	77.476	****	126.115	****	5.940	**
	<i>P. tremuloides</i>	35.979	****	32.580	****	8.568	**	33.329	****	9.787	***
	<i>P. balsamifera</i>	10.012	***	42.344	****	13.028	***	53.247	****	6.271	**

### 2.3.3 Comparison of optical metrics to photosynthesis

Correlations between photosynthetic activity and optical metrics, including  $F_s$  and reflectance indices (NDVI, PRI, and CCI), are shown in Figure 2.5, and summarized in Table 2.2a for evergreen species, and Table 2.2b for deciduous species. For evergreens, *P. mariana* and *P. glauca* showed weak correlations between the NDVI and photosynthetic activity ( $p > 0.05$ ), while *P. mariana* and *P. banksiana* showed a stronger correlation ( $p < 0.05$ ,  $p < 0.001$ , respectively) (Fig. 2.5a). All deciduous species showed strong correlations ( $p < 0.0001$ ) (Fig. 2.5e). For all evergreens, the PRI showed strong correlations with photosynthetic rate ( $p < 0.0001$ ) (Fig. 2.5b), while in broad-leaf deciduous species, the PRI showed moderate correlations ( $p < 0.01$ ), and in *L. laricina*, a strong correlation was found ( $p < 0.0001$ ) (Fig. 2.5f). Strong correlations emerged between the CCI and photosynthetic rate for all evergreen ( $p < 0.0001$ ) and deciduous species ( $p < 0.0001$ ) (Fig. 2.5c,g).  $F_s$  had strong correlations with photosynthetic rate for all evergreen species ( $p < 0.0001$ ) (Fig. 2.5d), but moderate correlations were seen for broad-leaf deciduous species ( $p < 0.05$ ), and no significant correlation was seen for *L. laricina* ( $p > 0.05$ ) (Fig. 2.5h).

**Table 2.2:** Coefficient of determination ( $R^2$ ) and  $p$ -values (asterisks) for regressions between canopy-level optical indices (normalized difference vegetation index (NDVI), photochemical reflectance index (PRI), chlorophyll/carotenoid index (CCI), and steady-state fluorescence ( $F_s$ )) and photosynthetic rate for evergreen (a) and deciduous (b) species. Data points from the spring transition in 2016 for *P. glauca* and *P. mariana* were excluded from analyses. The sample size for  $F_s$  was smaller than for reflectance indices, and is indicated in parentheses. \*,  $p < 0.05$ ; \*\*,  $p < 0.01$ ; \*\*\*,  $p < 0.001$ ; \*\*\*\*,  $p < 0.0001$ .

	Species	n	NDVI	PRI	CCI	$F_s$
a)	<i>P. mariana</i>	17 (10)	0.318 *	0.905 ****	0.945 ****	0.891 ****
	<i>P. banksiana</i>	21 (13)	0.556 ***	0.853 ****	0.928 ****	0.908 ****
	<i>P. glauca</i>	17 (10)	0.199	0.950 ****	0.914 ****	0.922 ****
b)	<i>L. laricina</i>	16 (9)	0.861 ****	0.796 ****	0.896 ****	0.307
	<i>P. tremuloides</i>	14 (8)	0.937 ****	0.505 **	0.881 ****	0.674 *
	<i>P. balsamifera</i>	14 (8)	0.828 ****	0.595 **	0.824 ****	0.692 *

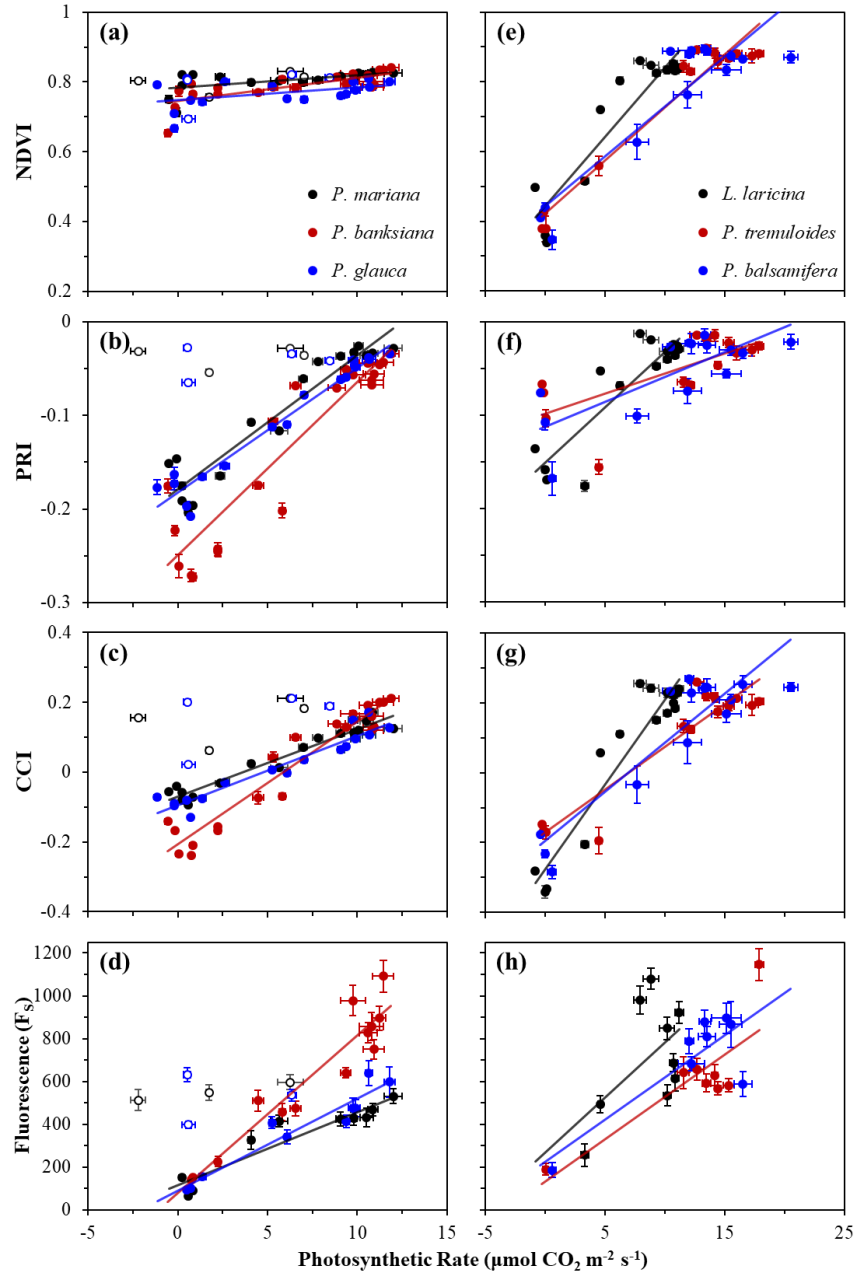


**Figure 2.5:** Relationships between photosynthetic rate ( $\mu\text{mol CO}_2 \text{ m}^{-2} \text{ s}^{-1}$ ) and the NDVI, PRI, CCI, or  $F_s$  for evergreen (a–d) and deciduous (e–h) species. Data points were obtained near solar noon from January 2016 to December 2016. Error bars denote  $\pm$ SE of the mean. Open points (a–d) denote dates when new branches were sampled for *P. mariana* and *P. glauca*; these points were excluded from analyses. The  $R^2$  and significance of each relationship are indicated in Table 2.2.

When comparing the relationships between optical measurements and photosynthetic rate across functional types (Table 2.3a), the slopes of the regressions between both the NDVI and PRI and photosynthetic rate were significantly different for evergreen and deciduous species ( $p < 0.0001$ ), indicating functionally distinct behavior of these indices in the two functional types. In general, NDVI showed a wider dynamic range for deciduous than evergreen species, and PRI showed the reverse pattern. The regression slopes between both the CCI and  $F_s$  and photosynthetic rate in evergreen and deciduous species were not significantly different ( $p > 0.05$ ).

**Table 2.3:**  $p$ -values for comparison of regression slopes (interaction) between evergreen and deciduous species grouped by type for optical measurements and photosynthetic rate (a), and between optical indices and  $F_s$  (b).

		NDVI	PRI	CCI	$F_s$
a)	Photosynthetic Rate	< 2E-16	6.52E-10	2.14E-01	5.83E-02
b)	$F_s$	2.50E-08	4.75E-02	2.85E-01	

Comparing regression slopes by species indicated differences within and across types (Table 2.4). Comparing the relationships between NDVI and photosynthetic rate (Table 2.4a), the slopes of the regressions for all evergreen species were significantly different from all deciduous species; no species differences were found within evergreen and deciduous types. Comparing the relationships between PRI and photosynthetic rate (Table 2.4b), all evergreen species were significantly different from deciduous species, except spruce species (*Picea* spp.), which were not different from *L. laricina*. Within types, only *P. glauca* and *P. banksiana* significantly differed from each other among evergreens, where as *L. laricina* was significantly different from both *P. tremuloides* and *P. balsamifera*. Comparing the relationships between CCI and photosynthetic rate (Table 2.4c), differences within and across types were noted. For evergreens, spruces species (*Picea* spp.) were not significantly different from each other but were different from *P. banksiana*. For deciduous species, broad-leaf aspen and poplar species (*Populus* spp.) were not different from each other but were significantly different from *L. laricina*. Comparing across types, all evergreen species were also significantly different from *L. laricina*, *P. mariana* was significantly different from *P. balsamifera*, and *P. banksiana* was significantly different from *P. tremuloides*. Comparing the relationships between  $F_s$  and photosynthetic rate (Table 2.4d), only *P. banksiana* was significantly different from other species, being different from both spruce species (*Picea* spp.) and both broad leaf species (*Populus* spp.).

**Table 2.4:** *p*-values from ANCOVA analysis comparing regression slopes (interaction) of optical measurements NDVI (a), PRI (b), CCI (c), and F<sub>S</sub> (d), plotted against photosynthetic rate between each study species. \*, *p* < 0.05; \*\*, *p* < 0.01; \*\*\*, *p* < 0.001; \*\*\*\*, *p* < 0.0001.

a)

Species	<i>P. mariana</i>	<i>P. banksiana</i>	<i>P. glauca</i>	<i>L. laricina</i>	<i>P. tremuloides</i>	<i>P. balsamifera</i>
<i>P. mariana</i>						
<i>P. banksiana</i>	1.24E-01					
<i>P. glauca</i>	9.86E-01	1.91E-01				
<i>L. laricina</i>	2.71E-09 ****	1.29E-09 ****	7.61E-09 ****			
<i>P. tremuloides</i>	3.80E-10 ****	2.92E-10 ****	2.34E-09 ****	5.85E-02		
<i>P. balsamifera</i>	3.16E-06 ****	2.99E-06 ****	5.70E-06 ****	6.65E-02	6.66E-01	

b)

Species	<i>P. mariana</i>	<i>P. banksiana</i>	<i>P. glauca</i>	<i>L. laricina</i>	<i>P. tremuloides</i>	<i>P. balsamifera</i>
<i>P. mariana</i>						
<i>P. banksiana</i>	7.21E-02					
<i>P. glauca</i>	4.95E-01	1.86E-02 *				
<i>L. laricina</i>	2.42E-01	1.35E-02 *	4.32E-01			
<i>P. tremuloides</i>	4.87E-06 ****	2.61E-07 ****	3.06E-06 ****	9.89E-04 ***		
<i>P. balsamifera</i>	2.83E-05 ****	1.27E-06 ****	2.27E-05 ****	3.89E-03 **	5.66E-01	

c)

Species	<i>P. mariana</i>	<i>P. banksiana</i>	<i>P. glauca</i>	<i>L. laricina</i>	<i>P. tremuloides</i>	<i>P. balsamifera</i>
<i>P. mariana</i>						
<i>P. banksiana</i>	1.56E-06 ****					
<i>P. glauca</i>	8.00E-01	5.95E-06 ****				
<i>L. laricina</i>	2.43E-07 ****	6.60E-03 **	5.22E-07 ****			
<i>P. tremuloides</i>	9.95E-02	3.82E-03 **	1.51E-01	6.02E-05 ****		
<i>P. balsamifera</i>	4.78E-02 *	9.96E-02	6.64E-02	1.79E-03 **	4.54E-01	

d)

Species	<i>P. mariana</i>	<i>P. banksiana</i>	<i>P. glauca</i>	<i>L. laricina</i>	<i>P. tremuloides</i>	<i>P. balsamifera</i>
<i>P. mariana</i>						
<i>P. banksiana</i>	2.39E-04 ***					
<i>P. glauca</i>	1.66E-01	2.96E-03 **				
<i>L. laricina</i>	4.80E-01	3.60E-01	7.33E-01			
<i>P. tremuloides</i>	6.28E-01	1.51E-02 *	7.89E-01	6.96E-01		
<i>P. balsamifera</i>	6.28E-01	1.21E-02 *	7.52E-01	6.83E-01	9.83E-01	

Correlations between  $F_S$  and reflectance indices (NDVI, PRI, and CCI) are shown in Figure 2.6, and summarized in Table 2.5a for evergreen species, and Table 2.5b for deciduous species. For the NDVI, weak correlations with  $F_S$  were seen in all evergreens ( $p > 0.05$ ) (Fig. 2.6a), except for *P. banksiana*, which yielded a good correlation ( $p < 0.001$ ), but with a very small range of NDVI values compared to deciduous species that had moderate correlations ( $p < 0.05$ ) (Fig. 2.6d). The PRI had strong correlations with  $F_S$  for all evergreen species ( $p < 0.0001$ ) (Fig. 2.6b), and moderate correlations for two deciduous species *L. laricina* ( $p < 0.05$ ), and *P. balsamifera* ( $p < 0.01$ ) (Fig. 2.6e). The CCI had strong correlations with  $F_S$  for all evergreen species ( $p < 0.0001$ ) (Fig. 2.6c), and moderate correlations for deciduous species (*P. tremuloides*,  $p < 0.05$ ; *L. laricina* & *P. balsamifera*,  $p < 0.001$ ) (Fig. 2.6f).

**Table 2.5:** Coefficient of determination ( $R^2$ ) and  $p$ -values (asterisks) for regressions between canopy-level optical indices NDVI, PRI, CCI and  $F_S$  for evergreen (a) and deciduous (b) species. Data points from the spring transition in 2016 for *P. glauca* and *P. mariana* were excluded from analyses. \*,  $p < 0.05$ ; \*\*,  $p < 0.01$ ; \*\*\*,  $p < 0.001$ ; \*\*\*\*,  $p < 0.0001$ .

	Species	n	NDVI	PRI	CCI
a)	<i>P. mariana</i>	14	0.001	0.873 ****	0.799 ****
	<i>P. banksiana</i>	14	0.642 ***	0.827 ****	0.885 ****
	<i>P. glauca</i>	14	0.104	0.900 ****	0.854 ****
b)	<i>L. laricina</i>	9	0.590 *	0.601 *	0.707 **
	<i>P. tremuloides</i>	9	0.501 *	0.393	0.471 *
	<i>P. balsamifera</i>	9	0.763 **	0.710 **	0.696 **

When comparing the relationships between optical indices and  $F_S$  across functional types (Table 2.3b), the slopes of the regressions between both the NDVI and PRI and  $F_S$  were significantly different in deciduous and evergreen species ( $p < 0.0001$ , and  $p < 0.05$ ), again indicating functionally distinct behavior of the NDVI and PRI in the two functional types. The regression slopes between the CCI and  $F_S$  in deciduous and evergreens were not significantly different ( $p > 0.05$ ).



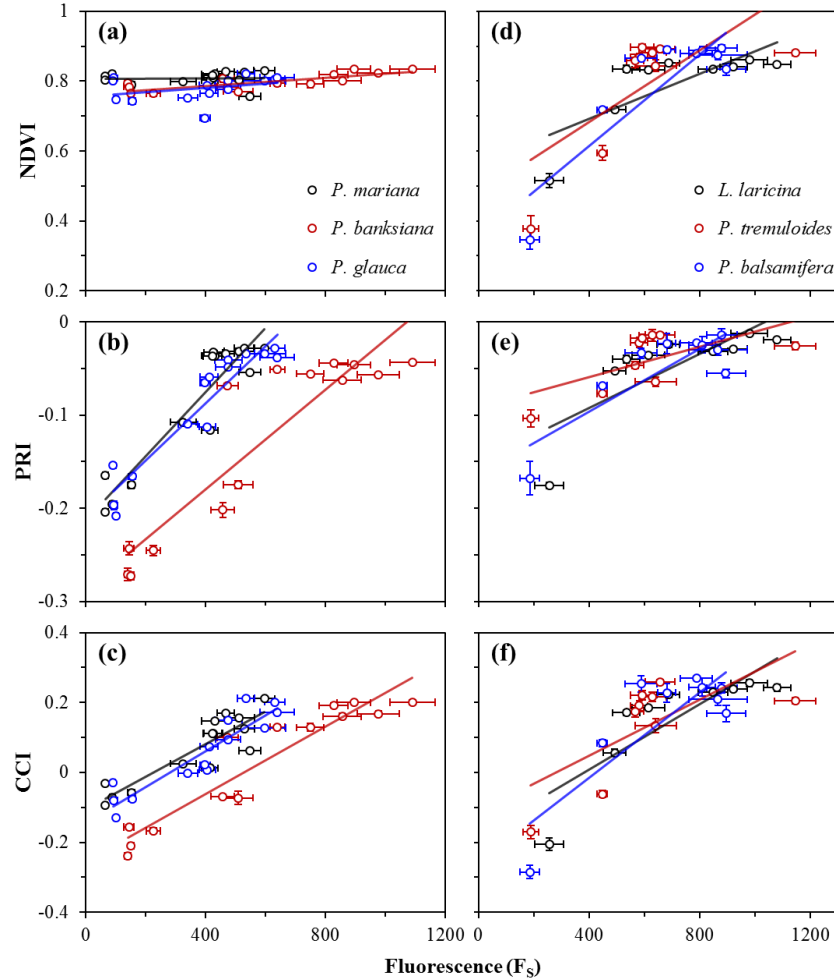


**Figure 2.6:** Relationships between  $F_s$  and canopy-level optical indices NDVI, PRI, and CCI for evergreen (a–c) and deciduous (d–f) species. Data points were obtained near solar noon from January 2016 to December 2016. Error bars denote  $\pm$ SE of the mean. The  $R^2$  and significance of each relationship are indicated in Table 2.4.

Comparing regression slopes for  $F_s$  and reflectance indices by species (Table 2.6) yielded similar results to analysis where species were grouped by type. For  $F_s$  and NDVI (Table 2.6a), the regression slopes for species within types were not significantly different but the slopes for all evergreen species were significantly different from all deciduous species. The results were similar for  $F_s$  and PRI (Table 2.6b), except for the slope for *P. banksiana* was not significantly different from *L. laricina* and *P. balsamifera*. Comparing the relationships between  $F_s$  and CCI (Table 2.6c) showed no significant differences between the slopes of any species.

**Table 2.6:** *p*-values from ANCOVA analysis comparing regression slopes of optical indices NDVI (a), PRI (b), and CCI (c), plotted against  $F_S$  between each study species. \*  $p < 0.05$ ; \*\*  $p < 0.01$ ; \*\*\*  $p < 0.001$ ; \*\*\*\*  $p < 0.0001$ .

a)

Species	<i>P. mariana</i>	<i>P. banksiana</i>	<i>P. glauca</i>	<i>L. laricina</i>	<i>P. tremuloides</i>	<i>P. balsamifera</i>
<i>P. mariana</i>						
<i>P. banksiana</i>	7.89E-02					
<i>P. glauca</i>	3.58E-01	9.85E-01				
<i>L. laricina</i>	3.91E-03 **	2.35E-03 **	1.95E-02 *			
<i>P. tremuloides</i>	7.97E-03 **	3.76E-03 **	1.65E-02 *	3.92E-01		
<i>P. balsamifera</i>	3.98E-05 ****	8.00E-06 ****	1.70E-04 ***	7.26E-02	5.70E-01	

b)

Species	<i>P. mariana</i>	<i>P. banksiana</i>	<i>P. glauca</i>	<i>L. laricina</i>	<i>P. tremuloides</i>	<i>P. balsamifera</i>
<i>P. mariana</i>						
<i>P. banksiana</i>	2.01E-01					
<i>P. glauca</i>	4.70E-01	4.42E-01				
<i>L. laricina</i>	2.59E-03 **	6.27E-02	4.70E-03 **			
<i>P. tremuloides</i>	9.83E-05 ****	6.85E-03 **	1.08E-04 ***	2.98E-01		
<i>P. balsamifera</i>	5.14E-03 **	1.41E-01	9.60E-03 **	7.01E-01	1.38E-01	

c)

Species	<i>P. mariana</i>	<i>P. banksiana</i>	<i>P. glauca</i>	<i>L. laricina</i>	<i>P. tremuloides</i>	<i>P. balsamifera</i>
<i>P. mariana</i>						
<i>P. banksiana</i>	9.08E-01					
<i>P. glauca</i>	6.41E-01	7.05E-01				
<i>L. laricina</i>	9.90E-01	9.13E-01	7.15E-01			
<i>P. tremuloides</i>	6.79E-01	5.80E-01	4.82E-01	7.43E-01		
<i>P. balsamifera</i>	3.60E-01	3.37E-01	5.05E-01	4.59E-01	3.63E-01	

## 2.4 Discussion

### 2.4.1 Seasonal Patterns and Variation

Based on visual inspection of the data, photosynthetic activity, fluorescence, and reflectance indices often exhibited seasonal responses that paralleled changing environmental conditions. However, the optical indices showed subtle differences from each other that indicated variation in their ability to track photosynthetic phenology. In parallel to seasonally changing temperature, optical and photosynthetic metrics in evergreen species (with the exception of the NDVI) changed gradually with temperature, whereas metrics in deciduous species showed abrupt changes that were typically limited to the spring and fall transition periods, and did not track temperature as closely as in evergreens. In particular, we noted that seasonal CCI patterns exhibited a close correlation with temperature for evergreen and deciduous species (supplemental Figure S2). The strong relationship between the CCI and temperature suggested a strong temperature driver in the CCI signal.

Gradual seasonal changes in photosynthetic activity for evergreen species, compared to more abrupt spring activation and fall declines of photosynthesis for deciduous species, based on visual inspection of the data, reflect a longer overall photosynthetic season for evergreens than for deciduous species [38]. While evergreens in boreal forests do not photosynthesize year-round, they can typically begin photosynthesis earlier in the spring and persist later in the fall than deciduous species [39]. The abrupt drop in photosynthetic rate for *P. mariana* and *P. glauca* during the spring transition was likely an artefact of leaf-level sampling. Budburst near branch tips for spruce trees made accurate sampling of mature needles difficult, leaving only young leaves to be sampled during this period. These young leaves are less productive than fully mature leaves [40].

The more abrupt transitions during spring and fall for deciduous species were expected as, unlike evergreens, deciduous species shed foliage during unfavorable seasons [38]. The higher overall photosynthetic rate observed in deciduous species compared visually to evergreens during the growing season was consistent with deciduous species having a higher rate of photosynthesis per unit leaf mass than evergreens [38]. Deciduous species have thinner leaves with a greater surface area than evergreens, allowing them to be more productive during favorable conditions, whereas evergreens have thick leaves that avoid damage brought on by frost or drought during unfavorable seasons [41]. The conifer *L. laricina*, though deciduous, showed very similar photosynthetic rates

to evergreen species, and typically has low summer rates of photosynthetic activity and growth [42].

When evaluating the efficacy of canopy reflectance indices in tracking photosynthetic phenology, we found that the NDVI was capable of tracking midday photosynthetic activity of deciduous species, showing strong seasonal variation associated with the development and loss of green foliage across seasons, as previously reported [17], but can change slightly with seasonally changing pigment levels, which likely accounts for the smaller (but sometimes significant) slopes in the NDVI-photosynthesis for some evergreens. The slight NDVI variation in evergreen species across seasons was expected, as evergreen canopy structure is relatively stable over seasons [17]. The small increase in the NDVI during the emergence of new foliage in *P. banksiana* suggested some sensitivity to the structural changes in evergreens associated with the flush of new leaves. However, in evergreens (relative to deciduous species), the NDVI fails to capture subtler changes in phenology (e.g., photosynthetic downregulation) [19] that occur during transitions into and out of winter.

The PRI was capable of tracking photosynthetic phenology for all evergreen species, and showed strong seasonal variation. These patterns were similar to seasonal trends shown in other studies that demonstrated that the PRI responds to seasonally changing chlorophyll and carotenoid pigment pool sizes [13,14,19]. The PRI is sensitive to changes in the chlorophyll/carotenoid ratios that are driven by the increase in carotenoids and the decline of chlorophyll concentrations in the winter, and their reversal in the summer [13]. These pigment changes are related to the cold-hardening process in response to changing temperature and photoperiod, and subsequent readjustment during the de-hardening period in the spring [6,7,9].

In deciduous species, the visibly smaller seasonal variation in PRI was likely a result of budburst and the increase in foliage and subsequent changes in pigment levels that occurred during transitions. The initial fall decrease in the PRI to values lower than the normal winter background may have been attributed to the breakdown of chlorophyll during senescence [43]; the more rapid breakdown of chlorophylls than carotenoids during senescence [44] alters chlorophyll/carotenoid ratios, to which the PRI is sensitive. The lower values of the PRI seen in *L. laricina* during winter periods compared to the broad-leaf deciduous species was likely due to the persistence of leaf litter on the top of the pots following senescence, causing lower values than was seen with bare soil.

The CCI showed strong seasonal variation in both evergreen and deciduous species, indicating that the CCI can effectively track photosynthetic phenology in both functional types, unlike the PRI and NDVI. The close parallels between the CCI and photosynthetic activity in evergreens were consistent with other findings indicating that changes in the CCI coincide with large pigment pool size shifts [15], which are known to closely track photosynthetic rates and GPP in evergreens [13–15]. Strong seasonal changes in the CCI for deciduous species were primarily driven by the presence and absence of canopy foliage. Similar to the PRI, the persistence of leaf litter on the top of pots was the likely cause of lower CCI values seen in *L. laricina*, compared to broad-leaf deciduous species, during winter periods. As with other reflectance indices, the CCI was also clearly affected by snow, which could have confounded the seasonal interpretation of this index. Consequently, more work may be needed to correct for these background effects.

The parallel seasonal patterns of the CCI and photosynthetic activity in deciduous species suggested that the CCI is sensitive to canopy structural changes, as well as the adjustment of pigments associated with leaf development in the spring, and senescence during the fall transition. The spikes in the CCI at the end of the spring transition for spruce species (*P. mariana* and *P. glauca*) and later in the summer for *P. banksiana* that coincided with needle expansion and shoot elongation indicated that the CCI is also sensitive to canopy structure in evergreens, which has not previously been reported. These results indicate that the CCI may be sensitive to a combination of canopy structural changes and pigment pool size adjustments for both functional types when tracking photosynthetic phenology. Consequently, the CCI appears well-suited to assess photosynthetic phenology consistently across evergreen, deciduous, and mixed forests, where the NDVI and PRI are likely to show different responses.

The increases in  $F_s$  during the spring and decreases during the fall observed in our three evergreen species were similar to seasonal patterns reported for *Pinus sylvestris* [45]. Maximum  $F_s$  values seen in the early spring for *L. laricina*, *P. mariana*, and *P. glauca*, and seen later in the season for *P. banksiana*, coincided with the emergence of new leaf tissues. As young leaves are less productive, with lower chlorophyll concentrations than mature leaves [40], they have more excess absorbed light to dissipate [46], and require greater photoprotection [47]. This excess light may result in greater dissipation through fluorescence. These leaf-level phenomena may not be

representative of the whole canopy, where multiple scattering and reabsorption can alter the fluorescence signal, and further studies at different spatial scales would be required to test this.

The seasonal changes observed in evergreens were likely related to changing NPQ with the adjustment of pigmentation (changing pigment pools and xanthophyll pigment activity) during the spring and fall transitions [7]. During the fall transition, pigmentation changes function to dissipate excess light energy through NPQ [7,9], which has been reported to be substantially greater in the winter months than summer months [45]; this increase in NPQ results in a quenching of the fluorescence signal [48]. The opposite is likely to have occurred during the growing season, with the increase in light availability reaching potentially saturating levels for photochemistry, combined with the reversal of cold-hardening pigment changes [7] and a reduction of NPQ with increasing temperature [45], all potentially resulting in increased dissipation of absorbed light through fluorescence during the spring transition. In deciduous species, the greater variability in  $F_S$  seen during the summer for broad-leaf species (*P. tremuloides* and *P. balsamifera*) compared to *L. laricina* was possibly due to the differential irradiance of individual leaves associated with more dynamic orientation of the broad-leaf species during sampling [49], with fluorescence adjusting quickly with changing light [11]. Further studies are warranted to evaluate the variability in the leaf-level fluorescence signals in relation to photosynthetic phenology, and to compare  $F_S$  to SIF in response to seasonally changing conditions. Here we used  $F_S$  as an indicator of likely SIF signals, but key differences in instrumentation and measurement protocols exist between these two methods [10].

#### **2.4.2 Complementarity Hypothesis**

Overall, our comparison of the NDVI and PRI to photosynthetic phenology reveal the complementary nature of the NDVI and PRI when sampling deciduous and evergreen vegetation, as evidenced by the strong relationships between NDVI and photosynthetic rate for deciduous species, and PRI and photosynthetic rate for evergreen species, which is consistent with the complementarity hypothesis [31,34]. However, NDVI related well to photosynthetic activity in some instances for evergreens, and PRI related well to photosynthetic activity for deciduous species, neither index tracked photosynthetic activity to the same extent or with the same dynamic range as in seen in the converse functional type. By contrast, the strong relationships between the CCI and photosynthetic activity in both evergreen and deciduous species indicated that the CCI is

sensitive to both seasonally changing pigment pools in evergreens, and canopy structural changes linked to photosynthetic activity in deciduous species, which has not previously been reported. If the CCI is sensitive to both canopy structural changes influencing absorbed light (APAR) and photosynthetic  $\epsilon$ , then the CCI can be used as a direct indicator of photosynthetic activity in multiple functional types, as proposed in Figure 2.1. SIF may also have a similar capability to the CCI in providing a direct indicator of photosynthetic activity [31], which has been suggested in large-scale studies linking fluorescence to GPP in multiple biomes [29], as it is known to be sensitive to absorbed light and photosynthetic downregulation [10].

The CCI showed strong parallels with  $F_S$  in evergreen species, and moderate parallels in deciduous species. The relatively poor relationships when comparing the CCI and  $F_S$  in deciduous species could be a consequence of comparing leaf-level  $F_S$  measurements to canopy-level reflectance indices, where the fewer  $F_S$  samples for deciduous species resulted from the lack of foliage year-round for sampling, and limited the sample size and sampling period for  $F_S$  to the growing season. Relative to the NDVI and PRI, stronger and more consistent correlations between the CCI and  $F_S$  for both evergreen and deciduous species suggested that these metrics might yield similar information about photosynthetic phenology, and further work at large scales and across multiple functional types would be required to confirm this.

### **2.4.3 Differences Between Species Within Functional Types**

While our results show differences in photosynthetic and optical phenology between deciduous and evergreens, they also indicate differences among species within each functional type. NDVI did not reveal differences within evergreen or deciduous types for NDVI, implying similar seasonal responses of canopy structure and greenness within each type. Our results also showed that for PRI, *P. banksiana* was different from the *Picea* species, and *L. laricina* was different from the *Populus* species but similar to the *Picea* species. Interestingly, for CCI we found that *L. laricina* was different from every other deciduous and evergreen species evaluated. These differences for PRI and CCI indicate that variation exists within each type (evergreen and deciduous), with closely related species (*Picea* spp. and *Populus* spp.) showing similar optical and physiological behavior, and *L. laricina* showing a similarities and differences to both evergreen and deciduous species suggesting a phylogenetic contribution to these patterns. These suggestions of a phylogenetic link

are broadly consistent with recent reports of significant relationships between leaf spectral diversity and functional and phylogenetic diversity [50].

Variation in optical and physiological behavior between evergreen and deciduous species is likely due to contrasting structural and physiological controls on plant growth between species, or genera, that reflect different evolutionary responses to environmental conditions [31,34], affecting the timing of seasonal activation and downregulation, as well as growth habits. This variation between and within functional types illustrates a need to better understand vegetation optical types: the classification by functionally different optical properties determined by a combination of leaf and canopy traits and phenology [51]. This optical behavior of vegetation needs to be better understood if it is to be effectively applied over larger spatial and temporal scales (e.g., airborne or satellite data).

#### ***2.4.4 Other Causes of Variation in Stand-Level Sampling***

While optical measurements can be used at both the leaf- and stand-levels as metrics of photosynthetic activity, there can be subtle differences in leaf- and canopy-level seasonal responses that might confound this relationship [14,15]. In our study, one likely cause of variation was the expansion of new branches and leaf tissues, which would have affected leaf- and canopy-level signals related to pigments and canopy structure differently.

Presumably, background signals (including soil, leaf litter, bark, and snow) also impacted optical measurements at the canopy- and stand-levels. While the NDVI and PRI are known to be influenced by these background signals [52,53], the effects of background signals on the CCI, while not as well-understood, were clearly visible.

The presence of snowfall had noticeable impacts on all optical indices during winter months, which has been previously reported for the NDVI [54], but not for the PRI or CCI. During transition periods, snowfall can obscure changes in vegetation [54], and observing patterns of spring activation and fall downregulation becomes more challenging, particularly for reflectance indices that are clearly influenced by the high albedo of snow. The impacts of different background signals on canopy-level optical indices, including snowfall in higher-latitude temperate forests, must be considered when sampling over large spatial and temporal scales.



The measurements of leaf-level  $F_S$  using the PAM method had potential limitations that require further consideration [10]. Compared to other fluorescence parameters (e.g.,  $F_m$ ,  $F_v/F_m$ ),  $F_S$  tells little about underlying plant physiological processes on its own [55], and it changed rapidly according to light conditions. Unlike SIF, which is measured passively using spectrometers with very narrow bandwidth, PAM fluorescence is a broadband measurement isolated with a modulated light signal. However, unlike other PAM fluorescence parameters, but similar to SIF,  $F_S$  is measured under ambient sunlight without the application of a saturating pulse. The passive nature of  $F_S$  in ambient light makes it a more appropriate analogue to SIF than other PAM fluorescence metrics that require a saturating light pulse. In this study,  $F_S$  was used in place of a spectral fluorescence metric due to the lack of high spectral resolution from the spectrometers utilized in this study. Future studies should investigate the seasonal responses of both  $F_S$  and SIF in response to seasonally changing conditions.

Some aspects of this study may not be reflective of natural environmental conditions due to the small-scale and synthetic nature of the design, limiting the ability to draw direct conclusions for natural forests. Our study took place on a rooftop, where the average temperature was often warmer than that of natural forests in the same region, potentially resulting in a slightly longer growing season than would normally be seen. Presumably, other aspects of surface energy balance were also different between rooftop conditions and natural forest environments. Our plants were well-watered with periodic nutrient applications to ensure proper growth. In natural environments, plants would be exposed to a wide range of water and nutrient conditions, and would experience drought and nutrient stress, which would impact plant physiology and optical properties. Accordingly, proper extension and application of these must be done in natural ecosystems at larger scales. To investigate the potential for upscaling, further studies are underway using satellite data and the flux tower network [15].

## **2.5 Conclusions**

The goals of this study were to gain further insight into the dynamics of optical signals and how optical signals relate to photosynthetic activity in boreal trees. As this work can be very difficult to conduct on natural forest stands, this study provided a means to understand the behaviour of optical signals for boreal stands by using synthetic stands of seedlings, a more tractable option to provide a foundation for the interpretation of satellite measurements.

Our results show the varying efficacy of  $F_S$  and reflectance indices (NDVI, PRI, and CCI) in tracking photosynthetic phenology for evergreen and deciduous species. As expected, the NDVI was primarily sensitive to canopy structural changes associated with leaf development and senescence, and detected changing photosynthetic activity in deciduous, but less so evergreen, species. The PRI was able to track photosynthetic activity driven by changes in pigment pool size, which can be observed in both functional types, but was better seen in evergreens. The CCI was able to track photosynthetic phenology in both deciduous and evergreen species, reflecting seasonal changes in both pigment pool size and canopy structural changes. In many cases,  $F_S$  showed similar responses to the CCI, but with weaker correlations with photosynthetic phenology, partly due to the limitations of smaller sample sizes. These findings demonstrate the value of remotely measured optical indices to better understand and monitor changing vegetation phenology, especially the spring transition, with changing climatic conditions.

Our findings support the complementary nature of the reflectance indices NDVI and PRI, with respect to the LUE model. As expected, the NDVI and PRI provided information relevant to the  $A_{PAR}$  and  $\epsilon$  terms in the model, respectively. By contrast, the CCI and  $F_S$  seem to have provided similar information regarding photosynthetic activity, and may have been sensitive to both  $A_{PAR}$  (via chlorophyll content and canopy structure) and  $\epsilon$  (mediated via relative pigment concentrations and NPQ). We also showed that the CCI correlated well with actual rates of photosynthesis and could perhaps transcend the LUE model by providing a direct metric of productivity, as proposed for SIF.  $F_S$  (a leaf-level analog for SIF) may have a similar potential, but further work at larger scales is needed to explore the cause of these differences apparent in our leaf ( $F_S$ ) and canopy (CCI) comparisons. The development of new instruments for canopy-level SIF measurements in conjunction with reflectance should further clarify these relationships and their mechanistic underpinnings.

Different functional types (evergreen and deciduous) showed distinct optical and photosynthetic phenology, highlighting the importance of considering optical types when sampling at the ecosystem-level. With similar responses in both types, the CCI is well suited for detecting changes representative of both functional types, and can presumably be applied to mixed boreal stands, where deciduous and evergreen species both contribute to canopy optical properties and photosynthetic fluxes. When considering reflectance indices for evaluating photosynthetic

phenology of different functional types, the limitations of the NDVI and PRI, which responded differently for evergreen and deciduous species, are apparent.

The CCI and SIF both offer means of monitoring large-scale photosynthesis and productivity, and the tandem ability of these metrics to monitor photosynthetic phenology in both deciduous and evergreen vegetation will be a particularly valuable contribution to the planned FLEX mission and supporting studies. Relative to other metrics, the stronger ability of the CCI and SIF in tracking photosynthetic activity of different functional types, by detecting structural and physiological contributions to photosynthetic phenology, appear to offer a powerful means of estimating photosynthesis and primary productivity across ecosystems. This study on small synthetic stands provides insight for how remote sensing can be applied to assess gross primary productivity at larger spatial and temporal scales when monitoring how the boreal ecosystem responds to changing environmental conditions.

## 2.6 References

1. Dixon, R. K.; Browne, S.; Houghton, R. A.; Solomon, A. M.; Trexler, M. C.; Wosniewski, J. Carbon pools and flux of global forest ecosystems. *Science* 1994, 263, 185–190.
2. Pan, Y.; Birdsey, R. A.; Fang, J.; Houghton, R.; Kauppi, P. E.; Kurz, W. A.; Phillips, O. L.; Shvidenko, A.; Lewis, S. L.; Canadell, J. G. A Large and Persistent Carbon Sink in the World's Forests. *Science* 2011, 333, 988–993.
3. Goodale, C. L.; Apps, M. J.; Birdsey, R. A.; Field, C. B.; Heath, L. S.; Houghton, R. A.; Jenkins, J. C.; Kohlmaier, G. H.; Kurz, W.; Liu, S.; Nabuurs, G.; Nilsson, S.; Shvidenko, A. Z. Forest carbon sinks in the Northern Hemisphere. *Ecol. Appl.* 2002, 12, 891–899.
4. MacDonald, G. M. Global warming and the Arctic: a new world beyond the reach of the Grinnellian niche? *J. Exp. Biol.* 2010, 213, 855–861.
5. Estiarte, M.; Peñuelas, J. Alteration of the phenology of leaf senescence and fall in winter deciduous species by climate change: Effects on nutrient proficiency. *Glob. Chang. Biol.* 2015, 21, 1005–1017.
6. Öquist, G.; Huner, N. P. A. Photosynthesis of Overwintering Plants. *Annu. Rev. Plant Biol.* 2003, 54, 329–355.
7. Ottander, C.; Campbell, D.; Öquist, G. Seasonal changes in photosystem II organisation and pigment composition in *Pinus sylvestris*. *Planta* 1995, 197, 176–183.
8. Maxwell, K.; Johnson, G. N. Chlorophyll fluorescence - a practical guide. *J. Exp. Bot.* 2000, 51, 659–668.
9. Demmig-Adams, B.; Adams, W. W. The role of xanthophyll cycle carotenoids in the protection of photosynthesis. *Trends Plant Sci.* 1996, 1, 21–26.
10. Porcar-Castell, A.; Tyystjärvi, E.; Atherton, J.; Van Der Tol, C.; Flexas, J.; Pfündel, E. E.; Moreno, J.; Frankenberg, C.; Berry, J. A. Linking chlorophyll a fluorescence to photosynthesis for remote sensing applications: Mechanisms and challenges. *J. Exp. Bot.* 2014, 65, 4065–4095.
11. Jones, H. G. *Plants and Microclimate: A Quantitative Approach to Environmental Plant Physiology*; 3rd ed.; Cambridge University Press: Cambridge, United Kingdom, 2014.

12. Demmig, B.; Winter, K.; Krüger, A.; Czygan, F. C. Photoinhibition and zeaxanthin formation in intact leaves: a possible role of the xanthophyll cycle in the dissipation of excess light energy. *Plant Physiol.* 1987, 84, 218–224.
13. Wong, C. Y. S.; Gamon, J. A. Three causes of variation in the photochemical reflectance index (PRI) in evergreen conifers. *New Phytol.* 2015, 206, 187–195.
14. Wong, C. Y. S.; Gamon, J. A. The photochemical reflectance index provides an optical indicator of spring photosynthetic activation in evergreen conifers. *New Phytol.* 2015, 206, 196–208.
15. Gamon, J. A.; Huemmrich, K. F.; Wong, C. Y. S.; Ensminger, I.; Garrity, S.; Hollinger, D. Y.; Noormets, A.; Peñuelas, J. A remotely sensed pigment index reveals photosynthetic phenology in evergreen conifers. *Proc. Natl. Acad. Sci. U. S. A.* 2016, 113, 13087–13092.
16. Park, T.; Ganguly, S.; Tømmervik, H.; Euskirchen, E. S.; Høgda, K.; Karlsen, S. R.; Brovkin, V.; Nemani, R. R.; Myneni, R. B. Changes in growing season duration and productivity of northern vegetation inferred from long-term remote sensing data. *Environ. Res. Lett.* 2016, 11, 84001.
17. Gamon, J. A.; Field, C. B.; Goulden, M. L.; Griffin, K. L.; Hartley, A. E.; Joel, G.; Peñuelas, J.; Valentini, R. Relationships Between NDVI, Canopy Structure, and Photosynthesis in Three Californian Vegetation Types. *Ecol. Appl.* 1995, 5, 28–41.
18. Running, S. W.; Nemani, R. R.; Heinsch, F. A.; Zhao, M.; Reeves, M.; Hashimoto, H. A Continuous Satellite-Derived Measure of Global Terrestrial Primary Production. *Bioscience* 2004, 54, 547.
19. Gamon, J. A.; Kovalchuck, O.; Wong, C. Y. S.; Harris, A.; Garrity, S. R. Monitoring seasonal and diurnal changes in photosynthetic pigments with automated PRI and NDVI sensors. *Biogeosciences* 2015, 12, 4149–4159.
20. Jönsson, A. M.; Eklundh, L.; Hellström, M.; Bärring, L.; Jönsson, P. Annual changes in MODIS vegetation indices of Swedish coniferous forests in relation to snow dynamics and tree phenology. *Remote Sens. Environ.* 2010, 114, 2719–2730.
21. Gamon, J. A.; Peñuelas, J.; Field, C. B. A Narrow-Waveband Spectral Index That Tracks Diurnal Changes in Photosynthetic Efficiency. *Remote Sens. Environ.* 1992, 44, 35–44.

22. Gamon, J. A.; Berry, J. A. Facultative and constitutive pigment effects on the Photochemical Reflectance Index (PRI) in sun and shade conifer needles. *Isr. J. Plant Sci.* 2012, 60, 85–95.
23. Gamon, J. A.; Serrano, L.; Surfus, J. S. The photochemical reflectance index: an optical indicator of photosynthetic radiation use efficiency across species, functional types, and nutrient levels. *Oecologia* 1997, 112, 492–501.
24. Goerner, A.; Reichstein, M.; Rambal, S. Tracking seasonal drought effects on ecosystem light use efficiency with satellite-based PRI in a Mediterranean forest. *Remote Sens. Environ.* 2009, 113, 1101–1111.
25. Garbulsky, M. F.; Peñuelas, J.; Ogaya, R.; Filella, I. Leaf and stand-level carbon uptake of a Mediterranean forest estimated using the satellite-derived reflectance indices EVI and PRI. *Int. J. Remote Sens.* 2013, 34, 1282–1296.
26. Baker, N. R.; Rosenqvist, E. Applications of chlorophyll fluorescence can improve crop production strategies: An examination of future possibilities. *J. Exp. Bot.* 2004, 55, 1607–1621.
27. Meroni, M.; Rossini, M.; Guanter, L.; Alonso, L.; Rascher, U.; Colombo, R.; Moreno, J. Remote sensing of solar-induced chlorophyll fluorescence: Review of methods and applications. *Remote Sens. Environ.* 2009, 113, 2037–2051.
28. Frankenberg, C.; Fisher, J. B.; Worden, J.; Badgley, G.; Saatchi, S. S.; Lee, J. E.; Toon, G. C.; Butz, A.; Jung, M.; Kuze, A.; Yokota, T. New global observations of the terrestrial carbon cycle from GOSAT: Patterns of plant fluorescence with gross primary productivity. *Geophys. Res. Lett.* 2011, 38, 1–6.
29. Joiner, J.; Yoshida, Y.; Vasilkov, A. P.; Schaefer, K.; Jung, M.; Guanter, L.; Zhang, Y.; Garrity, S.; Middleton, E. M.; Huemmrich, K. F.; Gu, L.; Beletti Marchesini, L. The seasonal cycle of satellite chlorophyll fluorescence observations and its relationship to vegetation phenology and ecosystem atmosphere carbon exchange. *Remote Sens. Environ.* 2014, 152, 375–391.
30. Walther, S.; Voigt, M.; Thum, T.; Gonsamo, A.; Zhang, Y.; Köhler, P.; Jung, M.; Varlagin, A.; Guanter, L. Satellite chlorophyll fluorescence measurements reveal large-scale decoupling of photosynthesis and greenness dynamics in boreal evergreen forests. *Glob. Chang. Biol.* 2016, 22, 2979–2996.

31. Gamon, J. A. Reviews and Syntheses: Optical sampling of the flux tower footprint. *Biogeosciences* 2015, 12, 4509–4523.
32. Gamon, J. A.; Qiu, H.-L. Ecological applications of remote sensing at multiple scales. In *Handbook of Functional Plant Ecology*; Pugnaire, F. I.; Valladares, F., Eds.; Marcel Dekker, Inc.: New York, USA, 1999; pp. 805–846.
33. Gamon, J. A.; Field, C. B.; Fredeen, A. L.; Thayer, S. Assessing photosynthetic downregulation in sunflower stands with an optically-based model. *Photosynth. Res.* 2001, 67, 113–25.
34. Garbulsky, M. F.; Peñuelas, J.; Gamon, J.; Inoue, Y.; Filella, I. The photochemical reflectance index (PRI) and the remote sensing of leaf, canopy and ecosystem radiation use efficiencies. A review and meta-analysis. *Remote Sens. Environ.* 2011, 115, 281–297.
35. Kraft, S.; Bézy, J.-L.; Del Bello, U.; Berlich, R.; Drusch, M.; Franco, R.; Gabriele, A.; Harnisch, B.; Meynart, R.; Silvestrin, P. FLORIS: phase A status of the fluorescence imaging spectrometer of the Earth Explorer mission candidate FLEX. *Proc. SPIE* 2013, 8889, 1–12.
36. Government of Canada Canadian Climate Normals [http://climate.weather.gc.ca/climate\\_normals/index\\_e.html](http://climate.weather.gc.ca/climate_normals/index_e.html) (accessed Mar 23, 2017).
37. Gamon, J. A.; Cheng, Y.; Claudio, H.; MacKinney, L.; Sims, D. A. A mobile tram system for systematic sampling of ecosystem optical properties. *Remote Sens. Environ.* 2006, 103, 246–254.
38. Givnish, T. J. Adaptive significance of evergreen vs. deciduous leaves: Solving the triple paradox. *Silva Fenn.* 2002, 36, 703–743.
39. Gower, S. T.; Richards, J. H. Larches: Deciduous Conifers in an Evergreen World carbon gain similar to evergreens. *Bioscience* 1990, 40, 818–826.
40. Krause, G. H.; Virgo, A.; Winter, K. High susceptibility to photoinhibition of young leaves of tropical forest trees. *Planta* 1995, 197, 583–591.
41. Chabot, B. F.; Hicks, D. J. The Ecology of Leaf Life Spans. *Annu. Rev. Ecol. Syst.* 1982, 13, 229–259.

42. Schulze, E.D.; Schulze, W.; Kelliher, F.M., Vygodskaya, N. N.; Ziegler, W.; Kobak, K. I.; Koch, H.; Arneith, A.; Kusnetsova, W. A.; Sogatchev, A.; Issajev, A.; Bauer, G.; Hollinger, D. Y. Aboveground biomass and nitrogen nutrition in a chronosequence of pristine Dahurian Larix stands in eastern Siberia. *Can. J. For. Res.* 1995, 25, 943–960.
43. Hörtensteiner, S.; Kräutler, B. Chlorophyll breakdown in higher plants. *Biochim. Biophys. Acta - Bioenerg.* 2011, 1807, 977–988.
44. Nakaji, T.; Oguma, H.; Fujinuma, Y. Seasonal changes in the relationship between photochemical reflectance index and photosynthetic light use efficiency of Japanese larch needles. *Int. J. Remote Sens.* 2006, 27, 493–509.
45. Porcar-Castell, A. A high-resolution portrait of the annual dynamics of photochemical and non-photochemical quenching in needles of *Pinus sylvestris*. *Physiol. Plant.* 2011, 143, 139–153.
46. Jiang, C. D.; Gao, H. Y.; Zou, Q.; Jiang, G. M.; Li, L. H. Leaf orientation, photorespiration and xanthophyll cycle protect young soybean leaves against high irradiance in field. *Environ. Exp. Bot.* 2006, 55, 87–96.
47. Zhu, H.; Zhang, T. J.; Zhang, P.; Peng, C. L. Pigment patterns and photoprotection of anthocyanins in the young leaves of four dominant subtropical forest tree species in two successional stages under contrasting light conditions. *Tree Physiol.* 2016, 36, 1092–1104.
48. Müller, P.; Li, X. P.; Niyogi, K. K. Non-photochemical quenching. A response to excess light energy. *Plant Physiol.* 2001, 125, 1558–1566.
49. Roden, J. S.; Pearcy, R. W. The Effect of Leaf Flutter on the Flux of CO<sub>2</sub> in Poplar Leaves. *Funct. Ecol.* 1993, 7, 669–675.
50. Schweiger, A.; Cavender-Bares, J.; Townsend, P.; Hobbie, S.; Madritch, M.; Wang, R.; Tilman, D.; Gamon, J. Leaf spectral diversity explains productivity, functional and phylogenetic diversity in a grassland experiment. *Nat. Ecol. Evol.* (Accepted)
51. Ustin, S. L.; Gamon, J. A. Remote sensing of plant functional types. *New Phytol.* 2010, 186, 795–816.



52. Hall, F. G.; Huemmrich, K. F.; Goetz, S. J.; Sellers, P. J.; Nickeson, J. E. Satellite remote sensing of surface energy balance - Success, failures, and unresolved issues in FIFE. *J. Geophys. Res.* 1992, 97, 19061–19089.
53. Barton, C. V. M.; North, P. R. J. Remote sensing of canopy light use efficiency using the photochemical reflectance index model and sensitivity analysis. *Remote Sens. Environ.* 2001, 78, 264–273.
54. Eklundh, L.; Jin, H.; Schubert, P.; Guzinski, R.; Heliasz, M. An optical sensor network for vegetation phenology monitoring and satellite data calibration. *Sensors* 2011, 11, 7678–7709.
55. Baker, N. R. Chlorophyll Fluorescence: A Probe of Photosynthesis In Vivo. *Annu. Rev. Plant Biol.* 2008, 59, 89–113.

## Chapter 3: Discussion and Conclusions

### 3.1 Summary and Contributions

The importance of the boreal forest as a global carbon sink and a key component of the global climate system is well established [1]. As our climate changes, accurate monitoring of the boreal forest will be essential to understanding how changing climatic conditions will affect forest function and its feedbacks on the global climate system. Remote sensing will play a key role in accomplishing this.

The main goal of this work was to evaluate the efficacy of remotely detected optical indices, the normalized difference vegetation index (NDVI), the photochemical reflectance index (PRI), the chlorophyll/carotenoid index (CCI), and steady-state chlorophyll fluorescence ( $F_s$ ) as a measure of solar-induced fluorescence (SIF), at tracking seasonal changes in photosynthetic activity (photosynthetic phenology) of boreal trees. The primary focus was testing the hypothesis that different functional types have contrasting optical properties based on complementary structural and physiological controls. By using a combination of evergreen and deciduous tree species, this study clarified which optical indices were most suited for sampling different functional types, providing an important foundation for the application of optical remote sensing across the boreal forest. By comparing optical phenology to changes in photosynthetic activity, this study was able to directly test the hypothetical relationships between different optical indices and plant productivity outlined in the complementarity hypothesis. The major findings of this study were:

1. The NDVI and PRI were each capable of tracking photosynthetic activity in only a single functional type, where CCI and, less accurately,  $F_s$  more closely tracked actual productivity in both functional types. Seasonal changes in NDVI showed close parallels to photosynthetic activity and strong seasonal variability in deciduous species, with NDVI driven by changes in canopy structure and foliar display, but NDVI had limited seasonal variability for evergreen species that had relatively little change in canopy structure across seasons. PRI showed the opposite ability, closely paralleling photosynthetic activity with strong seasonal variation in evergreens, reflecting subtle changes in pigment pool sizes across seasons, whereas for deciduous species, changes in PRI were not as prominent, but did show seasonal variability that was driven by the emergence and senescence of green foliage. By contrast, CCI closely paralleled photosynthetic phenology and displayed strong

seasonal variation in both evergreen and deciduous tree species; showing sensitivity to both canopy structural changes as well as changes in pigment pool sizes. Steady state fluorescence ( $F_s$ ) showed a similar ability to CCI, but was visibly more variable.

2. NDVI and PRI provided complementary information with respect to the light-use efficiency (LUE) model when sampling evergreen and deciduous species, supporting the original complementarity hypothesis. NDVI strongly related to seasonally changing photosynthetic activity for deciduous species, reflecting changes in absorbed radiation (APAR), but not for all evergreen species. In evergreens, the dynamic range of NDVI across seasons was far less than in deciduous species. PRI closely followed changes in photosynthetic activity for evergreen species, indicating changes in light-use efficiency ( $\epsilon$ ), but was a less effective indicator of photosynthetic activity and efficiency in deciduous species, with a smaller dynamic range in deciduous than in evergreen species. CCI, on the other hand, similarly tracked changes in photosynthetic activity for both functional types, indicating sensitivity to both subtle foliar changes related to efficiency ( $\epsilon$ ) and structural changes related to APAR. Because it is sensitive to both terms of the LUE model, CCI may be a more direct indicator of photosynthetic activity than NDVI or PRI. Similar relationships were found between steady state fluorescence ( $F_s$ , an indicator of solar induced fluorescence, SIF) and photosynthetic activity, particularly for evergreens but less so for deciduous species, suggesting that  $F_s$  has a similar ability as CCI to directly estimate photosynthetic activity. Whether the lower accuracy of  $F_s$ , relative to CCI, was due to the differences in spatial scales of employed measurements or rather a result of optical indices being inherently different is still unclear.
3. Optical and photosynthetic phenology showed distinctly different patterns for deciduous and evergreen species, presumably reflecting different the structural and physiological controls impacting optical properties. Variation in optical phenology also existed within functional types, with closely related species of the same functional type exhibiting more similar responses than more distantly related species, suggesting a phylogenetic component to these responses. Of the metrics used, CCI appears to be best suited to detecting changes in optical properties across and within functional types in boreal forest ecosystems.

## 3.2 Limitations and Future Work

### 3.2.1 *Expanding Upon Small-Scale Studies*

The rooftop setting of this study allowed for convenient long-term monitoring of boreal trees while they were subject to the same environmental conditions, analogous to a ‘common garden’. This experiment was conducted at proximal (leaf and canopy) scales using synthetic tree plots. However, the age and spacing of the trees used to establish the synthetic rooftop plots may not fully represent tree stands in natural ecosystems. Similar studies in natural forests are required to clarify any potential artefacts from this small-scale study on potted trees. Artefacts may have arisen from any number of effects the synthetic setting may have had on optical signals, such as the different stand structure of seedling versus mature stands, or the influence of various background signals (snow, leaf litter, soil).

In context of the complementarity hypothesis, this study clearly shows that different functional types (evergreen and deciduous) had distinct optical and photosynthetic phenology. While this provides clear support to the idea that different functional types in different ecosystems have contrasting structural and physiological controls on optical and physiological properties [2,3], studies assessing a greater diversity of species from multiple ecosystems are still required to fully test this concept in order to evaluate functional types beyond “evergreen” and “deciduous” trees. Such studies would help to clarify the concept of vegetation optical types: vegetation classified by optical properties [4]. This concept states that the optical properties of vegetation are determined by combination of specific physiological leaf traits [5,6] canopy structure [7] and the phenology of vegetation [8]. The potential classification of vegetation based on optical behavior needs to be better understood to effectively apply optical sampling to estimate photosynthetic phenology over larger spatial and temporal scales.

Additionally, the design of this study was limited in replication. This study utilized only one plot per species (unreplicated at the species level) and included a technical replication (pseudoreplication) during sampling. In future studies, species replication at the plot level with nested treatments would allow for stronger conclusions to be drawn regarding the variability of optical properties at the species level. To further expand on this work, future studies should also monitor more species within each functional type as well as incorporating species from other

functional types to better understand optical and phenological variation within and across functional types.

### ***3.2.2 Upscaling with New Technologies***

The phenomena observed in this setting provide an important foundation for the application of these methods across larger spatial and temporal scales. Studies combining proximal remote sampling with flux measurements are required to understand finer-scale plant processes that can be missed by large-scale remote techniques [3]. The current flux tower network (e.g. FLUXNET) allows for sampling atmosphere biosphere interactions in terrestrial ecosystems [9]. The use of automated portable sensors [10,11] in association with flux measurements can provide a mechanistic understanding of the relationships between optical and flux measurements at proximal levels that provides the basis for interpreting remote data at larger spatial scales. The integration of optical remote sensing and flux measurements at proximal scales is necessary to fully understand the relationships between optical properties, plant physiological processes and changing environmental conditions, providing essential ground validation for large-scale optical sampling through satellite (e.g. MODIS) or airborne measurements. While no single satellite can measure all the optical indices explored here, the upcoming FLEX satellite missions [12] will benefit from the understanding gained from this and similar proximal studies.

The current tools available to measure both optical and physiological properties of ecosystems at large scales can be used to further understand plant optical diversity as it applies to functional processes such as photosynthesis. Applying the findings of this study to larger spatial scales (upscaling) also requires proximal studies that look at a greater number of species in both monocultural and mixed settings, representing wider assemblages of plant communities, to further understand how canopy heterogeneity impacts the sampling of optical and photosynthetic metrics. Future work should explore the optical and physiological properties of vegetation from variety of ecosystems, such as tundra or prairie grasslands, and deciduous or tropical forests. Understanding how the optical properties of vegetation from these different ecosystems relates to photosynthesis at proximal scales will be vital for the interpretation of ecosystem level optical and photosynthetic phenology.

The groundwork laid in this study for the upscaling of optical remote sensing to monitor entire ecosystems will provide critical information on how fundamental properties and processes of

vegetation in the boreal forest, as well as in other biomes and ecoregions, will respond to a globally changing climate. Insight into changing phenology and productivity expected for the boreal forest in response to altered environmental conditions (water and temperature regimes) can be gained by the proper application and integration of a variety remote sensing techniques.

### **3.3 Conclusions**

Remote sensing provides a powerful means of monitoring and estimating biophysical properties of plants at multiple scales. With the emergence of new technologies, structural and physiological properties of vegetation that control productivity can be more accurately measured and related to plant productivity. However, continued work that integrates earth observational sciences, traditional plant physiology, and ecological principles is essential to properly understanding how plant physiological processes and structure impact remote measurements and productivity. Further experimental studies that integrate optical sampling with ecosystem carbon fluxes at different scales are needed to understanding the structural and physiological controls on photosynthetic activity. An understanding of the behavior of plant optical properties will be essential to understand how to apply and interpret large scale optical remote sensing measurements across ecosystems.

While the LUE model provides a useful framework for using remote sensing to estimate plant productivity, the emergence of new optical parameters and their continued study may change how we apply remote sensing metrics to models of plant productivity across ecosystems. This leaves several questions that are yet to be answered: Can we consistently parameterize the LUE model using multiple remote measurements, or can new metrics (CCI or  $F_s$ ) lead to a model that potentially transcends the LUE model to estimating productivity more directly? Is there a universal model for estimating carbon uptake in terrestrial environments? Or do models require ecosystem specific calibration according to varying vegetation physiology and structure? If so, can we use optical properties to elaborate on the concept of optical types, and categorize vegetation that are functionally and optically similar? These are questions that need to be answered using continued interdisciplinary studies. As our climate continues to shift, accurate monitoring of vegetation phenology and productivity at large scales is a vital to understanding how ecosystems will respond to changing climate.

### 3.4 References

1. Bonan, G. B. Forests and climate change: forcings, feedbacks, and the climate benefits of forests. *Science*. 2008, 320, 1444–1449.
2. Garbulsky, M. F.; Peñuelas, J.; Gamon, J.; Inoue, Y.; Filella, I. The photochemical reflectance index (PRI) and the remote sensing of leaf, canopy and ecosystem radiation use efficiencies. A review and meta-analysis. *Remote Sens. Environ.* 2011, 115, 281–297.
3. Gamon, J. A. Reviews and Syntheses: Optical sampling of the flux tower footprint. *Biogeosciences* 2015, 12, 4509–4523.
4. Ustin, S. L.; Gamon, J. A. Remote sensing of plant functional types. *New Phytol.* 2010, 186, 795–816.
5. Sánchez-Azofeifa, G. A.; Castro, K.; Wright, S. J.; Gamon, J.; Kalacska, M.; Rivard, B.; Schnitzer, S. A.; Feng, J. L. Differences in leaf traits, leaf internal structure, and spectral reflectance between two communities of lianas and trees: Implications for remote sensing in tropical environments. *Remote Sens. Environ.* 2009, 113, 2076–2088.
6. Niinemets, Ü.; Keenan, T. F.; Hallik, L. A worldwide analysis of within-canopy variations in leaf structural, chemical and physiological traits across plant functional types. *New Phytol.* 2015, 205, 973–993.
7. Knyazikhin, Y.; Schull, M. A.; Stenberg, P.; Mottus, M.; Rautiainen, M.; Yang, Y.; Marshak, A.; Latorre Carmona, P.; Kaufmann, R. K.; Lewis, P.; Disney, M. I.; Vanderbilt, V.; Davis, A. B.; Baret, F.; Jacquemoud, S.; Lyapustin, A.; Myneni, R. B. Hyperspectral remote sensing of foliar nitrogen content. *Proc. Natl. Acad. Sci.* 2013, 110, E185–E192.
8. Chavana-Bryant, C.; Malhi, Y.; Wu, J.; Asner, G. P.; Anastasiou, A.; Enquist, B. J.; Cosio Caravasi, E. G.; Doughty, C. E.; Saleska, S. R.; Martin, R. E.; Gerard, F. F. Leaf aging of Amazonian canopy trees as revealed by spectral and physiochemical measurements. *New Phytol.* 2016, 214, 1049–1063.
9. Baldocchi, D.; Falge, E.; Gu, L.; Olson, R.; Hollinger, D.; Running, S.; Anthoni, P.; Bernhofer, C.; Davis, K.; Evans, R.; Fuentes, J.; Goldstein, A.; Katul, G.; Law, B.; Lee, X.; Malhi, Y.; Meyers, T.; Munger, W.; Oechel, W.; Paw, U. K. T.; Pilegaard, K.; Schmid, H. P.; Valentini, R.; Verma,

S.; Vesala, T.; Wilson, K.; Wofsy, S. FLUXNET: A New Tool to Study the Temporal and Spatial Variability of Ecosystem-Scale Carbon Dioxide, Water Vapor, and Energy Flux Densities. *Bull. Am. Meteorol. Soc.* 2001, 82, 2415–2434.

10. Gamon, J. A.; Kovalchuck, O.; Wong, C. Y. S.; Harris, A.; Garrity, S. R. Monitoring seasonal and diurnal changes in photosynthetic pigments with automated PRI and NDVI sensors. *Biogeosciences* 2015, 12, 4149–4159.

11. Nestola, E.; Calfapietra, C.; Emmerton, C. A.; Wong, C. Y. S.; Thayer, D. R.; Gamon, J. A. Monitoring grassland seasonal carbon dynamics, by integrating MODIS NDVI, proximal optical sampling, and eddy covariance measurements. *Remote Sens.* 2016, 8.

12. Kraft, S.; Bézy, J.-L.; Del Bello, U.; Berlich, R.; Drusch, M.; Franco, R.; Gabriele, A.; Harnisch, B.; Meynart, R.; Silvestrin, P. FLORIS: phase A status of the fluorescence imaging spectrometer of the Earth Explorer mission candidate FLEX. *Proc. SPIE* 2013, 8889, 1–12.



## Bibliography

- Adams, W. W. and Demmig-Adams, B.: Carotenoid composition and down-regulation of photosystem II in three conifer species during the winter, *Physiol. Plant.*, 92(3), 451–458, 1994.
- Adams, W. W., Demmig-Adams, B., Rosenstiel, T. N., Brightwell, A. K. and Ebbert, V.: Photosynthesis and Photoprotection in Overwintering Plants, *Plant Biol.*, 4, 545–557, doi:10.1055/s-2002-35434, 2002.
- Baker, N. R.: Chlorophyll Fluorescence: A Probe of Photosynthesis In Vivo, *Annu. Rev. Plant Biol.*, 59, 89–113, doi:10.1146/annurev.arplant.59.032607.092759, 2008.
- Baker, N. R. and Rosenqvist, E.: Applications of chlorophyll fluorescence can improve crop production strategies: An examination of future possibilities, *J. Exp. Bot.*, 55(403), 1607–1621, doi:10.1093/jxb/erh196, 2004.
- Baldocchi, D., Falge, E., Gu, L., Olson, R., Hollinger, D., Running, S., Anthoni, P., Bernhofer, C., Davis, K., Evans, R., Fuentes, J., Goldstein, A., Katul, G., Law, B., Lee, X., Malhi, Y., Meyers, T., Munger, W., Oechel, W., Paw, U. K. T., Pilegaard, K., Schmid, H. P., Valentini, R., Verma, S., Vesala, T., Wilson, K. and Wofsy, S.: FLUXNET: A New Tool to Study the Temporal and Spatial Variability of Ecosystem-Scale Carbon Dioxide, Water Vapor, and Energy Flux Densities, *Bull. Am. Meteorol. Soc.*, 82(11), 2415–2434, doi:10.1175/1520-0477(2001)082<2415:FANTTS>2.3.CO;2, 2001.
- Balzarolo, M., Vescovo, L., Hammerle, A., Gianelle, D., Papale, D., Tomelleri, E. and Wohlfahrt, G.: On the relationship between ecosystem-scale hyperspectral reflectance and CO<sub>2</sub> exchange in European mountain grasslands, *Biogeosciences*, 12(10), 3089–3108, doi:10.5194/bg-12-3089-2015, 2015.
- Balzarolo, M., Vicca, S., Nguy-Robertson, A. L., Bonal, D., Elbers, J. A., Fu, Y. H., Grünwald, T., Horemans, J. A., Papale, D., Peñuelas, J., Suyker, A. and Veroustraete, F.: Matching the phenology of Net Ecosystem Exchange and vegetation indices estimated with MODIS and FLUXNET in-situ observations, *Remote Sens. Environ.*, 174, 290–300, doi:10.1016/j.rse.2015.12.017, 2016.
- Barr, A., Black, T. A. and McCaughey, H.: Climatic and Phenological Controls of the Carbon and Energy Balances of Three Contrasting Boreal Forest Ecosystems in Western Canada, in *Phenology of Ecosystem Processes*, edited by A. Noormets, pp. 3–34, Springer, New York, NY., 2009.
- Barton, C. V. M. and North, P. R. J.: Remote sensing of canopy light use efficiency using the photochemical reflectance index model and sensitivity analysis, *Remote Sens. Environ.*, 78(3), 264–273, doi:10.1016/S0034-4257(01)00224-3, 2001.
- Bhatia, S. and Sharma, K.: *Microenvironmentation in Micropropagation*, Elsevier Inc., 2015.

- Bhatt, U. S., Walker, D. A., Reynolds, M. K., Comiso, J. C., Epstein, H. E., Jia, G., Gens, R., Pinzon, J. E., Tucker, C. J., Tweedie, C. E. and Webber, P. J.: Circumpolar Arctic tundra vegetation change is linked to sea ice decline, *Earth Interact.*, 14(8), doi:10.1175/2010EI315.1, 2010.
- Black, T. A., Gaumont-Guay, D., Jassa, R. S., D'Amiro, B., Jarvis, P. G., Gower, S. T., Kelliher, F. M., Dunn, A. L. and Wofsy, S. C.: Measurement of CO<sub>2</sub> exchange between boreal forest and the atmosphere, in *The Carbon Balance of Forest Biomes*, vol. 57, edited by H. Griffith and P. Jarvis, pp. 151–186, Taylor & Francis Group, New York, NY., 2005.
- Bonan, G. B.: Forests and climate change: forcings, feedbacks, and the climate benefits of forests., *Science*, 320(5882), 1444–1449, doi:10.1126/science.1155121, 2008.
- Bunn, A. G., Goetz, S. J., Kimball, J. S. and Zhang, K.: Northern high-latitude ecosystems respond to climate change, *Eos, Trans. Am. Geophys. Union*, 88(34), 333–335, doi:10.1029/2007EO340001, 2007.
- Burns, R. M. and Honkala, B. H.: *Silvics of North America: 1. Conifers*. Agricultural Handbook 654, 654th ed., U.S. Department of Agriculture, Forest Service, Washington, DC., 1990a.
- Burns, R. M. and Honkala, B. H.: *Silvics of North America: 2. Hardwoods*. Agriculture Handbook 654, U.S. Department of Agriculture, Forest Service, Washington, DC., 1990b.
- Chabot, B. F. and Hicks, D. J.: The Ecology of Leaf Life Spans, *Annu. Rev. Ecol. Syst.*, 13(1), 229–259, doi:10.1146/annurev.es.13.110182.001305, 1982.
- Chavana-Bryant, C., Malhi, Y., Wu, J., Asner, G. P., Anastasiou, A., Enquist, B. J., Cosio Caravasi, E. G., Doughty, C. E., Saleska, S. R., Martin, R. E. and Gerard, F. F.: Leaf aging of Amazonian canopy trees as revealed by spectral and physiochemical measurements, *New Phytol.*, 214(3), 1049–1063, doi:10.1111/nph.13853, 2016.
- D'Odorico, P., Gonsamo, A., Gough, C. M., Bohrer, G., Morison, J., Wilkinson, M., Hanson, P. J., Gianelle, D., Fuentes, J. D. and Buchmann, N.: The match and mismatch between photosynthesis and land surface phenology of deciduous forests, *Agric. For. Meteorol.*, 214–215, 25–38, doi:10.1016/j.agrformet.2015.07.005, 2015.
- Demmig-Adams, B. and Adams, W. W.: The role of xanthophyll cycle carotenoids in the protection of photosynthesis, *Trends Plant Sci.*, 1(1), 21–26, doi:10.1016/S1360-1385(96)80019-7, 1996.
- Demmig, B., Winter, K., Krüger, A. and Czygan, F. C.: Photoinhibition and zeaxanthin formation in intact leaves: a possible role of the xanthophyll cycle in the dissipation of excess light energy., *Plant Physiol.*, 84(2), 218–224, doi:10.1104/pp.84.2.218, 1987.
- Dixon, R. K., Browne, S., Houghton, R. A., Solomon, A. M., Trexler, M. C. and Wosniewski, J.: Carbon pools and flux of global forest ecosystems, *Science*, 263(5144), 185–190, doi:10.1126/science.263.5144.185, 1994.

- Eklundh, L., Jin, H., Schubert, P., Guzinski, R. and Heliasz, M.: An optical sensor network for vegetation phenology monitoring and satellite data calibration, *Sensors*, 11(8), 7678–7709, doi:10.3390/s110807678, 2011.
- Ensminger, I., Sveshnikov, D., Campbell, D. A., Funk, C., Jansson, S., Lloyd, J., Shibistova, O. and Öquist, G.: Intermittent low temperatures constrain spring recovery of photosynthesis in boreal Scots pine forests, *Glob. Chang. Biol.*, 10(6), 995–1008, doi:10.1111/j.1365-2486.2004.00781.x, 2004.
- Estiarte, M. and Peñuelas, J.: Alteration of the phenology of leaf senescence and fall in winter deciduous species by climate change: Effects on nutrient proficiency, *Glob. Chang. Biol.*, 21(3), 1005–1017, doi:10.1111/gcb.12804, 2015.
- Fischlin, A., Midgley, G. F., Price, J. T., Leemans, R., Gopal, B., Turley, C., Rounsevell, M. D. A., Dube, O. P., Tarazona, J. and Velichko, A. A.: Ecosystems, their properties, goods and services., 2007.
- Frankenberg, C., Fisher, J. B., Worden, J., Badgley, G., Saatchi, S. S., Lee, J. E., Toon, G. C., Butz, A., Jung, M., Kuze, A. and Yokota, T.: New global observations of the terrestrial carbon cycle from GOSAT: Patterns of plant fluorescence with gross primary productivity, *Geophys. Res. Lett.*, 38(17), 1–6, doi:10.1029/2011GL048738, 2011.
- Gamon, J. A.: Reviews and Syntheses: Optical sampling of the flux tower footprint, *Biogeosciences*, 12(14), 4509–4523, doi:10.5194/bg-12-4509-2015, 2015.
- Gamon, J. A. and Berry, J. A.: Facultative and constitutive pigment effects on the Photochemical Reflectance Index (PRI) in sun and shade conifer needles, *Isr. J. Plant Sci.*, 60(1–2), 85–95, doi:10.1560/IJPS.60.1-2.85, 2012.
- Gamon, J. A. and Qiu, H.-L.: Ecological applications of remote sensing at multiple scales, in *Handbook of Functional Plant Ecology*, edited by F. I. Pugnaire and F. Valladares, pp. 805–846, Marcel Dekker, Inc., New York, USA., 1999.
- Gamon, J. A., Peñuelas, J. and Field, C. B.: A Narrow-Waveband Spectral Index That Tracks Diurnal Changes in Photosynthetic Efficiency, *Remote Sens. Environ.*, 44, 35–44, 1992.
- Gamon, J. A., Field, C. B., Goulden, M. L., Griffin, K. L., Hartley, A. E., Joel, G., Peñuelas, J. and Valentini, R.: Relationships Between NDVI, Canopy Structure, and Photosynthesis in Three Californian Vegetation Types, *Ecol. Appl.*, 5(1), 28–41, doi:10.2307/1942049, 1995.
- Gamon, J. A., Serrano, L. and Surfus, J. S.: The photochemical reflectance index: an optical indicator of photosynthetic radiation use efficiency across species, functional types, and nutrient levels, *Oecologia*, 112(4), 492–501, doi:10.1007/s004420050337, 1997.

- Gamon, J. A., Field, C. B., Fredeen, A. L. and Thayer, S.: Assessing photosynthetic downregulation in sunflower stands with an optically-based model., *Photosynth. Res.*, 67(1–2), 113–25, doi:10.1023/A:1010677605091, 2001.
- Gamon, J. A., Cheng, Y., Claudio, H., MacKinney, L. and Sims, D. A.: A mobile tram system for systematic sampling of ecosystem optical properties, *Remote Sens. Environ.*, 103(3), 246–254, doi:10.1016/j.rse.2006.04.006, 2006.
- Gamon, J. A., Kovalchuck, O., Wong, C. Y. S., Harris, A. and Garrity, S. R.: Monitoring seasonal and diurnal changes in photosynthetic pigments with automated PRI and NDVI sensors, *Biogeosciences*, 12(13), 4149–4159, doi:10.5194/bg-12-4149-2015, 2015.
- Gamon, J. A., Huemmrich, K. F., Wong, C. Y. S., Ensminger, I., Garrity, S., Hollinger, D. Y., Noormets, A. and Peñuelas, J.: A remotely sensed pigment index reveals photosynthetic phenology in evergreen conifers., *Proc. Natl. Acad. Sci. U. S. A.*, 113(46), 13087–13092, doi:10.1073/pnas.1606162113, 2016.
- Garbulsky, M. F., Peñuelas, J., Gamon, J., Inoue, Y. and Filella, I.: The photochemical reflectance index (PRI) and the remote sensing of leaf, canopy and ecosystem radiation use efficiencies. A review and meta-analysis, *Remote Sens. Environ.*, 115(2), 281–297, doi:10.1016/j.rse.2010.08.023, 2011.
- Garbulsky, M. F., Peñuelas, J., Ogaya, R. and Filella, I.: Leaf and stand-level carbon uptake of a Mediterranean forest estimated using the satellite-derived reflectance indices EVI and PRI, *Int. J. Remote Sens.*, 34(4), 1282–1296, doi:10.1080/01431161.2012.718457, 2013.
- GISTEMP Team: GISS Surface Temperature Analysis (GISTEMP), NASA Goddard Inst. Sp. Stud. [online] Available from: <https://data.giss.nasa.gov/gistemp/> (Accessed 21 September 2017), 2017.
- Givnish, T. J.: Adaptive significance of evergreen vs. deciduous leaves: Solving the triple paradox, *Silva Fenn.*, 36(3), 703–743, doi:10.14214/sf.535, 2002.
- Goerner, A., Reichstein, M. and Rambal, S.: Tracking seasonal drought effects on ecosystem light use efficiency with satellite-based PRI in a Mediterranean forest, *Remote Sens. Environ.*, 113(5), 1101–1111, doi:10.1016/j.rse.2009.02.001, 2009.
- Goetz, S. J., Bunn, A. G., Fiske, G. J. and Houghton, R. A.: Satellite-observed photosynthetic trends across boreal North America associated with climate and fire disturbance., *Proc. Natl. Acad. Sci. U. S. A.*, 102(38), 13521–5, doi:10.1073/pnas.0506179102, 2005.
- Goodale, C. L., Apps, M. J., Birdsey, R. A., Field, C. B., Heath, L. S., Houghton, R. A., Jenkins, J. C., Kohlmaier, G. H., Kurz, W., Liu, S., Nabuurs, G., Nilsson, S. and Shvidenko, A. Z.: Forest carbon sinks in the Northern Hemisphere, *Ecol. Appl.*, 12(3), 891–899, doi:10.1890/1051-0761, 2002.

Gordo, O. and Sanz, J. J.: Long-term temporal changes of plant phenology in the Western Mediterranean, *Glob. Chang. Biol.*, 15(8), 1930–1948, doi:10.1111/j.1365-2486.2009.01851.x, 2009.

Government of Canada: Canadian Climate Normals, [online] Available from: [http://climate.weather.gc.ca/climate\\_normals/index\\_e.html](http://climate.weather.gc.ca/climate_normals/index_e.html) (Accessed 23 March 2017), 2017.

Gower, S. T. and Richards, J. H.: Larches: Deciduous Conifers in an Evergreen World carbon gain similar to evergreens, *Bioscience*, 40(11), 818–826, doi:https://doi.org/10.2307/1311484, 1990.

Gustafson, E. J., Shvidenko, A. Z., Sturtevant, B. R. and Scheller, R. M.: Predicting global change effects on forest biomass and composition in south-central Siberia, *Ecol. Appl.*, 20(3), 700–715, doi:10.1890/08-1693.1, 2010.

Hall, F. G., Huemmrich, K. F., Goetz, S. J., Sellers, P. J. and Nickeson, J. E.: Satellite remote sensing of surface energy balance - Success, failures, and unresolved issues in FIFE, *J. Geophys. Res.*, 97(17), 19061–19089, doi:10.1029/92JD02189, 1992.

Hanes, J. M., Richardson, A. D. and Klosterman, S.: Mesic Temperate Deciduous Forest Phenology, in *Phenology: An Integrative Environmental Science*, edited by M. D. Schwartz, pp. 211–224, Springer, Dordrecht., 2013.

Hansen, J., Ruedy, R., Sato, M. and Lo, K.: Global surface temperature change, *Rev. Geophys.*, 48(4), RG4004, doi:10.1029/2010RG000345.1.INTRODUCTION, 2010.

Havranek, W. M. and Tranquillini, W.: Physiological Processes during Winter Dormancy and Their Ecological Significance, in *Ecophysiology of Coniferous Forests*, pp. 95–124, ACADEMIC PRESS, INC., 1995.

Heinsch, F. A., Zhao, M., Running, S. W., Kimball, J. S., Nemani, R. R., Davis, K. J., Bolstad, P. V., Cook, B. D., Desai, A. R., Ricciuto, D. M., Law, B. E., Oechel, W. C., Kwon, H., Luo, H., Wofsy, S. C., Dunn, A. L., Munger, J. W., Baldocchi, D. D., Xu, L., Hollinger, D. Y., Richardson, A. D., Stoy, P. C., Siqueira, M. B. S., Monson, R. K., Burns, S. P. and Flanagan, L. B.: Evaluation of remote sensing based terrestrial productivity from MODIS using regional tower eddy flux network observations, *IEEE Trans. Geosci. Remote Sens.*, 44(7), 1908–1923, doi:10.1109/TGRS.2005.853936, 2006.

Hörtensteiner, S.: Chlorophyll Degradation During Senescence, *Annu. Rev. Plant Biol.*, 57(1), 55–77, doi:10.1146/annurev.arplant.57.032905.105212, 2006.

Hörtensteiner, S. and Kräutler, B.: Chlorophyll breakdown in higher plants, *Biochim. Biophys. Acta - Bioenerg.*, 1807(8), 977–988, doi:10.1016/j.bbambio.2010.12.007, 2011.

Jiang, C. D., Gao, H. Y., Zou, Q., Jiang, G. M. and Li, L. H.: Leaf orientation, photorespiration and xanthophyll cycle protect young soybean leaves against high irradiance in field, *Environ. Exp. Bot.*, 55(1–2), 87–96, doi:10.1016/j.envexpbot.2004.10.003, 2006.

Joiner, J., Yoshida, Y., Vasilkov, A. P., Schaefer, K., Jung, M., Guanter, L., Zhang, Y., Garrity, S., Middleton, E. M., Huemmrich, K. F., Gu, L. and Belelli Marchesini, L.: The seasonal cycle of satellite chlorophyll fluorescence observations and its relationship to vegetation phenology and ecosystem atmosphere carbon exchange, *Remote Sens. Environ.*, 152, 375–391, doi:10.1016/j.rse.2014.06.022, 2014.

Jones, H. G.: *Plants and Microclimate: A Quantitative Approach to Environmental Plant Physiology*, 3rd ed., Cambridge University Press, Cambridge, United Kingdom., 2014.

de Jong, R., Verbesselt, J., Schaepman, M. E. and de Bruin, S.: Trend changes in global greening and browning: Contribution of short-term trends to longer-term change, *Glob. Chang. Biol.*, 18(2), 642–655, doi:10.1111/j.1365-2486.2011.02578.x, 2012.

Jönsson, A. M., Eklundh, L., Hellström, M., Barring, L. and Jönsson, P.: Annual changes in MODIS vegetation indices of Swedish coniferous forests in relation to snow dynamics and tree phenology, *Remote Sens. Environ.*, 114(11), 2719–2730, doi:10.1016/j.rse.2010.06.005, 2010.

Kattge, J. and Knorr, W.: Temperature acclimation in a biochemical model of photosynthesis: A reanalysis of data from 36 species, *Plant, Cell Environ.*, 30(9), 1176–1190, doi:10.1111/j.1365-3040.2007.01690.x, 2007.

Knyazikhin, Y., Schull, M. A., Stenberg, P., Mottus, M., Rautiainen, M., Yang, Y., Marshak, A., Latorre Carmona, P., Kaufmann, R. K., Lewis, P., Disney, M. I., Vanderbilt, V., Davis, A. B., Baret, F., Jacquemoud, S., Lyapustin, A. and Myneni, R. B.: Hyperspectral remote sensing of foliar nitrogen content, *Proc. Natl. Acad. Sci.*, 110(3), E185–E192, doi:10.1073/pnas.1210196109, 2013.

Kraft, S., Bézy, J.-L., Del Bello, U., Berlich, R., Drusch, M., Franco, R., Gabriele, A., Harnisch, B., Meynart, R. and Silvestrin, P.: FLORIS: phase A status of the fluorescence imaging spectrometer of the Earth Explorer mission candidate FLEX, *Proc. SPIE*, 8889(88890T), 1–12, doi:10.1117/12.2032060, 2013.

Krause, G. H., Virgo, A. and Winter, K.: High susceptibility to photoinhibition of young leaves of tropical forest trees, *Planta*, 197(4), 583–591, doi:10.1007/BF00191564, 1995.

Lloyd, J.: The CO<sub>2</sub> dependence of photosynthesis, plant growth responses to elevated CO<sub>2</sub> concentrations and their interaction with soil nutrient status, II. Temperate and boreal forest productivity and the combined effects of increasing CO<sub>2</sub> concentrations and increased nitrogen deposition at a global scale, *Funct. Ecol.*, 13(4), 439–459, doi:10.1046/j.1365-2435.1999.00350.x, 1999.

MacDonald, G. M.: Global warming and the Arctic: a new world beyond the reach of the Grinnellian niche?, *J. Exp. Biol.*, 213(6), 855–861, doi:10.1242/jeb.039511, 2010.

Maxwell, K. and Johnson, G. N.: *Chlorophyll fluorescence - a practical guide.*, *J. Exp. Bot.*, 51(345), 659–668, doi:10.1093/jexbot/51.345.659, 2000.

- Meroni, M., Rossini, M., Guanter, L., Alonso, L., Rascher, U., Colombo, R. and Moreno, J.: Remote sensing of solar-induced chlorophyll fluorescence: Review of methods and applications, *Remote Sens. Environ.*, 113(10), 2037–2051, doi:10.1016/j.rse.2009.05.003, 2009.
- Monteith, J. L.: Climate and the efficiency of crop production in Britain, *Phil. Trans. R. Soc. Lond. B*, 281, 277–294, doi:10.1098/rstb.1977.0140, 1977.
- Müller, P., Li, X. P. and Niyogi, K. K.: Non-photochemical quenching. A response to excess light energy., *Plant Physiol.*, 125(4), 1558–1566, doi:10.1104/pp.125.4.1558, 2001.
- Nakaji, T., Oguma, H. and Fujinuma, Y.: Seasonal changes in the relationship between photochemical reflectance index and photosynthetic light use efficiency of Japanese larch needles, *Int. J. Remote Sens.*, 27(3), 493–509, doi:10.1080/01431160500329528, 2006.
- NASA-ABOVE: A Notional Airborne Science Research Strategy for NASA’s Arctic Boreal Vulnerability Experiment (ABOVE). [online] Available from: [https://above.nasa.gov/pdfs/Notional Airborne Remote Sensing Strategy for ABOVE - 2016-05-27.pdf](https://above.nasa.gov/pdfs/Notional%20Airborne%20Remote%20Sensing%20Strategy%20for%20ABOVE%20-%202016-05-27.pdf), 2016.
- Nestola, E., Calfapietra, C., Emmerton, C. A., Wong, C. Y. S., Thayer, D. R. and Gamon, J. A.: Monitoring grassland seasonal carbon dynamics, by integrating MODIS NDVI, proximal optical sampling, and eddy covariance measurements, *Remote Sens.*, 8(3), doi:10.3390/rs8030260, 2016.
- Niinemets, Ü., Keenan, T. F. and Hallik, L.: A worldwide analysis of within-canopy variations in leaf structural, chemical and physiological traits across plant functional types, *New Phytol.*, 205(3), 973–993, doi:10.1111/nph.13096, 2015.
- Olson, J. S.: Productivity of Forest Ecosystems, in *Productivity of World Ecosystems*, pp. 33–43, National Academy of Sciences, Washington, DC., 1975.
- Van Ommen Kloeke, A. E. E., Douma, J. C., Ordoñez, J. C., Reich, P. B. and Van Bodegom, P. M.: Global quantification of contrasting leaf life span strategies for deciduous and evergreen species in response to environmental conditions, *Glob. Ecol. Biogeogr.*, 21(2), 224–235, doi:10.1111/j.1466-8238.2011.00667.x, 2012.
- Öquist, G. and Huner, N. P. A.: Photosynthesis of Overwintering Plants, *Annu. Rev. Plant Biol.*, 54(1), 329–355, doi:10.1146/annurev.arplant.54.072402.115741, 2003.
- Ottander, C., Campbell, D. and Öquist, G.: Seasonal changes in photosystem II organisation and pigment composition in *Pinus sylvestris*, *Planta*, 197(1), 176–183, doi:10.1007/BF00239954, 1995.
- Pan, Y., Birdsey, R. A., Fang, J., Houghton, R., Kauppi, P. E., Kurz, W. A., Phillips, O. L., Shvidenko, A., Lewis, S. L. and Canadell, J. G.: A Large and Persistent Carbon Sink in the World’s Forests, *Science*, 333(6045), 988–993, doi:10.1126/science.1201609, 2011.

Park, T., Ganguly, S., Tømmervik, H., Euskirchen, E. S., Høgda, K., Karlsen, S. R., Brovkin, V., Nemani, R. R. and Myneni, R. B.: Changes in growing season duration and productivity of northern vegetation inferred from long-term remote sensing data, *Environ. Res. Lett.*, 11, 84001, doi:10.1088/1748-9326/11/8/084001, 2016.

Porcar-Castell, A.: A high-resolution portrait of the annual dynamics of photochemical and non-photochemical quenching in needles of *Pinus sylvestris*, *Physiol. Plant.*, 143(2), 139–153, doi:10.1111/j.1399-3054.2011.01488.x, 2011.

Porcar-Castell, A., Tyystjärvi, E., Atherton, J., Van Der Tol, C., Flexas, J., Pfündel, E. E., Moreno, J., Frankenberg, C. and Berry, J. A.: Linking chlorophyll a fluorescence to photosynthesis for remote sensing applications: Mechanisms and challenges, *J. Exp. Bot.*, 65(15), 4065–4095, doi:10.1093/jxb/eru191, 2014.

Reich, P. B., Ellsworth, D. S. and Walters, M. B.: Leaf structure (specific leaf area) modulates photosynthesis – nitrogen relations: evidence from within and across species and functional groups, *Funct. Ecol.*, 12, 948–958, doi:10.1046/j.1365-2435.1998.00274.x, 1998.

Richardson, A. D., Keenan, T. F., Migliavacca, M., Ryu, Y., Sonnentag, O. and Toomey, M.: Climate change, phenology, and phenological control of vegetation feedbacks to the climate system, *Agric. For. Meteorol.*, 169, 156–173, doi:10.1016/j.agrformet.2012.09.012, 2013.

Roden, J. S. and Percy, R. W.: The Effect of Leaf Flutter on the Flux of CO<sub>2</sub> in Poplar Leaves, *Funct. Ecol.*, 7(6), 669–675, doi:10.2307/2390187, 1993.

Rohde, A. and Bhalerao, R. P.: Plant dormancy in the perennial context, *Trends Plant Sci.*, 12(5), 217–223, doi:10.1016/j.tplants.2007.03.012, 2007.

Running, S. W., Nemani, R. R., Heinsch, F. A., Zhao, M., Reeves, M. and Hashimoto, H.: A Continuous Satellite-Derived Measure of Global Terrestrial Primary Production, *Bioscience*, 54(6), 547, doi:10.1641/0006-3568(2004)054[0547:ACSMOG]2.0.CO;2, 2004.

Sabine, C. L., Heimann, M., Artaxo, P., Bakker, D. C. E., Chen, C.-T. A., Field, C. B., Gruber, N., Le Quéré, C., Prinn, R. G. and Richey, J. E.: Current status and past trends of the global carbon cycle, in *The Global Carbon Cycle: Integrating Humans, Climate, and the Natural World*, vol. 62, pp. 17–44., 2004.

Sánchez-Azofeifa, G. A., Castro, K., Wright, S. J., Gamon, J., Kalacska, M., Rivard, B., Schnitzer, S. A. and Feng, J. L.: Differences in leaf traits, leaf internal structure, and spectral reflectance between two communities of lianas and trees: Implications for remote sensing in tropical environments, *Remote Sens. Environ.*, 113(10), 2076–2088, doi:10.1016/j.rse.2009.05.013, 2009.

Schulze, E.D., Schulze, W., Kelliher, F.M., Vygodskaya, N. N., Ziegler, W., Kobak, K. I., Koch, H., Arneth, A., Kusnetsova, W. A., Sogatchev, A., Issajev, A., Bauer, G. and Hollinger, D. Y.:



Aboveground biomass and nitrogen nutrition in a chronosequence of pristine Dahurian Larix stands in eastern Siberia, *Can. J. For. Res.*, 25(6), 943–960, doi:10.1139/x95-103, 1995.

Schweiger, A., Cavender-Bares, J., Townsend, P., Hobbie, S., Madritch, M., Wang, R., Tilman, D. and Gamon, J.: Leaf spectral diversity explains productivity, functional and phylogenetic diversity in a grassland experiment, *Nat. Ecol. Evol.*, Accepted.

Seidl, R., Thom, D., Kautz, M., Martin-Benito, D., Peltoniemi, M., Vacchiano, G., Wild, J., Ascoli, D., Petr, M., Honkaniemi, J., Lexer, M. J., Trotsiuk, V., Mairota, P., Svoboda, M., Fabrika, M., Nagel, T. A. and Reyer, C. P. O.: Forest disturbances under climate change, *Nat. Clim. Chang.*, 7(6), 395–402, doi:10.1038/nclimate3303, 2017.

Serreze, M. C. and Barry, R. G.: Processes and impacts of Arctic amplification: A research synthesis, *Glob. Planet. Change*, 77(1–2), 85–96, doi:10.1016/j.gloplacha.2011.03.004, 2011.

Sims, D. A., Luo, H., Hastings, S., Oechel, W. C., Rahman, A. F. and Gamon, J. A.: Parallel adjustments in vegetation greenness and ecosystem CO<sub>2</sub> exchange in response to drought in a Southern California chaparral ecosystem, *Remote Sens. Environ.*, 103(3), 289–303, doi:10.1016/j.rse.2005.01.020, 2006.

Soolanayakanahally, R. Y., Guy, R. D., Silim, S. N., Drewes, E. C. and Schroeder, W. R.: Enhanced assimilation rate and water use efficiency with latitude through increased photosynthetic capacity and internal conductance in balsam poplar (*Populus balsamifera* L.), *Plant, Cell Environ.*, 32(12), 1821–1832, doi:10.1111/j.1365-3040.2009.02042.x, 2009.

Swann, A. L., Fung, I. Y., Levis, S., Bonan, G. B. and Doney, S. C.: Changes in Arctic vegetation amplify high-latitude warming through the greenhouse effect, *Proc. Natl. Acad. Sci.*, 107(4), 1295–1300, doi:10.1073/pnas.0913846107, 2010.

Thakur, N., Sharma, V. and Kishore, K.: Leaf senescence: an overview, *Indian J. Plant Physiol.*, 21(3), 225–238, doi:10.1007/s40502-016-0234-3, 2016.

Tjoelker, M. G., Oleksyn, J. and Reich, P. B.: Seedlings of five boreal tree seedlings differ in acclimation of photosynthesis to elevated CO<sub>2</sub> and temperature, *Tree Physiol.*, 18, 715–726, 1998.

Tucker, C. J., Townshend, J. R. G. and Goff, T. E.: African land-cover classification using satellite data, *Science*, 227(4685), 369–75, doi:10.1126/science.227.4685.369, 1985.

Ustin, S. L. and Gamon, J. A.: Remote sensing of plant functional types, *New Phytol.*, 186(4), 795–816, doi:10.1111/j.1469-8137.2010.03284.x, 2010.

Walker, A. P., Beckerman, A. P., Gu, L., Kattge, J., Cernusak, L. A., Domingues, T. F., Scales, J. C., Wohlfahrt, G., Wullschleger, S. D. and Woodward, F. I.: The relationship of leaf photosynthetic traits - V<sub>max</sub> and J<sub>max</sub> - to leaf nitrogen, leaf phosphorus, and specific leaf area: A meta-analysis and modeling study, *Ecol. Evol.*, 4(16), 3218–3235, doi:10.1002/ece3.1173, 2014.

- Walther, S., Voigt, M., Thum, T., Gonsamo, A., Zhang, Y., Köhler, P., Jung, M., Varlagin, A. and Guanter, L.: Satellite chlorophyll fluorescence measurements reveal large-scale decoupling of photosynthesis and greenness dynamics in boreal evergreen forests, *Glob. Chang. Biol.*, 22(9), 2979–2996, doi:10.1111/gcb.13200, 2016.
- Way, D. A. and Oren, R.: Differential responses to changes in growth temperature between trees from different functional groups and biomes: a review and synthesis of data, *Tree Physiol.*, 669–688, doi:10.1093/treephys/tpq015, 2010.
- Wilson, K. B., Baldocchi, D. D. and Hanson, P. J.: Leaf age affects the seasonal pattern of photosynthetic capacity and net ecosystem exchange of carbon in a deciduous forest, *Plant, Cell Environ.*, 24(2001), 571–583, doi:10.1046/j.0016-8025.2001.00706.x, 2001.
- Winton, M.: Amplified Arctic climate change: What does surface albedo feedback have to do with it?, *Geophys. Res. Lett.*, 33(3), 1–4, doi:10.1029/2005GL025244, 2006.
- Wong, C. Y. S. and Gamon, J. A.: The photochemical reflectance index provides an optical indicator of spring photosynthetic activation in evergreen conifers, *New Phytol.*, 206(1), 196–208, doi:10.1111/nph.13251, 2015a.
- Wong, C. Y. S. and Gamon, J. A.: Three causes of variation in the photochemical reflectance index (PRI) in evergreen conifers, *New Phytol.*, 206(1), 187–195, doi:10.1111/nph.13159, 2015b.
- Zhu, H., Zhang, T. J., Zhang, P. and Peng, C. L.: Pigment patterns and photoprotection of anthocyanins in the young leaves of four dominant subtropical forest tree species in two successional stages under contrasting light conditions, *Tree Physiol.*, 36(9), 1092–1104, doi:10.1093/treephys/tpw047, 2016.

## Appendix

**Table S1:** Summary of measurements performed on tree plots.

Measurement	Equipment Used	Sampling Level	Samples per plot	Measurements per plant
Photosynthetic Rate	LI-6400 Gas Exchange System	Plant (branch or leaf)	5	5
Canopy Reflectance (for calculating indices)	UniSpec DC Spectrometer	Canopy	5	n/a
Steady-State Fluorescence	Walz Mini-PAM Fluorometer	Plant (leaf)	6	3

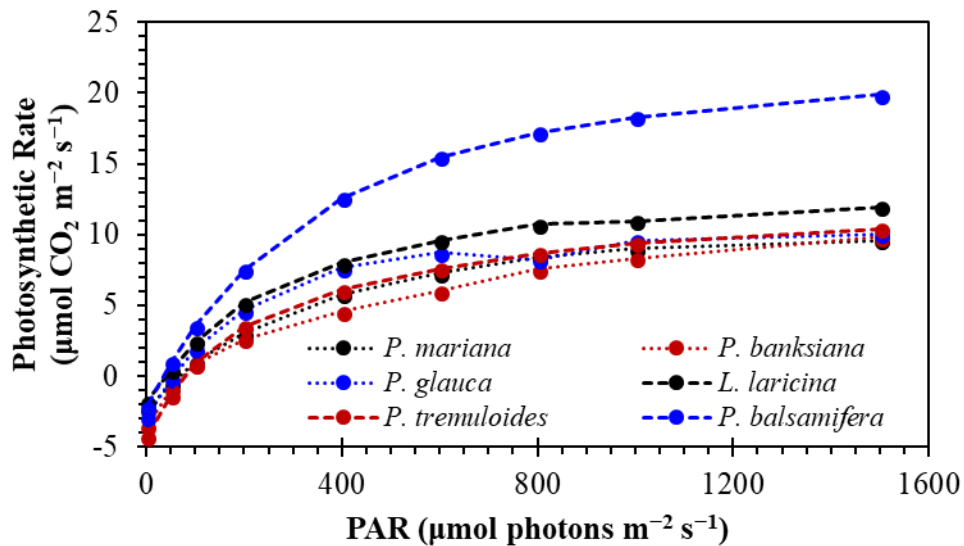


**Figure S1:** Growing season photosynthetic light response curves for evergreen (dotted lines) and deciduous species (dashed lines). The light curve was set to monitor photosynthesis at light intensity values of 1500, 1000, 800, 600, 400, 100, 50 and 0  $\mu\text{mol photons m}^{-2} \text{s}^{-1}$ . For each stage, there was a 1-3 min acclimation time before measurement and changing to the next light level. Measurements were performed on within 1 hour of solar noon on July 27, 2016. Based on these light-response curves, 1500 was selected as the “saturating” light level for seasonal photosynthetic trends.

**Table S2:** Copy of Table 2.1 indicating  $p$ -values for each t-statistic numerically.

	Photosynthetic Rate		NDVI		PRI		CCI		Fs	
	t-stat	$p$	t-stat	$p$	t-stat	$p$	t-stat	$p$	t-stat	$p$
a) Evergreen spp.	85.762	1.359E-04	3.373	7.778E-02	13.274	5.628E-03	6.236	2.476E-02	5.233	3.463E-02
Deciduous spp.	9.060	1.197E-02	21.280	2.201E-03	3.086	9.092E-02	7.779	1.613E-02	36.420	7.531E-04
b) <i>P. mariana</i>	22.239	2.420E-05	8.012	1.317E-03	72.815	2.132E-07	72.022	2.227E-07	11.995	7.103E-05
<i>P. banksiana</i>	15.549	9.987E-05	8.279	1.162E-03	30.160	7.198E-06	86.473	1.072E-07	21.730	3.830E-06
<i>P. glauca</i>	28.247	9.347E-06	15.679	9.664E-05	67.416	2.900E-07	151.682	1.133E-08	15.595	1.970E-05
c) <i>L. laricina</i>	21.667	2.684E-05	59.100	4.909E-07	77.476	1.663E-07	126.115	2.371E-08	5.940	1.931E-03
<i>P. tremuloides</i>	35.979	3.562E-06	32.580	5.292E-06	8.568	1.019E-03	33.329	4.833E-06	9.787	1.895E-04
<i>P. balsamifera</i>	10.012	5.594E-04	42.344	1.859E-06	13.028	2.004E-04	53.247	7.446E-07	6.271	1.514E-03

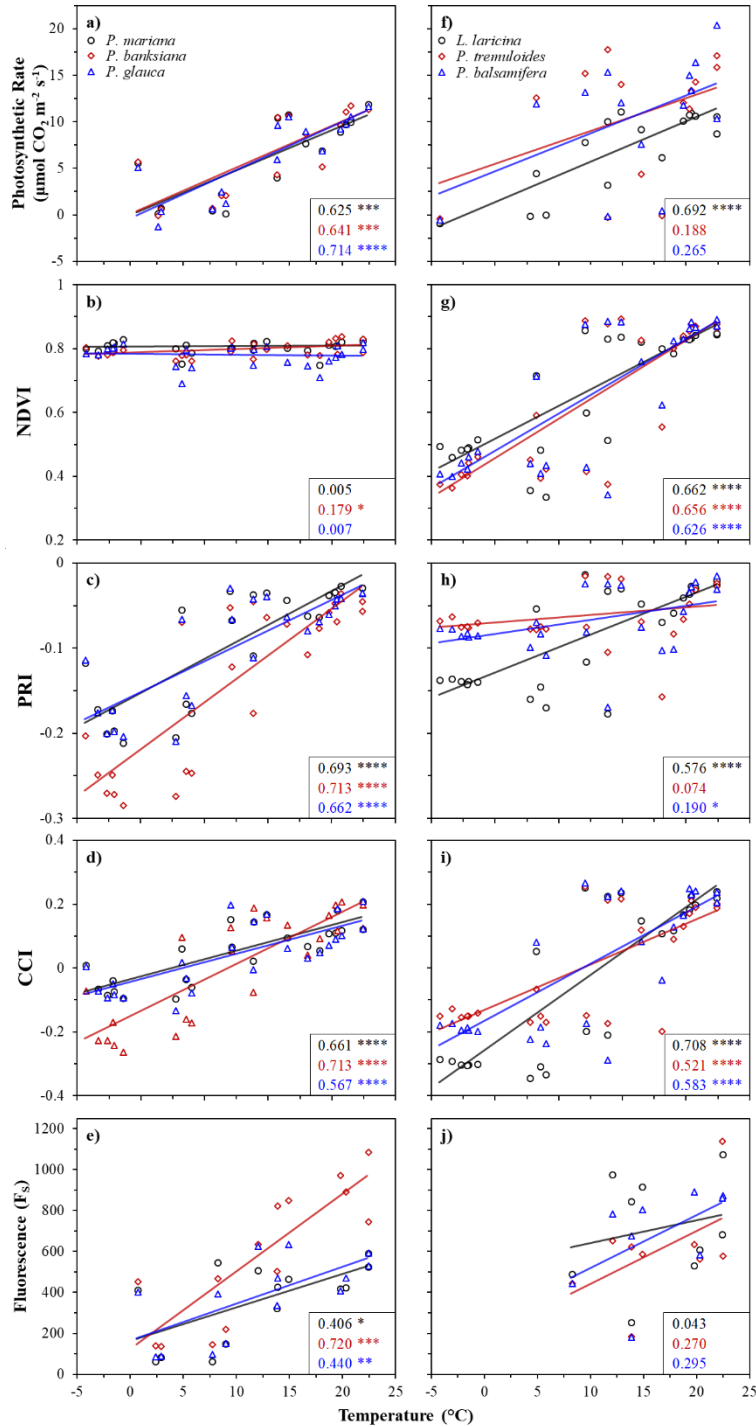


**Figure S2:** Relationships between daily average temperature and measurements of photosynthetic rate ( $\mu\text{mol CO}_2 \text{ m}^{-2} \text{ s}^{-1}$ ), NDVI, PRI, CCI, and  $F_s$  for evergreen (a-e) and deciduous (f-j) species. Temperature is expressed as a daily average. Data points for other metrics were obtained near solar noon from January 2016 to December 2016. For reflectance indices (NDVI, PRI, CCI), canopy data with snow present were excluded.  $R^2$  values and significance are given in the figure legends. \*,  $p < 0.05$ ; \*\*,  $p < 0.01$ ; \*\*\*,  $p < 0.001$ ; \*\*\*\*,  $p < 0.0001$ .

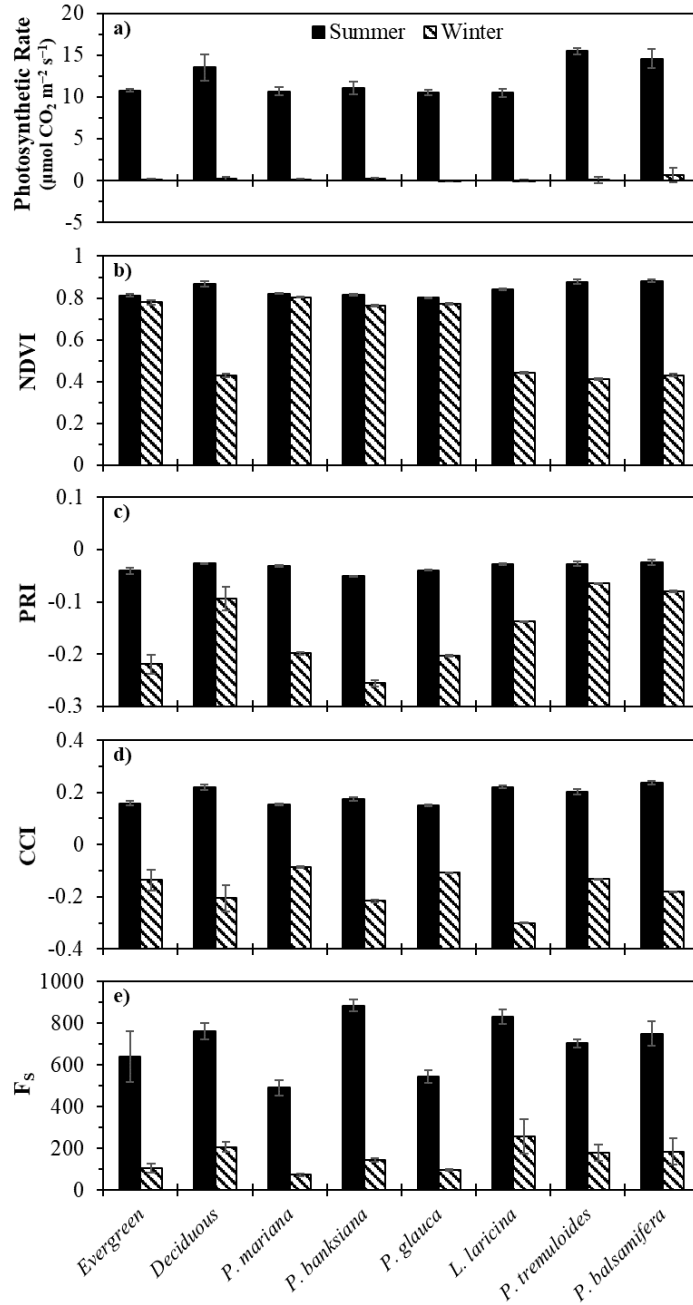


**Figure S3:** Summer and winter period averages for Photosynthetic rate (a), NDVI (b), PRI (c), CCI (d), and  $F_s$  (e). For evergreen and deciduous types, average summer and winter values for each species within each type were used for comparison ( $n=3$ ). Average photosynthetic rate for each plant ( $n=5$ ), the average value for NDVI, PRI, and CCI from each region within a plot ( $n=5$ ), and the average  $F_s$  for each plant ( $n=6$ ) from all sampling intervals in each period. For photosynthetic rate, dates when new branches were sampled for *P. mariana* and *P. glauca* (open points, Fig. 2.4a) were excluded from analyses. For NDVI, PRI, and CCI, data in winter where snow was present on canopies were excluded from statistical analyses. For  $F_s$ , winter values for deciduous species were taken from a single time point (see supplemental Figure S4). Error bars denote  $\pm$ SE of the mean.

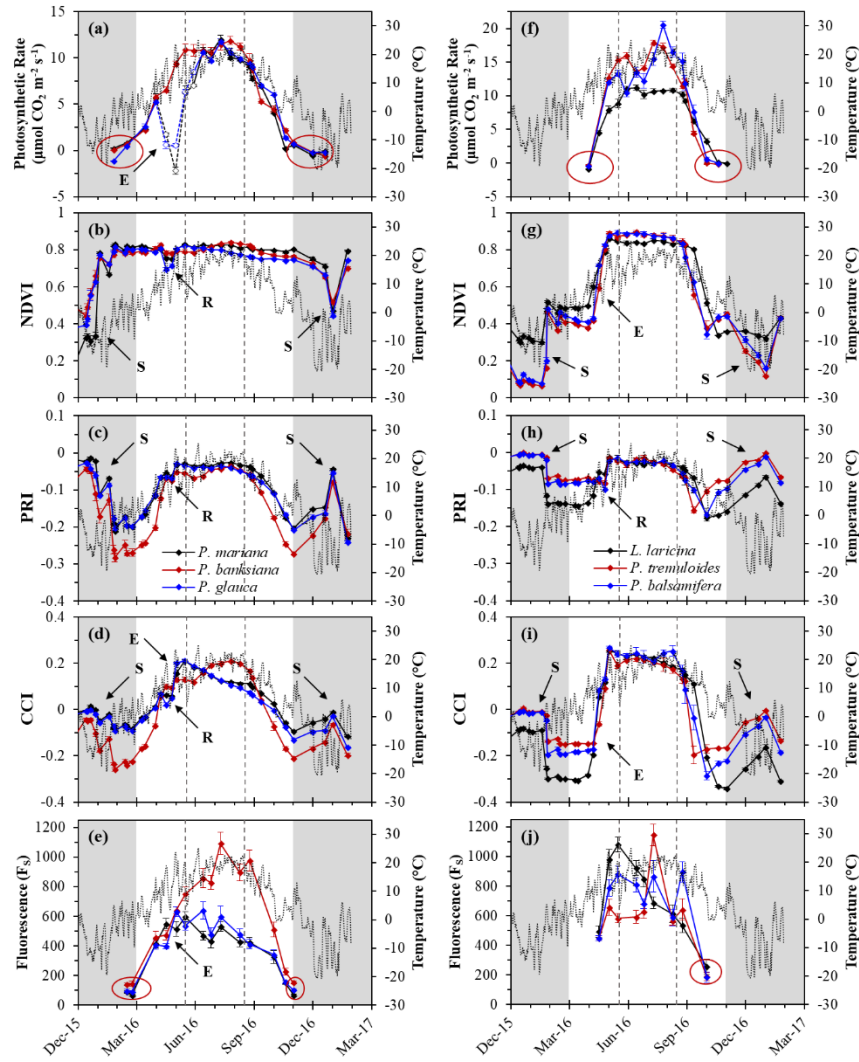


**Figure S4:** Copy of Figure 2.4 of data chapter with annotations indicating period of summer (between dashed lines) in addition to period of winter, indicated by the grey regions, highlighting time points used for calculating average summer and winter values for each measurement by plant/plot region. For leaf level measurements (photosynthetic rate,  $F_s$ ), points closest to the winter period were used, as there were no measurements performed during the defined winter period (circled); winter points for leaf-level measurements for evergreen species are also circled.